



Universidad de Oviedo

**PROGRAMA DE DOCTORADO EN FÍSICA DE LA MATERIA  
CONDENSADA, NANOCIENCIA Y BIOFÍSICA**

**Estudio del papel del citoesqueleto en las  
propiedades físicas y mecánicas de células  
cancerosas.**

**Marina Pilar López Yubero**

Tesis doctoral dirigida por

**Prof. Francisco Javier Tamayo de Miguel**

Tutor:

**Prof. Jaime Ferrer Rodríguez**

Oviedo, 2023





Universidad de Oviedo

**PROGRAMA DE DOCTORADO EN FÍSICA DE LA MATERIA  
CONDENSADA, NANOCIENCIA Y BIOFÍSICA**

**Disentangling the role of cytoskeleton in physical  
and mechanical properties of cancer cells.**

**Marina Pilar López Yubero**

Supervised by

**Prof. Francisco Javier Tamayo de Miguel**

Tutor:

**Prof. Jaime Ferrer Rodríguez**

Oviedo, 2023

This thesis was developed in the Bionanomechanics Lab at the Instituto de Micro y Nanotecnología (IMN-CNM), belonging to the Spanish National Research Council (CSIC) under the supervision of Professor Francisco Javier Tamayo de Miguel. It was tutored by Professor Jaime Ferrer Rodríguez from University of Oviedo.

This thesis was supported by the European Union's Horizon 2020 research and innovation program under European Research Council Grant 681275-LIQUIDMASS-ERC-CoG-2015, under Grant Agreement Number 73186-VIRUSCAN and by the Spanish Science, Innovation and Universities Ministry through project CELLTANGLE, reference RTI2018-099369-B-I00. Also by the Comunidad de Madrid through the project iLUNG B2017/BMD-3884 with support from EU (FEDER, FSE) and the Global Health Interdisciplinary Platform (PTI) of the CSIC through the project 202050E156-CSIC-COV19-035.

The service from the X-SEM Laboratory in the Instituto de Micro y Nanotecnología (IMN-CNM, CSIC) is funded by Comunidad de Madrid (project SpaceTec, S2013/ICE2822), Ministerio de Asuntos Económicos y Transformación Digital (MINECO, project CSIC13-4E-1794) and European Union (FEDER, FSE).

**©2023**

**Marina P. López Yubero**

All rights reserved





## RESUMEN DEL CONTENIDO DE TESIS DOCTORAL

1.- Título de la Tesis	
Español/Otro Idioma: Estudio del papel del citoesqueleto en las propiedades físicas y mecánicas de células cancerosas.	Inglés: Disentangling the role of cytoskeleton in physical and mechanical properties of cancer cells.
2.- Autor	
Nombre: Marina Pilar López Yubero	DNI/Pasaporte/NIE:
Programa de Doctorado: Programa de Doctorado en Física de la Materia Condensada, Nanociencia y Biofísica (Interuniversitario).	
Órgano responsable: Departamento de Física de la Universidad de Oviedo	

### RESUMEN (en español)

En los últimos años, el estudio de las propiedades mecánicas de las células ha cobrado mayor importancia en el mundo científico. Dado que la célula es la unidad anatómica fundamental de los seres vivos, capaz de reagruparse en tejidos, y que a su vez se organizan en órganos, el estudio de sus características físicas parece clave para entender su biología y cómo se relaciona la célula con lo que le rodea.

Se han desarrollado numerosas técnicas físicas para el estudio de propiedades mecánicas de células animales y vegetales, siendo el Microscopio de Fuerzas Atómicas (AFM) una de las más utilizadas por su versatilidad.

En esta tesis, se ha empleado el AFM para estudiar las propiedades mecánicas de células humanas en cultivo en base a dos parámetros de sus propiedades: el módulo de elasticidad aparente,  $E_0$ , y el exponente  $\beta$ , relacionado con las propiedades viscoelásticas. Con estas dos medidas se puede realizar un fenotipado mecánico de células individuales que puede incluso ser usado como ensayo de efectos de fármacos.

Usando esta metodología, se han estudiado las líneas celulares de cáncer de mama MCF10-A (línea sana), MCF-7 (línea tumoral no metastática) y MDA-MB-231 (línea tumoral invasiva), logrando un fenotipado mecánico de las tres líneas.

Cuando una célula se vuelve tumoral, sufre cambios y reprogramaciones tanto en su metabolismo como en su cortex de actina. Para estudiar el papel del metabolismo y del citoesqueleto en la contribución a las propiedades mecánicas de estas líneas celulares hemos aplicado tres tratamientos a las células. En primer lugar, hemos desorganizado los filamentos de actina usando citocalasina D, en segundo lugar, hemos inhibido los motores moleculares de miosina-II con blebistatina y, finalmente, hemos impedido el correcto funcionamiento del metabolismo celular agotando el ATP disponible en el medio. Con esto hemos descubierto cómo las distintas células establecen sus características físicas de diferente manera según su malignidad y en función de su metabolismo.

Las células de mama sanas basan sus propiedades mecánicas en la polimerización de fibras de actina, gastando ATP. Las células metastáticas utilizan la actividad de los motores moleculares de miosina-II para mantener su rigidez y las células tumorales no invasivas muestran unas alteraciones metabólicas que les permiten mantener sus



propiedades mecánicas intactas, incluso en ausencia casi total de energía en forma de ATP.

También hemos empleado esta técnica de AFM con tres líneas de cáncer de pulmón de células no pequeñas, o no microcíticos, (NSCLC). En las líneas celulares A549 y NCI-H226, las propiedades mecánicas de células individuales son similares, mientras que son muy diferentes a las de la línea celular NCI-H23. Estas tres líneas muestran diferentes mutaciones conductoras (*driver*), que son aquellas que le confieren a la célula una ventaja selectiva en su crecimiento. Entre éstas, las hay que afectan a dos conocidos genes relacionados con el cáncer: el oncogén *KRAS* y el gen supresor de tumores *TP53*. NCI-H226 es wild-type para ambos, NCI-H23 muestra mutaciones en ambos, y A549 tiene mutado *KRAS*.

Para saber si las alteraciones en estos dos genes afectan a las propiedades mecánicas de estas líneas celulares, hemos mutado *KRAS* con una sustitución G12V y hemos eliminado *TP53* en líneas celulares salvajes para ambos. Así, cada línea actúa como control de sí misma.

Los resultados de AFM muestran que *TP53* sí afecta a las propiedades mecánicas de las células investigadas, mientras que la mutación G12V en *KRAS* no lo hace. Así, se muestra que hay una conexión directa entre algunas alteraciones en rutas moleculares y las propiedades mecánicas de las células.

### RESUMEN (en Inglés)

In recent years, the study of the mechanical properties of cells has become a promising scientific field. Given that the cell is the basic anatomical unit of living beings, which is capable of regrouping into tissues and which finally organize themselves into organs, the study of a cell's physical characteristics seems to be key for understanding its biology and how the cell relates to its surroundings.

Numerous physical techniques have been developed to study the physical properties of animal and plant cells, being the Atomic Force Microscope (AFM) one of the most commonly used due to its versatility.

In this thesis, AFM has been used to study the mechanical properties of human cells in culture based on two parameters of their properties: the apparent elastic modulus,  $E_0$ , and the exponent  $\beta$ , related to its viscoelastic properties. With these two quantities, a mechanical phenotyping of individual cells can be performed, which can even be used as a drug effects assay.

Using this methodology, breast cancer cell lines MCF10-A (healthy line), MCF-7 (non-metastatic tumor line), and MDA-MB-231 (invasive tumor line) have been studied, achieving a mechanical phenotyping of the three lines.

When a cell becomes tumoral, it undergoes changes and reprogramming in both its metabolism and actin cortex. To study the role of metabolism and the cytoskeleton contribution to the mechanical properties of these cell lines, we have applied three treatments to the cells. Firstly, we have disorganized actin filaments using cytochalasin D, secondly, we have inhibited the molecular motors of myosin-II with blebbistatin, and finally we have prevented the proper functioning of cellular metabolism by depleting the available ATP in the medium. This has revealed how different cells establish their physical characteristics differently depending on their malignancy and according to their metabolism.



Universidad de Oviedo

Healthy cells base their mechanical properties on the polymerization of actin fibers, consuming ATP. Metastatic cells use the activity of myosin-II molecular motors to maintain their rigidity, and non-invasive tumor cells show metabolic alterations that allow them to maintain their mechanical properties intact, even in the total absence of ATP.

We have also used this AFM technique with three lines of non-small cell lung cancer (NSCLC). In the cell lines A549 and NCI-H226, the mechanical properties of individual cells are similar, while they are very different from those of the cell line NCI-H23. These three lines show different driver mutations, which confer a selective growth advantage to the cell. Among these, there are those that affect two well-known cancer-related genes: the oncogene *KRAS* and the tumor suppressor gene *TP53*. NCI-H226 is wild-type for both, NCI-H23 shows mutations in both, and A549 has mutated *KRAS*.

To determine whether alterations in these two genes affect the mechanical properties of these cell lines, we mutated *KRAS* with a G12V substitution and eliminated *TP53* in wild-type cell lines for both. Thus, each line acts as a control for itself.

Our results show that *TP53* does in fact affect the mechanical properties of the investigated cells, but *KRAS* G12V mutation does not have any impact on these properties. Thus, it is shown that there is a direct connection between alterations in some molecular routes and mechanical properties in single cells.

**SR. PRESIDENTE DE LA COMISIÓN ACADÉMICA DEL PROGRAMA DE DOCTORADO EN FÍSICA DE LA MATERIA CONDENSADA, NANOCIENCIA Y BIOFÍSICA**

This thesis was developed in the Bionanomechanics Lab at the Instituto de Micro y Nanotecnología (IMN-CNM), belonging to the Spanish National Research Council (CSIC) under the supervision of Professor Francisco Javier Tamayo de Miguel. It was tutored by Professor Jaime Ferrer Rodríguez from University of Oviedo.

This thesis was supported by the European Union's Horizon 2020 research and innovation program under European Research Council Grant 681275-LIQUIDMASS-ERC-CoG-2015, under Grant Agreement Number 73186-VIRUSCAN and by the Spanish Science, Innovation and Universities Ministry through project CELLTANGLE, reference RTI2018-099369-B-I00. Also by the Comunidad de Madrid through the project iLUNG B2017/BMD-3884 with support from EU (FEDER, FSE) and the Global Health Interdisciplinary Platform (PTI) of the CSIC through the project 202050E156-CSIC-COV19-035.

The service from the X-SEM Laboratory in the Instituto de Micro y Nanotecnología (IMN-CNM, CSIC) is funded by Comunidad de Madrid (project SpaceTec, S2013/ICE2822), Ministerio de Asuntos Económicos y Transformación Digital (MINECO, project CSIC13-4E-1794) and European Union (FEDER, FSE).

**©2023**

**Marina P. López Yubero**

All rights reserved

*Thank you. How grand we are this morning!*

*Gracias. ¡Qué grandes estamos esta mañana!*

*Ulysses, James Joyce, 1922.*



A grayscale microscopic image showing a dense field of cells. Some cells are in the process of dividing, appearing as pairs of small circles. The cells have irregular, somewhat rounded shapes with visible internal structures. The background is a light gray, and the cells are darker, creating a high-contrast image.

## Resumen

En los últimos años, el estudio de las propiedades mecánicas de las células ha cobrado mayor importancia en el mundo científico. Dado que la célula es la unidad anatómica fundamental de los seres vivos, capaz de reagruparse en tejidos, y que a su vez se organizan en órganos, el estudio de sus características físicas resulta clave para entender su biología y cómo se relaciona la célula con lo que le rodea.

Se han desarrollado numerosas técnicas físicas para el estudio de propiedades mecánicas de células animales y vegetales, siendo el Microscopio de Fuerzas Atómicas (AFM) una de las más utilizadas por su versatilidad.

En esta tesis, se ha empleado el AFM para estudiar las propiedades mecánicas de células humanas en cultivo en base a dos parámetros de sus propiedades: el módulo de elasticidad aparente,  $E_0$ , y el exponente  $\beta$ , relacionado con las propiedades viscoelásticas. Con estas dos medidas se puede realizar un fenotipado mecánico de células individuales que puede



---

incluso ser usado como ensayo de efectos de fármacos.

Usando esta metodología, se han estudiado las líneas celulares de cáncer de mama MCF10-A (línea sana), MCF-7 (línea tumoral no metastática) y MDA-MB-231 (línea tumoral invasiva), logrando un fenotipado mecánico de las tres líneas.

Cuando una célula se vuelve tumoral, sufre cambios y reprogramaciones tanto en su metabolismo como en su cortex de actina. Para estudiar el papel del metabolismo y del citoesqueleto en la contribución a las propiedades mecánicas de estas líneas celulares hemos aplicado tres tratamientos a las células. En primer lugar, hemos desorganizado los filamentos de actina usando citocalasina D, en segundo lugar, hemos inhibido los motores moleculares de miosina-II con blebistatina y, finalmente, hemos impedido el correcto funcionamiento del metabolismo celular agotando el ATP disponible en el medio. Con esto hemos descubierto cómo las distintas células establecen sus características físicas de diferente manera según su malignidad y en función de su metabolismo.

Las células de mama sanas basan sus propiedades mecánicas en la polimerización de fibras de actina, gastando ATP. Las células metastáticas utilizan la actividad de los motores moleculares de miosina-II para mantener su rigidez y las células tumorales no invasivas muestran unas alteraciones metabólicas que les permiten mantener sus propiedades mecánicas intactas, incluso en ausencia casi total de energía en forma de ATP.

También hemos empleado esta técnica de AFM con tres líneas de cáncer de pulmón de células no pequeñas, o no microcíticos, (NSCLC). En las líneas celulares A549 y NCI-H226, las propiedades mecánicas de células



---

individuales son similares, mientras que son muy diferentes a las de la línea celular NCI-H23. Estas tres líneas muestran diferentes mutaciones conductoras (o *driver*), que son aquellas que le confieren a la célula una ventaja selectiva en su crecimiento. Entre éstas, las hay que afectan a dos conocidos genes relacionados con el cáncer: el oncogén *KRAS* y el gen supresor de tumores *TP53*. NCI-H226 es wild-type para ambos, NCI-H23 muestra mutaciones en ambos, y A549 tiene mutado *KRAS*.

Para saber si las alteraciones en estos dos genes afectan a las propiedades mecánicas de estas líneas celulares, hemos mutado *KRAS* con una sustitución G12V y hemos eliminado *TP53* en líneas celulares salvajes para ambos. Así, cada línea actúa como control de sí misma.

Los resultados de AFM muestran que *TP53* sí afecta a las propiedades mecánicas de las células investigadas, mientras que la mutación G12V en *KRAS* no lo hace. Así, se muestra que hay una conexión directa entre algunas alteraciones en rutas moleculares y las propiedades mecánicas de las células.



A grayscale microscopic image showing a dense field of cells. The cells are irregular in shape, with some appearing as small, rounded clusters and others as larger, more elongated structures. The background is a textured, light gray. A dark, circular spot is visible in the upper right quadrant. A green-bordered white box with the word 'Abstract' is overlaid on the bottom left of the image.

## Abstract

In recent years, the study of the mechanical properties of cells has become a promising scientific field. Given that the cell is the basic anatomical unit of living beings, which is capable of regrouping into tissues and which finally organize themselves into organs, the study of a cell's physical characteristics seems to be key for understanding its biology and how the cell relates to its surroundings.

Numerous physical techniques have been developed to study the physical properties of animal and plant cells, being the Atomic Force Microscope (AFM) one of the most commonly used due to its versatility. In this thesis, AFM has been used to study the mechanical properties of human cells in culture based on two parameters of their properties: the apparent elastic modulus,  $E_0$ , and the exponent  $\beta$ , related to its viscoelastic properties. With these two quantities, a mechanical phenotyping of individual cells can be performed, which can even be used as a drug effects assay.

---

Using this methodology, breast cancer cell lines MCF10-A (healthy line), MCF-7 (non-metastatic tumor line), and MDA-MB-231 (invasive tumor line) have been studied, achieving a mechanical phenotyping of the three lines.

When a cell becomes tumoral, it undergoes changes and reprogramming in both its metabolism and actin cortex. To study the role of metabolism and the cytoskeleton contribution to the mechanical properties of these cell lines, we have applied three treatments to the cells. Firstly, we have disorganized actin filaments using cytochalasin D, secondly, we have inhibited the molecular motors of myosin-II with blebbistatin, and finally we have prevented the proper functioning of cellular metabolism by depleting the available ATP in the medium. This has revealed how different cells establish their physical characteristics differently depending on their malignancy and according to their metabolism.

Healthy cells base their mechanical properties on the polymerization of actin fibers, consuming ATP. Metastatic cells use the activity of myosin-II molecular motors to maintain their rigidity, and non-invasive tumor cells show metabolic alterations that allow them to maintain their mechanical properties intact, even in the total absence of ATP.

We have also used this AFM technique with three lines of non-small cell lung cancer (NSCLC). In the cell lines A549 and NCI-H226, the mechanical properties of individual cells are similar, while they are very different from those of the cell line NCI-H23. These three lines show different driver mutations, which confer a selective growth advantage to the cell. Among these, there are those that affect two well-known cancer-related genes:

---

the oncogene *KRAS* and the tumor suppressor gene *TP53*. NCI-H226 is wild-type for both, NCI-H23 shows mutations in both, and A549 has mutated *KRAS*.

To determine whether alterations in these two genes affect the mechanical properties of these cell lines, we mutated *KRAS* with a G12V substitution and eliminated *TP53* in wild-type cell lines for both. Thus, each line acts as a control for itself.

Our results show that *TP53* does in fact affect the mechanical properties of the investigated cells, but *KRAS* G12V mutation does not have any impact on these properties. Thus, it is shown that there is a direct connection between alterations in some molecular routes and mechanical properties in single cells.

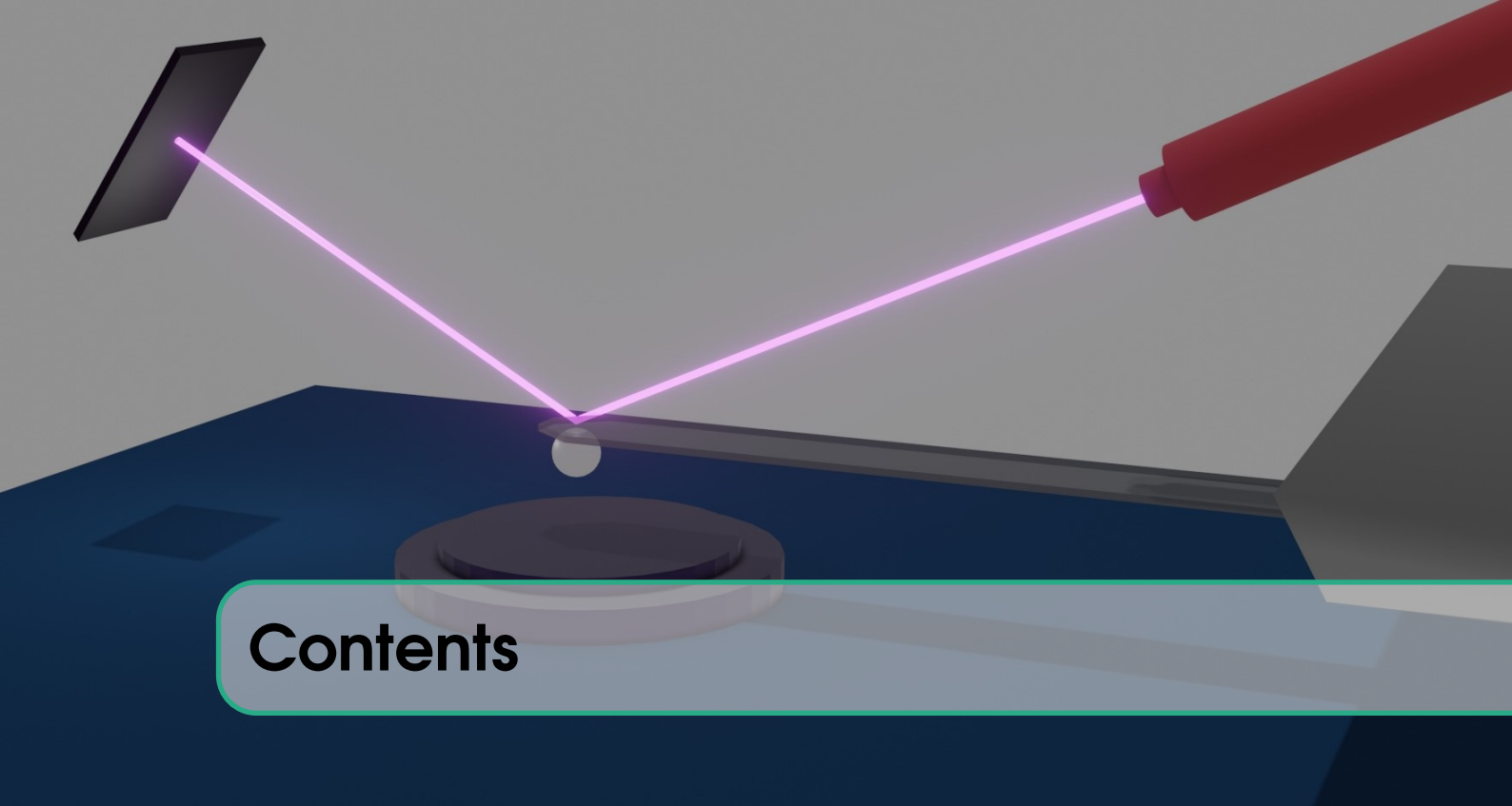


## List of abbreviations

- ADP - Adenosine Diphosphate
- AFM - Atomic Force Microscope
- ATP - Adenosine Triphosphate
- BSA - Bovine Serum Albumin
- CRISPR - Clustered Regularly Interspaced Short Palindromic Repeats
- DAPI - 2-(4-amidinophenyl)-1*H*-indole-6-carboxamide
- DHM - Digital Holographic Microscopy
- DMEM - Dulbecco's Modified Eagle's Medium
- DMSO - Dimethyl Sulfoxide
- EDTA - Ethylenediaminetetraacetic Acid
- FBS - Fetal Bovine Serum
- HEPES - (4-(2-hydroxyethyl)-1-piperazineethanesulfonic acid)
- PBS - Phosphate Buffer Saline
- PLR - Power Law Rheology

- RIPA - Radio-Immunoprecipitation Assay
- RPMI - Roswell Park Memorial Institute medium
- SDS - Sodium Dodecyl Sulfate
- SDS-PAGE - Sodium Dodecyl Sulfate Polyacrylamide Gel Electrophoresis
- SPM - Scanning Probe Microscopes
- STM - Scanning Tunnelling Microscopy
- TBS - Tris-Buffered Saline
- WT - Wild-type





# Contents

Resumen .....	1
Abstract .....	5
List of abbreviations .....	9
List of figures .....	16
List of tables .....	17

## I Introduction

1 Thesis motivation .....	21
1.1 Motivation	21
1.2 Objectives	22

<b>2</b>	<b>Cell mechanics and cancer</b> .....	<b>25</b>
2.1	Introduction	25
2.2	Cell cytoskeleton and actin cortex	26
2.3	Mechanical properties of cells and cancer	30
2.4	Cell metabolism and cancer	35
2.5	Cancer and genetics	37
	Bibliography	39
<b>3</b>	<b>Atomic Force Microscopy</b> .....	<b>43</b>
3.1	Introduction	43
3.2	Principle of operation	44
3.3	Force spectroscopy	47
3.4	Cell mechanics characterization	48
	Bibliography	51
<b>4</b>	<b>Materials and Methods</b> .....	<b>53</b>
4.1	Cell culture	53
4.2	Immunocytochemistry	55
4.3	<i>Wound healing</i> assay	56
4.4	Knock-out of <i>TP53</i> and mutation of <i>KRAS</i> in lung cells	56
4.5	Western blot analysis	57
4.6	AFM experiments	59
	Bibliography	60

**II****Breast cancer cells**

<b>5</b>	<b>Mechanical properties of breast cancer cells obtained by AFM</b> .....	<b>65</b>
5.1	Introduction	65
5.2	AFM results	69
5.3	Immunocytochemistry imaging	71
5.4	Wound healing assay of breast cancer cells	72
5.5	Conclusions	75
	Bibliography	76
<b>6</b>	<b>Effects of energy metabolism on the mechanical properties of breast cells</b> .....	<b>81</b>
6.1	Introduction	81
6.2	Breast cancer cells metabolism	82
6.3	ATP depletion and effect of drugs directed to the cytoskeleton	83
6.4	Immunocytochemistry imaging	87
6.5	Contribution of active processes to cell elasticity	89
6.6	Conclusions	92
	Bibliography	93

**III****Lung cancer cells**

<b>7</b>	<b>Lung cancer cells</b> .....	<b>99</b>
7.1	Introduction	99
7.1.1	<i>KRAS</i> mutations .....	99
7.1.2	Tumor suppressor <i>TP53</i> .....	101
7.2	Mechanical properties of lung cancer cell lines	104

<b>7.3</b>	<b>Effects of KRAS-G12V mutation and p53 knock-out</b>	<b>107</b>
7.3.1	NCI-H226 cell line .....	108
7.3.2	A549 cell line .....	111
<b>7.4</b>	<b>Conclusions</b>	<b>114</b>
	<b>Bibliography</b>	<b>115</b>

## IV

## Conclusiones/Conclusions

<b>Conclusiones</b> .....	<b>121</b>
<b>Conclusions</b> .....	<b>125</b>
<b>List of publications</b> .....	<b>127</b>

## List of Figures

2.1	Cytoskeleton in animal cells	27
2.2	Actin polymerization	28
2.3	Actin-binding proteins.	29
2.4	Cancer statistics in 2020	31
2.5	Cancer statistics in 2020 according to gender.	32
2.6	Microrheology techniques	34
2.7	Warburg effect in cancer cells	36
3.1	AFM setup	45
3.2	Force-distance curves on glass and cells.	48
3.3	Method used to obtain the PLR parameters of cells	49
4.1	Transfection of p53 and KRAS mutated in lung cells	57
5.1	Optical microscopy images of breast cancer cell culture	66
5.2	Experimental setup of the AFM	70
5.3	PLR parameters of breast cancer cells	71
5.4	Immunofluorescence imaging of F-actin organization	72
5.5	Wound healing assay in breast cancer cells	74

6.1	Sketch of breast cell lines metabolism	82
6.2	Effects of treatments in breast cancer cells.	85
6.3	PLR parameters in breast cancer cells	86
6.4	Confocal fluorescence imaging of immunocytochemistry of F-actin.	88
6.5	Proposal model of PLR response of breast cancer cells	89
7.1	KRAS activation and signalling cascade	100
7.2	TP53 pathway.	102
7.3	TP53 and actin dynamics feedback in the case of DNA damage.	103
7.4	PLR parameters of lung cancer cells	105
7.5	Word clouds of cancer drivers in A549, NCI-H226 and NCI-H23	106
7.6	Western blot of H226 mutated cells.	109
7.7	Immunofluorescence of H226 wild-type and mutated cells.	109
7.8	Effects of p53 knock-out and KRAS G12V mutation in H226 cells.	111
7.9	Western blot of A549 mutated cells.	112
7.10	Immunofluorescence of A549 wild-type and TP53 KO cells.	112
7.11	Effects of p53 knock-out in A549 cells.	113

## List of Tables

4.1	Primary antibodies used for Western Blot assay. . . . .	58
5.1	Summary of selected experiments on stiffness or related parameters of breast cancer cells . . . . .	67
7.1	<i>TP53</i> mutation in NCI-H23. . . . .	107
7.2	<i>KRAS</i> mutations in A549 and NCI-H23. . . . .	108
7.3	Summary of mutations performed in lung cell lines. . . . .	108







# Introduction

<b>1</b>	<b>Thesis motivation .....</b>	<b>21</b>
1.1	Motivation	
1.2	Objectives	
<b>2</b>	<b>Cell mechanics and cancer ....</b>	<b>25</b>
2.1	Introduction	
2.2	Cell cytoskeleton and actin cortex	
2.3	Mechanical properties of cells and cancer	
2.4	Cell metabolism and cancer	
2.5	Cancer and genetics	
	Bibliography	
<b>3</b>	<b>Atomic Force Microscopy .....</b>	<b>43</b>
3.1	Introduction	
3.2	Principle of operation	
3.3	Force spectroscopy	
3.4	Cell mechanics characterization	
	Bibliography	
<b>4</b>	<b>Materials and Methods .....</b>	<b>53</b>
4.1	Cell culture	
4.2	Immunocytochemistry	
4.3	<i>Wound healing</i> assay	
4.4	Knock-out of <i>TP53</i> and mutation of <i>KRAS</i> in lung cells	
4.5	Western blot analysis	
4.6	AFM experiments	
	Bibliography	



A grayscale microscopic image showing a dense field of cells, likely cancer cells, with various shapes and sizes, some showing prominent nuclei and nucleoli. A dark, curved shape is visible in the lower-left quadrant.

# 1. Thesis motivation

## 1.1 Motivation

Cancer is a complex disease that involves changes in metabolism, genetics and mechanical properties within single cells. These changes cause an uncontrollable division and expansion of cells that eventually provoke organic malfunctioning and can cause death.

Carcinogenesis is a very intricate process which transforms cells from healthy to tumorigenic cells. This mechanism can progress and eventually can lead to malignant cells that cause metastasis. When cancer appears, cells acquire capabilities to overcome cell-cycle checkpoints and proliferate uncontrollably, known as cancer hallmarks [1].

Tumors are complex tissues formed by heterogeneous cancer cell clusters, deriving each from a common altered single cell. These differences among the cells within a tumor promote cancer progression and even metastasis and drug resistance. Thus, if a cancer is identified at its very early, single-cell

stage, its diagnosis and treatment could be implemented much faster with better survival rate and prognosis.

The use of physical techniques such as Atomic Force Microscopy in the field of cellular biology and oncology can help study mechanical properties of healthy and cancer single cells, leading to new physical biomarkers of disease, such as elastic and viscoelastic deformability. This can help us understand how cells become malignant and how their biomechanical properties are influenced by onsets and progression of the diseases.

## 1.2 Objectives

The main objectives in this thesis are to:

- Use AFM as a tool for phenotyping cancer cells according to their mechanical properties.
- Investigate the role of cytoskeleton in these mechanical properties in different cell lines.
- Link cell metabolism with the establishment and maintenance of cell stiffness.
- Find if there is any connection between alterations in molecular pathways regulation with mechanical properties in cancer cells.

Following these objectives, this thesis has been divided into three main parts. First, the introduction tries to set up all the theoretical basis used during this thesis. Chapter 2 collects information about cell biology and mechanical properties in healthy and cancer cells. Chapter 3 introduces the AFM methodology and the cell mechanics characterization performed

in this thesis. Finally, Chapter 4 refers to the methodology to extract the rheology parameters from cells, which are physical biomarkers for malignity.

The second part of this thesis studies breast cancer cells mechanics for different cell lines. Chapter 5 is an overview of the mechanical properties of the three main models of cell lines used to study different malignancy degrees of breast cancer cells. Chapter 6 takes a deeper approach to the biological origin for the differences observed in the mechanical properties among the three lines studied, treating them with cytoskeleton drugs and depleting the energy in the cells.

The third part is dedicated to lung cancer cells. In Chapter 7, three non-small lung cancer cell lines are tested by AFM. As they show different mutations in cancer drivers *TP53* and *KRAS*, we perform knock-out of the first one and a G12V mutation in the second one in the wild-type cell lines to observe if changes in these genes cause alterations in their mechanical properties.

At the end of this thesis there is a Conclusion which compiles the main results and includes conclusions from the previous chapters.



A blue-tinted microscopic image showing several spherical cells with textured surfaces. One cell in the center is smaller and has a spiky, star-like structure. The background is filled with faint, out-of-focus images of other cells and structures.

## 2. Cell mechanics and cancer

### 2.1 Introduction

The term *biophysics* was first introduced by Karl Pearson in 1982 as a science that could link Physics and Biology [2]. At that moment, he was aware that probably this "new" field would become important in an immediate future.

In this way, Biophysics is an interdisciplinary branch of science that tries to describe and analyze a biological phenomenon from different points of view, connecting biomolecular reactions with physical laws. The focus of biophysical studies comprises a lot of subjects such as gene regulation, cell biology, biomolecular structure of proteins, neuroscience, physiology and so on.

Cells are the basic structural units of all living beings. They are delimited from the outside by a cellular membrane, which is permeable to certain substances and plays a fundamental role in communication and cell signaling.



Inside this membrane there is the cytoplasm, the nucleus and various organelles which play a role in all the cellular activities.

Multicellular organisms as ourselves are organized in differentiated tissues that perform very specific tasks in our bodies. Also, our cells are subjected to a variety of stimuli to react to, such as mechanical forces generated by neighboring cells, fluid flow, gravity, and so on. In order to maintain their shape and functionality, cells must be at some level viscoelastic to face those changes. This means that they need to preserve their mechanical characteristics which are directly related to their health and functioning.

Recently, the interest in the study of mechanical properties of cells has greatly increased in the cell biology and biophysics fields. As we are going to see in this chapter, mechanical properties of cells are potential physical biomarkers for illnesses and malfunctioning. The knowledge of these physical properties can shed light on other cellular processes and reactions, as these are closely connected.

## **2.2 Cell cytoskeleton and actin cortex**

The cytoskeleton is the cell organelle responsible for the mechanical maintenance and shape of the cell. It also plays an important role in communication with adjacent cells and with the extracellular matrix. In eukaryote cells, it is a three-dimensional protein scaffold formed by actin filaments, microtubules and intermediate filaments (Figure 2.1). It is a highly dynamic and adaptable structure able to change in response to variations in the cell environment [3]. In cells, the cytoskeleton is the main responsible element that respond



to loading forces, acting as a polymer network far from thermal equilibrium [4].

Actin is the most abundant protein in eukaryotic cells, accounting for 5-10% of cell protein content, reaching up to 20% of the protein content in muscle cells. It is distributed heterogeneously through the cell and it can be found in the cytoplasm in a free monomer form (G-actin) or in a filamentous conformation (F-actin).

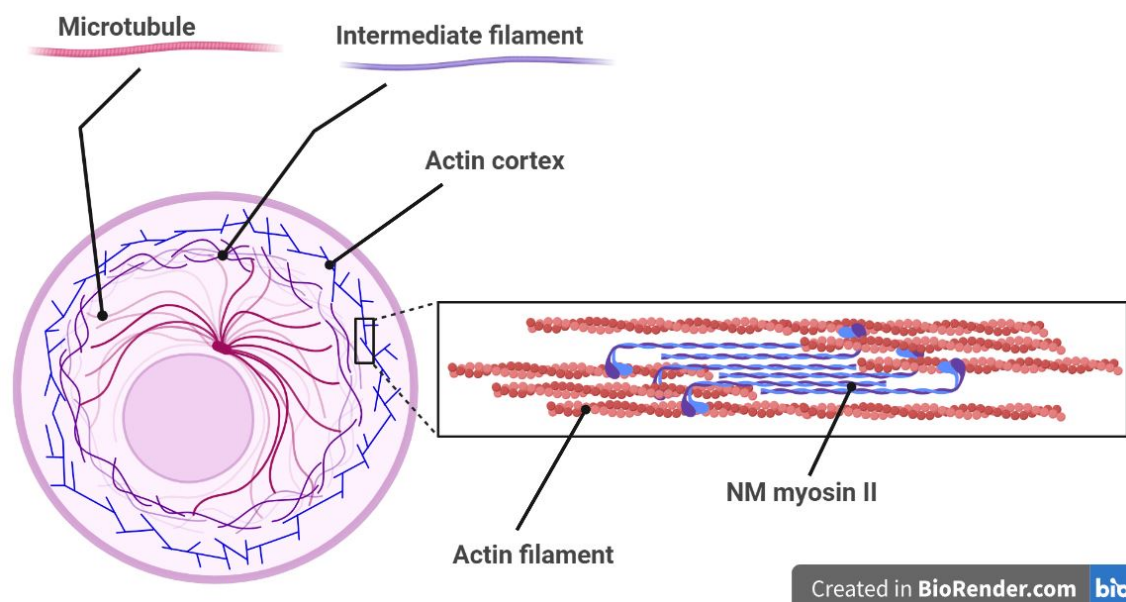


Figure 2.1: **Scheme of the cytoskeleton in animal cells.** Inset of the actin cortex, formed by actin filaments crosslinked by non-muscle (NM) myosin II.

G-actin monomers undergo polymerization and form two chains that roll up in a helical thread. This filament has polarity. The plus end is called the barbed end, its monomers are bound to ATP and it indicates the growing end of an actin filament. The minus end is called the pointed end and its monomers are bound to ADP. This indicates the shrinking end of the filament [5].

Actin polymerization is reversible, so actin filaments are continuously

growing and shrinking. In vitro, actin polymerization shows three different phases (see Figure 2.2): first, a lag phase when no filaments are visible, followed by a phase of rapid filament elongation. Finally, there is an equilibrium state where the actin monomers' incorporation rate and the dissociation of monomers' rate are the same. While this is happening, the polymer maintains a stable length. This is known as treadmilling and the G-actin concentration in the medium is known as critical concentration.

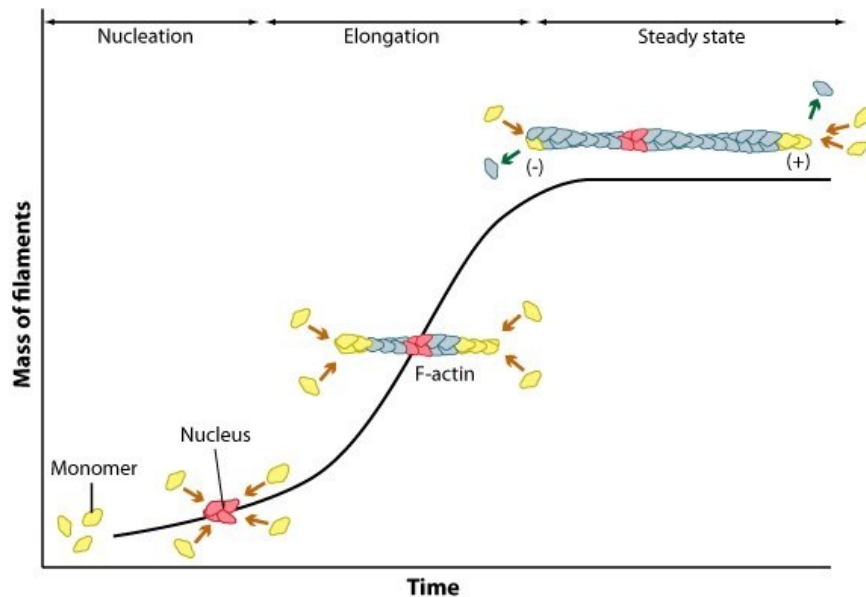


Figure 2.2: **Actin fibers polymerization.** Nucleation, elongation, and steady state phase of actin filament assembly. From MBInfo, Mechanobiology Institute, National University of Singapore.

In the cytosol, what determines the growth or shrinkage of the filament is the available monomer concentration around the ends of the filaments. If cytosolic G-actin concentration in both barbed and pointed ends is higher than the critical concentration, the filament will grow. If cytosolic G-actin concentration in both barbed and pointed ends is less than the critical concentration, there will be depolymerization of the filament. Cells tend to

maintain a sufficiently high enough globular actin concentration to maintain a certain length of the polymers [6].

Actin filaments are regulated by a huge number of actin-binding proteins that help maintenance, polymerization and depolymerization of the filaments [7]. They regulate filament branching, actin polymerization, depolymerization and even 3D organization in the cell. Actin-binding proteins and its function are depicted in Figure 2.3.

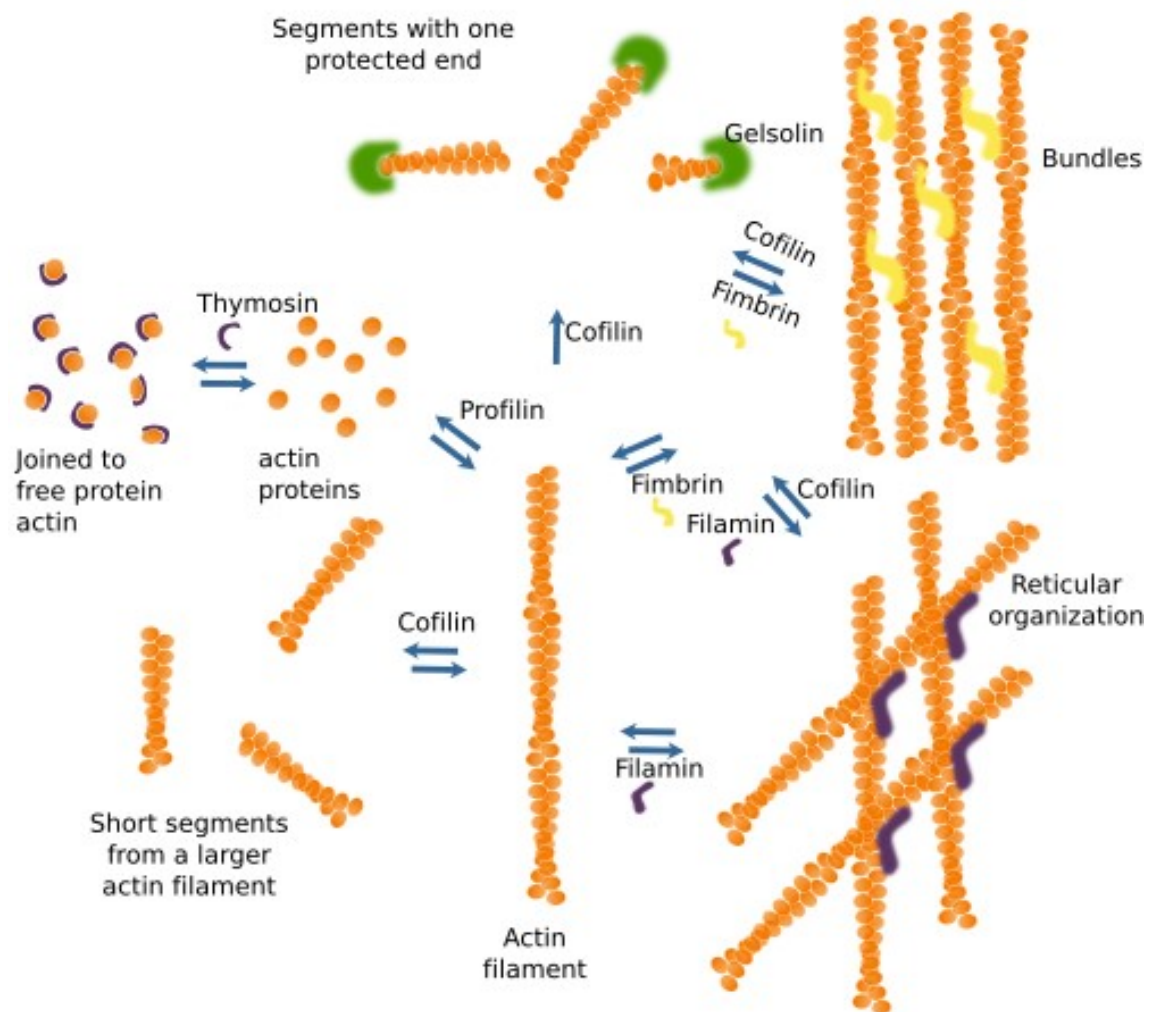


Figure 2.3: **Actin-binding proteins and their functions.** From [5].

Actin filaments form the cell cortex, which is located underneath the cell membrane (Figure 2.1, inset). It is a dense network in charge of cell shape

and movement of the cell surface, being the main determinant of cellular mechanics [8, 9, 10]. In mammal cells, this cortex is compounded not only by F-actin, but also by myosin motors and actin-binding proteins.

Non-muscle (NM) myosin II motors create contractile stress by pulling the actin filaments from each other. The energy needed for producing this tension is provided by hydrolysis of ATP, which takes place in the ATPase domain of the NM myosin II molecule [11]. As myosin motors are crucial elements of the cell cortex, it is also referred to as actomyosin cortex.

Actin-myosin network can form stress fibers that are involved in cell elasticity and stiffness [12]. These stress fibers can exert forces that provoke contraction, migration or cytoskeletal reorganization of the cell, and can tolerate compression [13].

Cells are subjected to forces and tension, generated locally by cell-cell or cell-extracellular matrix interactions. It is known that these forces are crucial in stem cell differentiation, tissue development and homeostasis. Cells have response mechanisms to mechanical stimuli and are able to alter their behavior and modify their environment, such as altering their extracellular matrix [14].

### 2.3 Mechanical properties of cells and cancer

According to the World Health Organization (WHO), cancer is *the rapid creation of abnormal cells that grow beyond their usual boundaries, and which can then invade adjoining parts of the body and spread to other organs.*

Living cells exist far from equilibrium. They are continuously subjected

to external and internal physical forces that they need to react to. This means that there are many active processes that may alter their mechanical properties and their normality [15, 16]. These alterations in the biochemical routes are joined by changes in cellular mechanics through cancer progression.

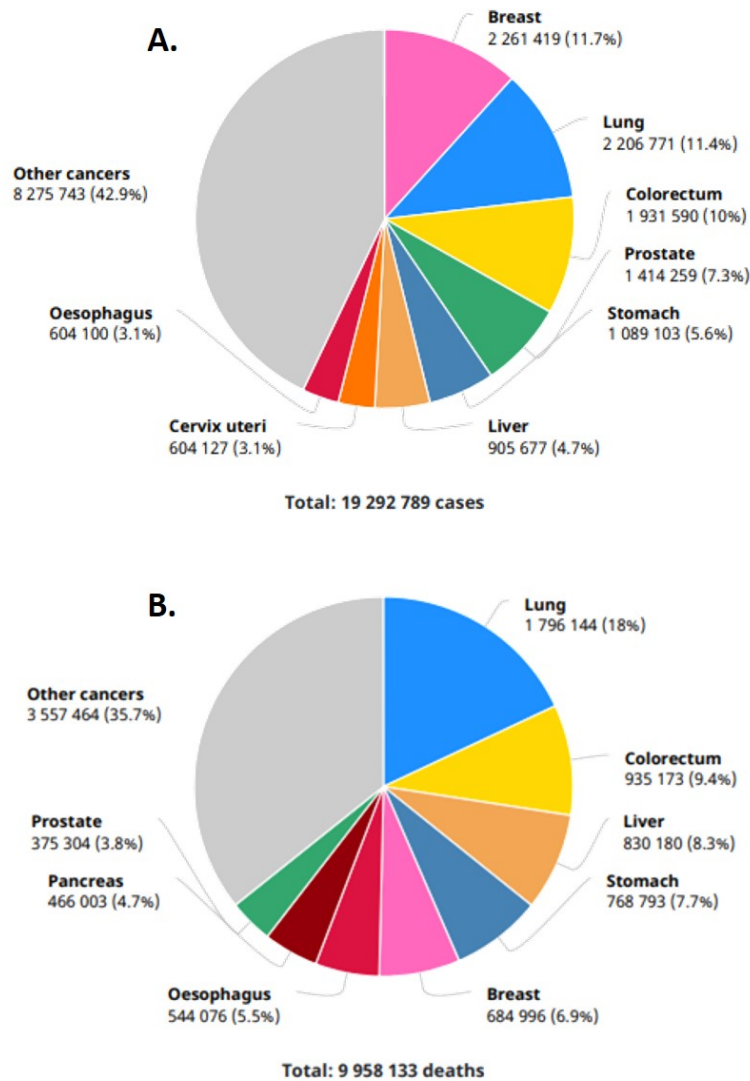


Figure 2.4: **Cancer statistics in 2020.** **A.** Number of new cancer types in 2020 for both sexes and all ages. **B.** Number of deaths by cancer types in 2020 for both sexes and all ages. From The Global Cancer Observatory, December 2020.

About 19.3 million new cancer cases were diagnosed and around 9 million deaths by cancer were reported in 2020 worldwide (Figure 2.4).

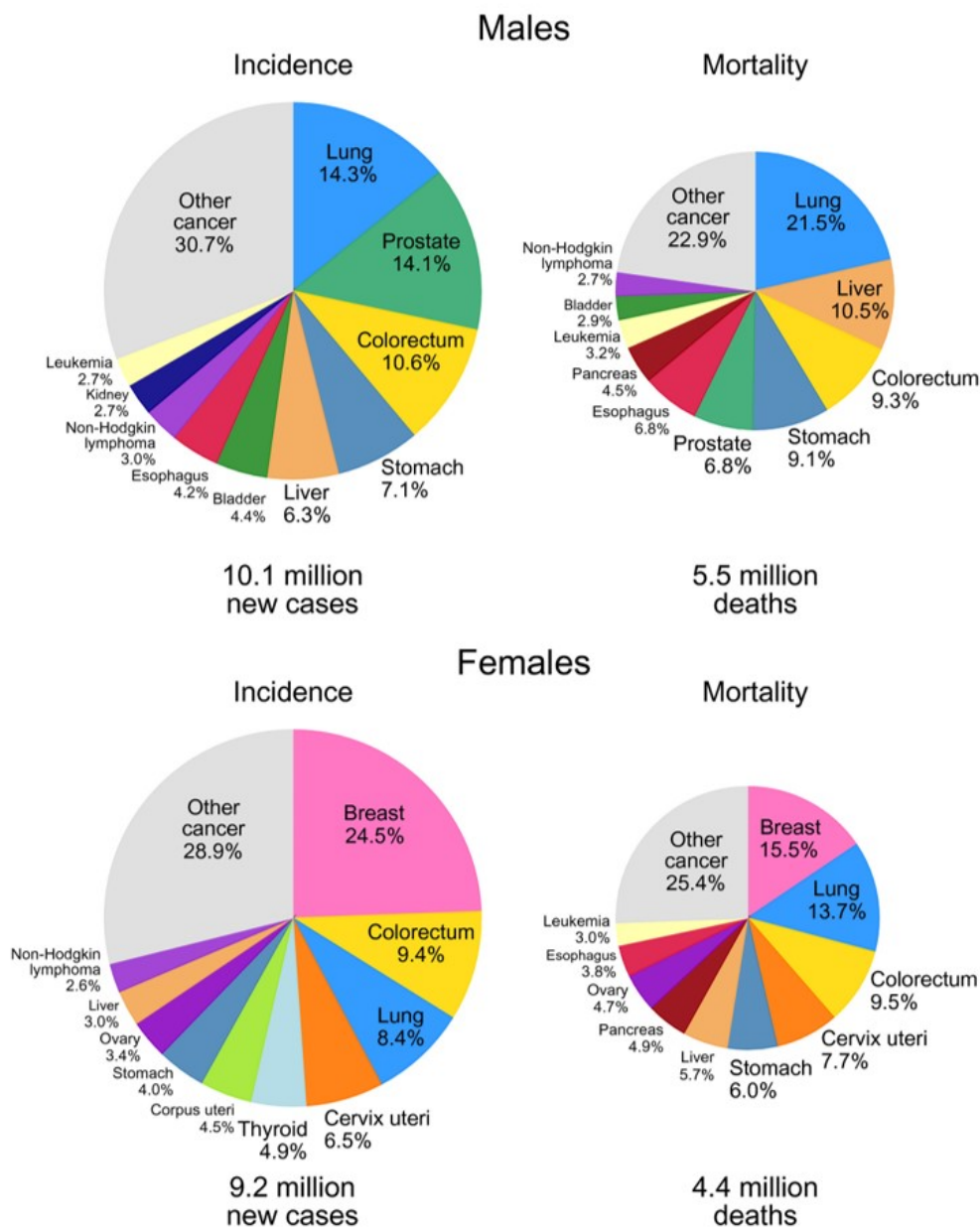


Figure 2.5: **Cancer statistics in 2020 according to gender. Top.** Number of new cancer types in 2020 in males. **Bottom.** Number of new cancer types in 2020 in females. From The Global Cancer Observatory, December 2020.

Lung and breast cancers are the two most diagnosed cancers in 2020, the first one being the most common cause of cancer death in 2020 [17] (Figure 2.4). Lung cancer was the most frequent cancer in men, also leading the mortality rate in this group, while the incidence and mortality rate of breast cancer is higher in women (Figure 2.5).

Cancer has been considered as a "mechanical disease". Biochemical alterations can shift mechanical properties and vice versa. For this, biophysics has emerged as a powerful field that could provide promising diagnosis and treatment tools, even at a single-cell scale [18].

Rheology is the science for measuring deformation in materials, to study how they react to an applied force. There are many techniques available, each with its own advantages and inconveniences. Cells are so small and have an extremely low stiffness that those deformations and forces applied need to be in the range of nanometers and nano-Newtons, respectively. For this, new adapted technologies have emerged, such as optical or magnetic tweezers, microplates, atomic force microscopy... [19, 20]. Some examples of these techniques are represented in Figure 2.6.

The basis of rheology are that simple fluids like water have an insignificant elasticity and dissipate energy through viscous flow, while simple solids are characterized by an elastic modulus and can not flow. There are many materials that do not behave as a simple fluid or solid, but exhibit both viscous and elastic characteristics [21]. In this case, they store and dissipate energy simultaneously when deformed, property which is called viscoelasticity.

The mesh size of actin cortex fluctuates between 20 to 250 nm, which is a small magnitude when compared to the whole cell extension. Nevertheless, cell mechanics are greatly determined by the characteristics of this structure [8].



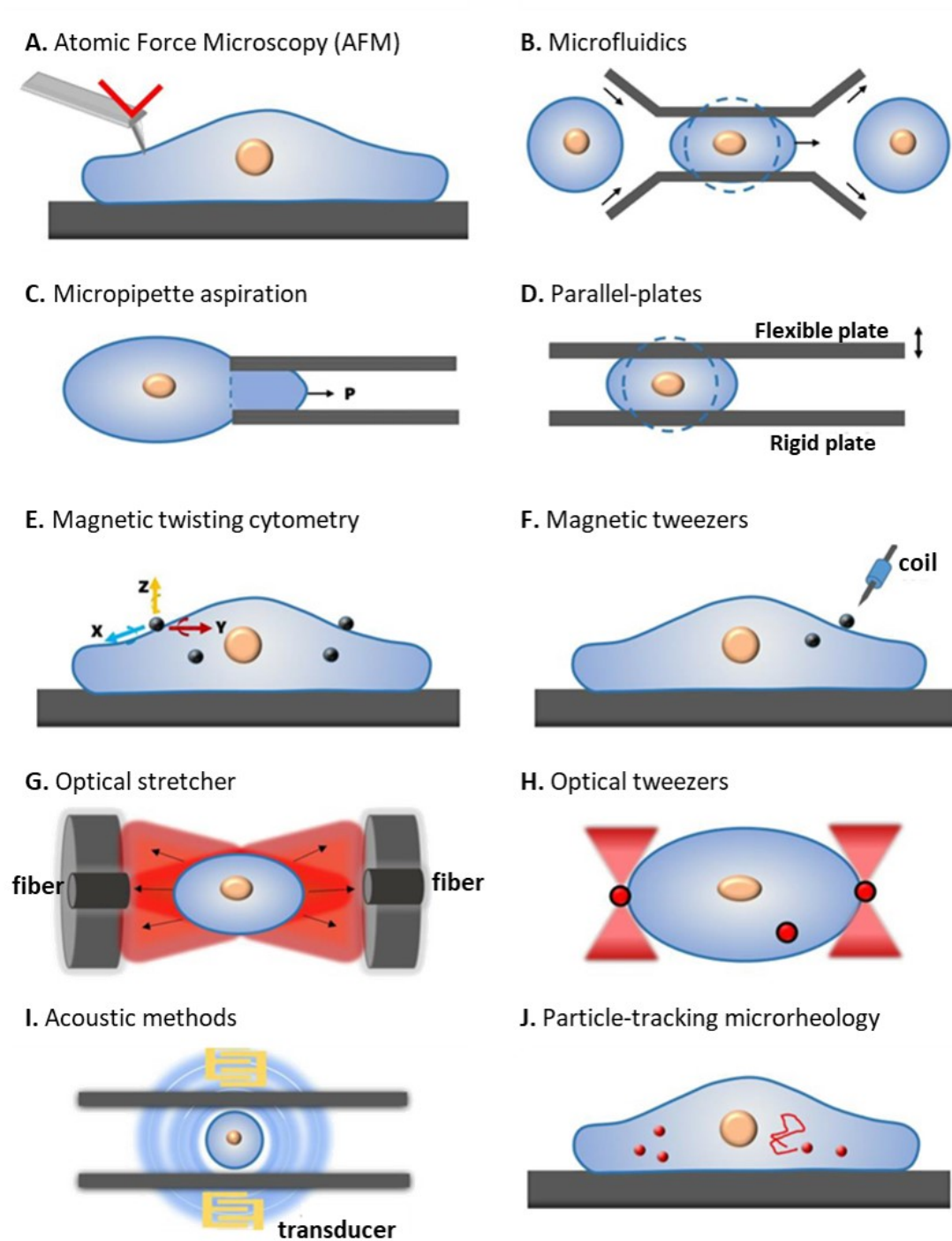


Figure 2.6: **Schematic illustration of different methods used for measuring single-cell mechanical properties.** Optical stretcher, optical tweezers and acoustic methods are non-contact techniques, while the rest of technologies depicted need contact measurement modes. From [20].



In cancer cells, a remodeling of the actin cortex network has been observed and it has been suggested that this change in conformation may be related to a change in rigidity and stiffness of cancerous cells. The great majority of mechanobiological studies agree with the fact that normal cells are stiffer than cancer cells in several tissues and that different degrees of malignancy exhibit different stiffness [15].

## 2.4 Cell metabolism and cancer

Cancer cells not only seem to be softer than healthy ones. There are other hallmarks that cancer cells acquire to become tumoral [1]. One of them is the deregulation of cellular energetics. This means that the cell can modified its metabolism to prioritize mechanisms such as invasion or proliferation.

Carbohydrates, proteins and lipids are oxidized by cells to obtain free energy, which is then stored in molecules with high-energy bonds that can be used when cells need it. The main molecule used for this purpose is adenosine triphosphate (ATP), known as "molecular unit of currency" which provides energy to carry on most of cell processes such as division, proliferation, migration and growth [22].

The main source of ATP in healthy cells is oxidizing glucose. This consists of three catabolic processes: glycolysis, tricarboxylic acid cycle (TCA or Krebs cycle) and oxidative phosphorylation. In glycolysis, one molecule of glucose is converted into two molecules of pyruvate. This pyruvate, in aerobic conditions, will be further oxidized in the mitochondria in the Krebs cycle, which produces carbon dioxide and energetic electron donors (NADH and FADH). These molecules, in presence of O<sub>2</sub>, are used by

the mitochondria to produce ATP by oxidative phosphorylation (OSPHOX). Up to 36 mols of ATPs per mol of processed glucose are obtained by this pathway.

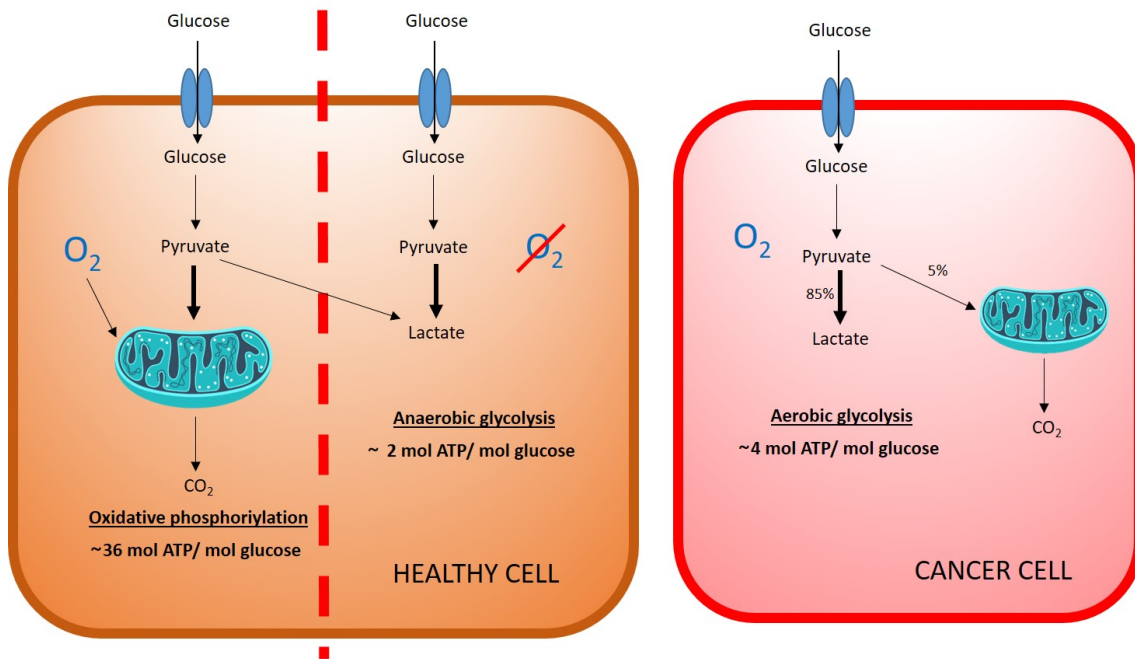


Figure 2.7: **Warburg effect in cancer cells.** Healthy cells obtain up to 36 mol of ATP per mol of glucose via oxidative phosphorylation in presence of oxygen, and 2 mol of ATP via anaerobic glycolysis when there is no oxygen. Cancer cells perform aerobic glycolysis, with an output of 4 mol of ATP per mol of glucose even in oxygen presence [23].

In anaerobic conditions, pyruvate produced by glycolysis is accumulated and converted to lactate by lactic acid fermentation. This takes place in the cytosol, not the mitochondria, with an efficiency of two mols of ATP per mol of processed glucose. This mechanism also transforms nutrients into biomass (lipids, nucleotides or amino acids) faster and more efficiently [23]. If there is oxygen available and aerobic metabolism is taking place in the mitochondria but pyruvate is building up faster than it is metabolized, then fermentation will take place.

Cancerous cells demand higher levels of energy because of their anomalous

energy metabolism. In the 1920s, Otto Warburg discovered that cancer cells preferred to metabolize glucose via glycolysis in the presence of oxygen instead via oxidative phosphorylation, which is a much more efficient way for ATP production [24]. The process is schemed in Figure 2.7. It is also suggested that cancer cells use this pathway because the intake of nutrients generates biomass needed to generate new cells.

This aerobic glycolysis is accepted as a hallmark of cancer, but its relationship with cancer progression remains unclear [25].

## 2.5 Cancer and genetics

As suggested before, biochemical alterations can shift mechanical properties and the other way around in cells. Cancer is also a genetic disease in which alterations in the DNA of cells causes neoplasms that become cancers.

Mutations are permanent changes in the DNA sequence of an organism. They can be caused by mistakes during DNA replication, by virus infections or by exposure to mutagens agents or radiation. This change in the DNA can lead to the wrong amino acid incorporation to a protein chain, resulting in a different amino acid codon which the ribosome recognizes and which is called a missense mutation. Missense mutations can make no difference at all to the protein function, can cause the protein to be less active in doing its job, or even can make the protein more effective.

If a mutation takes place in a sperm or egg cell (germ cells), it passes directly from a parent to a child at the time of conception. Therefore, it is hereditary. Cancer caused by germline mutations accounts for about 5% to 20% of all cancers (American Cancer Society<sup>®</sup>). On the other hand, the

most common cause of cancer is acquired mutations which take place in a particular cell during an organism's life. These somatic cells are not passed on to descendants, so they are not hereditary.

Most genetic changes in cancers can be divided in two origins: mutations in proto-oncogenes that activate and stimulate cell division and growth, or loss-of-function mutations in tumor suppressor genes that in normal conditions promote DNA repair and provides cell cycle checkpoints to guarantee normal cell proliferation [26].

Some of these mutations are recurrent and frequent for specific tissues. For example, germ line mutations in genes *BRCA1* or *BRCA2* increases risk of breast and ovarian cancers in women [27], and acquired mutations in *TP53* are found in more than 50% of cancers. All *BRCA1*, *BRCA2* and *TP53* are tumor suppressor genes.

In conclusion, cancer is a multifactorial disease which includes genetic, environmental factors, and lifestyle. The more we know about cancer, the better management of the disease we will have concerning prevention, diagnosis and treatment.

# Bibliography

- [1] Douglas Hanahan and Robert A Weinberg. “Hallmarks of cancer: the next generation”. In: *cell* 144.5 (2011), pages 646–674.
- [2] Karl Pearson. “The Grammar of Science. 2nd”. In: *London: Black* (1900).
- [3] Bruce Alberts et al. *Essential cell biology*. Garland Science, 2013.
- [4] Adrian F Pegoraro, Paul Janmey, and David A Weitz. “Mechanical properties of the cytoskeleton and cells”. In: *Cold Spring Harbor perspectives in biology* 9.11 (2017), a022038.
- [5] Thomas D Pollard. “Actin and actin-binding proteins”. In: *Cold Spring Harbor perspectives in biology* 8.8 (2016).
- [6] CG Dos Remedios et al. “Actin binding proteins: regulation of cytoskeletal microfilaments”. In: *Physiological reviews* 83.2 (2003), pages 433–473.
- [7] Thomas D Pollard et al. *Cell biology E-book*. Elsevier Health Sciences, 2016.
- [8] Guillaume Salbreux, Guillaume Charras, and Ewa Paluch. “Actin cortex mechanics and cellular morphogenesis”. In: *Trends in cell biology* 22.10 (2012), pages 536–545.
- [9] Marco Fritzsche et al. “Actin kinetics shapes cortical network structure and mechanics”. In: *Science advances* 2.4 (2016), e1501337.

- 
- [10] Martin P Stewart et al. “Hydrostatic pressure and the actomyosin cortex drive mitotic cell rounding”. In: *Nature* 469.7329 (2011), pages 226–230.
- [11] Miguel Vicente-Manzanares et al. “Non-muscle myosin II takes centre stage in cell adhesion and migration”. In: *Nature reviews Molecular cell biology* 10.11 (2009), pages 778–790.
- [12] Sari Tojkander, Gergana Gateva, and Pekka Lappalainen. “Actin stress fibers—assembly, dynamics and biological roles”. In: *Journal of cell science* 125.8 (2012), pages 1855–1864.
- [13] D Stamenović and Donald E Ingber. “Models of cytoskeletal mechanics of adherent cells”. In: *Biomechanics and modeling in mechanobiology* 1.1 (2002), pages 95–108.
- [14] Darci T Butcher, Tamara Alliston, and Valerie M Weaver. “A tense situation: forcing tumour progression”. In: *Nature Reviews Cancer* 9.2 (2009), pages 108–122.
- [15] Charlotte Alibert, Bruno Goud, and Jean-Baptiste Manneville. “Are cancer cells really softer than normal cells?” In: *Biology of the Cell* 109.5 (2017), pages 167–189.
- [16] Subra Suresh. “Biomechanics and biophysics of cancer cells”. In: *Acta Materialia* 55.12 (2007), pages 3989–4014.
- [17] Hyuna Sung et al. “Global cancer statistics 2020: GLOBOCAN estimates of incidence and mortality worldwide for 36 cancers in 185 countries”. In: *CA: a cancer journal for clinicians* 71.3 (2021), pages 209–249.
- [18] Mauro Ferrari. “Infernal mechanism”. In: *Mechanical Engineering* 132.03 (2010), pages 24–28.
- [19] Wei Liu and Chi Wu. “Rheological study of soft matters: A review of microrheology and microrheometers”. In: *Macromolecular Chemistry and Physics* 219.3 (2018), page 1700307.
- [20] Yansheng Hao et al. “Mechanical properties of single cells: Measurement methods and applications”. In: *Biotechnology Advances* 45 (2020), page 107648.
- [21] Ronald G Larson. *The structure and rheology of complex fluids*. Volume 150. Oxford university press New York, 1999.
- [22] Massimo Bonora et al. “ATP synthesis and storage”. In: *Purinergic signalling* 8.3 (2012), pages 343–357.

- 
- [23] Matthew G Vander Heiden, Lewis C Cantley, and Craig B Thompson. “Understanding the Warburg effect: the metabolic requirements of cell proliferation”. In: *Science* 324.5930 (2009), pages 1029–1033.
- [24] Otto Warburg. “On the origin of cancer cells”. In: *Science* 123.3191 (1956), pages 309–314.
- [25] Natalya N Pavlova and Craig B Thompson. “The emerging hallmarks of cancer metabolism”. In: *Cell metabolism* 23.1 (2016), pages 27–47.
- [26] Eva YHP Lee and William J Muller. “Oncogenes and tumor suppressor genes”. In: *Cold Spring Harbor perspectives in biology* 2.10 (2010), a003236.
- [27] Michael P Lux, Peter A Fasching, and Matthias W Beckmann. “Hereditary breast and ovarian cancer: review and future perspectives”. In: *Journal of molecular medicine* 84.1 (2006), pages 16–28.





A close-up photograph of an Atomic Force Microscope (AFM) probe tip. The tip is a small, orange, conical structure mounted on a black metal base. The background is blurred, showing other parts of the microscope.

## 3. Atomic Force Microscopy

### 3.1 Introduction

The Atomic Force Microscope (AFM) is a device of the known Scanning Probe Microscopes (SPMs), which were developed in the early 1980s with the invention of the Scanning Tunnelling Microscopy (STM) by Gerd Binnig and Heinrich Rohrer. They won the Nobel prize in Physics in 1986, and the same year Binnig, Calvin Quate and Christoph Gerber announced the development of the AFM, the second member of the SPM family [28].

There are three main features of AFM that make it a great tool for studying biological samples: first, it provides a high spatial resolution of the samples. Secondly, it allows precise control of the forces applied to the sample. And finally, its ability to operate in liquids allows biological samples to be embedded in their buffers, for example, cultured cells can be measured in their growth medium.

During the last decades, AFM modes have been developed to adapt to the

intricacy of biological samples. From direct contact with the surface to the multifrequency mode in which the sample is contoured by oscillating the tip at multiple frequencies, there is a methodology for each biological issue [29]. Also, AFM can be adapted to be used along with other techniques such as real-time fluorescence, and it is commercially available by many producers.

AFM can also be used to manipulate biological samples. By applying forces or by functionalization of the tip, specimens can be modified. This makes the AFM a useful utensil to cut, sculpt, or dissect biological samples with a nanometer resolution [30].

### 3.2 Principle of operation

The AFM is not an optical microscope with which the specimen is directly looked at. It generates images or information by "touching" the surface with a tip placed on the edge of a microcantilever. This cantilever is flexible and acts as a spring, measuring the force between tip and surface. These local forces bend the cantilever towards or away from the surface, depending on whether they attract or repulse.

To measure and transform this cantilever deviation into an electrical signal to produce an image, a laser beam is reflected on the cantilever and its reflection is collected on a photodetector (Figure 3.1). This photodiode is divided into four quadrants in order to calculate the laser spot position. If the cantilever deflects, this spot is moved on the photodiode, so the deflection signal can be calculated. An electronic control unit receives these analogical signals and sends them to a digital signal processor which translates them

into digital data. This allows new parameters to be computed according to the force set point introduced by the user through a computer.

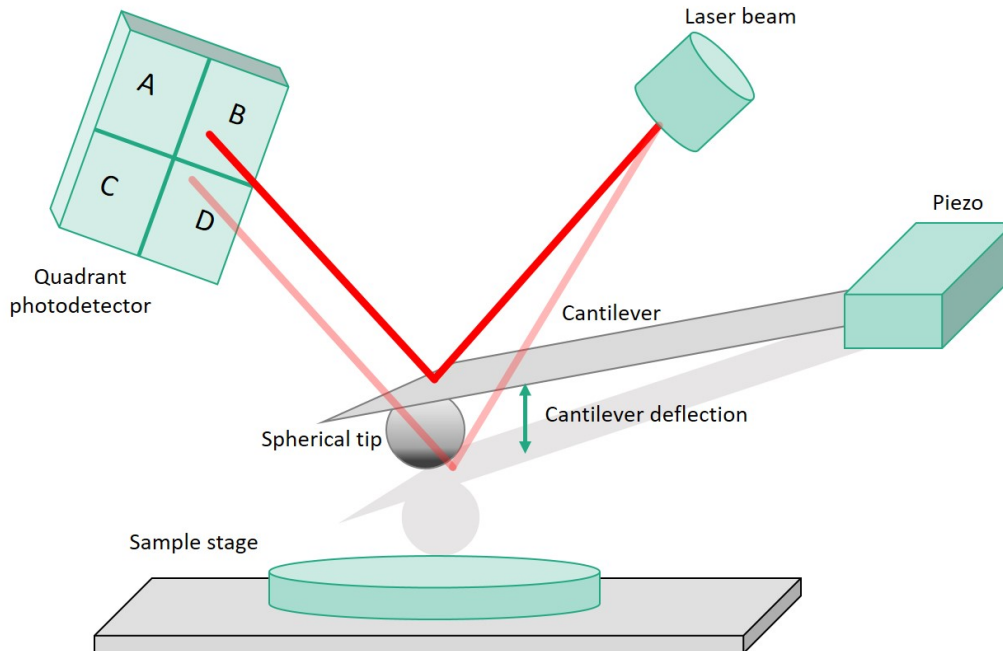


Figure 3.1: **Schematic of our AFM setup.** The piezo controls X, Y, Z movement of the cantilever and tip. A laser beam is focused on the back of the cantilever and the reflected spot is collected on a quadrant photodetector. The detector signal  $((A+B) - (C+D)) / ((A+B) + (C+D))$  is sent to the computer, where the final image is calculated.

Finally, the cantilever is fixed in a piezoelectric tube that can be moved in X, Y and Z positions by a feedback algorithm to facilitate accurate movements of the tip on a surface. Thus, a topographic map of the sample is obtained by scanning the surface.

The interaction force applied to the specimen is calculated by the equation 3.2.1.  $D$  is the deflection of the laser on the photodiode,  $k_c$  is the spring constant of the cantilever, and  $S$  is the sensitivity of the photodetector. This sensitivity connects the deflection in volts of the cantilever to its deflection in nanometers.

$$3.2.1 \quad F(nN) = D(V) * k_c(N/m) * S(nm/V)$$

To obtain these three AFM parameters, it is necessary to calibrate the instrument before each use. In our system, this calibration is performed automatically by thermal noise, which is based on the method described by Hutter and Bechhoefer [31]. This is performed by plotting the force spectrum of the cantilever based on this deflection to get the spring constant and the sensitivity of the photodetector.

AFM can be operated in contact or in dynamic mode. In the former case, the tip is directly placed on the sample, while in the latter one, the cantilever is oscillating over it.

The election of the microcantilever is also a crucial step for AFM measurement. A small spring constant of the microcantilever allows obtaining higher force sensitivity, as a smaller applied force produces a larger deflection on the detector. Also, adhesion forces between the tip and the sample and sample stiffness dictate the choice of the cantilever mechanical properties. Usually, cell studies use cantilevers between 0.01 - 0.6 N/m stiffness [32]. Additionally, while sharp tips should be used for cellular imaging, large colloidal probes are preferred to measure whole-cell mechanical properties [33], as is the case for the experiments performed in this thesis.

The main limitation of the AFM in cell biology is the fact that all measurements are executed on the cell surface, but there are many forces exerted and pressures inside the cells that also affect their mechanical properties [34].

### 3.3 Force spectroscopy

One of the unique features about the AFM is its ability to physically interact in a direct way with the sample. AFM allows pushing and deforming the specimen by using the tip of the instrument and recording the forces exerted and the reactions provoked by approaching or retracting the apex of the cantilever tip. One of the first quantitative cell mechanics study with AFM was the comparison of the elasticity of cell lines that possess different degrees of malignancy by cell indentation [35].

In our study, data are obtained by recording the z-piezo movement and the cantilever deflection during an approach and retract cycle of the AFM tip to a surface in contact mode. The first step to obtain information from these force-distance curves is to obtain the cantilever spring constant,  $k$ , and the photodetector sensibility, as the AFM uses optical detection for the cantilever displacement detection. In our AFM, cantilever spring constant is measured through the recorded thermal noise. Once we know the force exerted by the tip onto the surface, the resulting deformation can be measured. Note that force is not directly determined; it is cantilever deflection which is recorded.

Once calibration has been carried out, a force curve (FZ) is performed. The tip is approached to the sample, touches it, and it is retracted, being the deflection and the piezo height recorded.

Stiff materials, which are not deformable, show a cantilever deflection directly proportional to the relative position of the sample. A softer, deformable material, such as a cell, shows a smaller deflection, being the F-Z a non-linear curve, as seen in Figure 3.2.

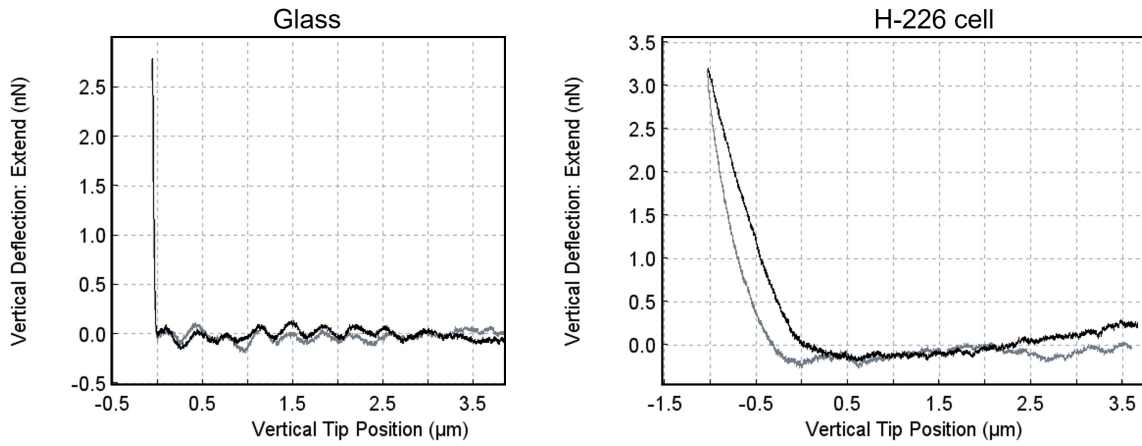


Figure 3.2: **Force-curves on glass (left) and on a H-226 cell (right).** Black line represents the approach curve and the grey line the retract one. A stiffer material shows a steep cantilever deflection, while a cell shows a non-linear curve.  $E_{0_{glass}} = 101.5kPa$ .  $E_{0_{cell}} = 747.4Pa$  (Hertz fit).

### 3.4 Cell mechanics characterization

Cells are exceptionally complex materials, but their mechanical behavior can be explained by a power law with a single exponent,  $\sim (i\omega)^\beta$ , where  $i = \sqrt{-1}$ .  $\beta$  is the power-law exponent that ranges between 0, which corresponds to an elastic solid, and 1, for viscous liquids [36, 37, 38].

Viscoelastic properties of cells are represented by hysteresis loops between the approach and retract curves. Commonly, those ramps are fitted to the Hertz model when a colloidal probe is used to obtain the apparent elastic modulus of the cells [39]. This model assumes that a cell is purely elastic as it does not take into account the retracting phase, and consequently ignores the viscoelasticity of the sample.

Recently, Efremov and Raman have developed a new numerical procedure based on Ting's model that allows integration of arbitrary linear viscoelastic constitutive equations to Hertz model [40]. Considering that the viscoelasticity emanates from the soft-glass behavior of the cells [41], the elasticity



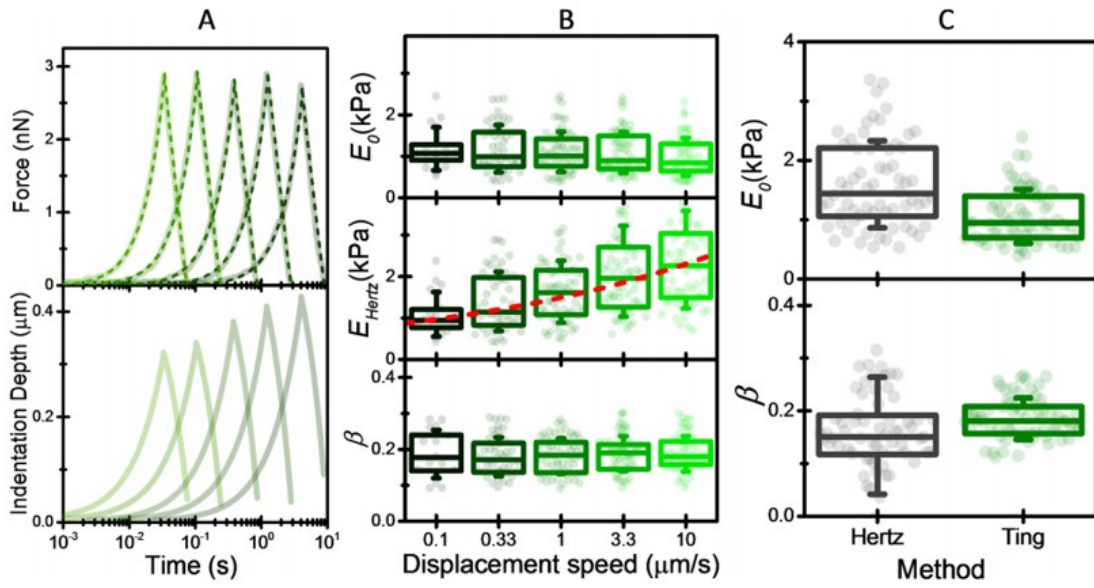


Figure 3.3: **Method used to obtain the PLR parameters of cells.** All curves correspond to a MCF10A cell indentation. **A.** Force and indentation depth as a function of indentation time for five loading rates of 0.1, 0.33, 1, 3.3 and 10  $\mu\text{m/s}$  fitted to the Ting’s model (dashed lines). **B.** Box plots of Power-Law Rheology (PLR) parameters,  $E_0$  and  $\beta$ , obtained by fitting the curves to Ting’s (top and bottom) and Hertz’s (middle) models for the five loading rates. Red line in Hertz model represents the fit of mean values to a power-law. **C.** Comparison of the PLR parameters obtained by fitting the loading-rate dependence of the Hertz elasticity modulus with those obtained by applying the Ting’s method at each force curve and averaging over the loading rates.

relaxation modulus of the cell can be calculated by equation  $E_0 \left( \frac{t}{t_0} \right)^\beta$ , where  $E_0$  is the apparent elasticity modulus given at an arbitrary time  $t_0$ , which is 1s in our case.

At the beginning of this thesis, Hertz model was applied to our measurements. In order to avoid dependence of loading rate of the tip, force curves were performed at five different loading rates, 0.1, 0.33, 1, 3.3 and 10  $\mu\text{m/s}$ . When those curves were fitted to the Ting’s model, the agreement between experiment and theory was excellent. Also, data showed a weak dependence of power-law behavior with loading rate (Figure 3.3B).

We compared the PRL parameters obtained by Hertz and Ting’s models,

showing that the distribution of the PRL parameters obtained by the second method is wider, as shown in figure 3.3C.

In this thesis, all the results provided and PRL parameters  $E_0$  and  $\beta$ , are obtained by Ting's model. In breast cancer cells (Chapters 5 and 6), the five loading rates of 0.1, 0.33, 1, 3.3 and 10  $\mu\text{m/s}$  were averaged by this method. In Chapter 7, force-distance curves were performed at 1  $\mu\text{m/s}$ . ANOVA analysis was performed in Origin data analysis software (OriginLab<sup>®</sup>) at a 95% confidence level ( $p < 0.05$ ).



## Bibliography

- [28] G Binnig and CF Quate. “Gerber Ch 1986 Atomic force microscope”. In: *Phys. Rev. Lett* 56.9 (), page 930.
- [29] Yves F Dufrêne et al. “Imaging modes of atomic force microscopy for application in molecular and cell biology”. In: *Nature nanotechnology* 12.4 (2017), pages 295–307.
- [30] Daniel J Müller and Yves F Dufrene. “Atomic force microscopy as a multifunctional molecular toolbox in nanobiotechnology”. In: *Nanoscience and technology: A collection of reviews from nature journals* (2010), pages 269–277.
- [31] Jeffrey L Hutter and John Bechhoefer. “Calibration of atomic-force microscope tips”. In: *Review of scientific instruments* 64.7 (1993), pages 1868–1873.
- [32] Núria Gavara. “A beginner’s guide to atomic force microscopy probing for cell mechanics”. In: *Microscopy research and technique* 80.1 (2017), pages 75–84.
- [33] Kristina Haase and Andrew E Pelling. “Investigating cell mechanics with atomic force microscopy”. In: *Journal of The Royal Society Interface* 12.104 (2015), page 20140970.
- [34] Michael Krieg et al. “Atomic force microscopy-based mechanobiology”. In: *Nature Reviews Physics* 1.1 (2019), pages 41–57.

- 
- [35] Malgorzata Lekka et al. “Elasticity of normal and cancerous human bladder cells studied by scanning force microscopy”. In: *European Biophysics Journal* 28.4 (1999), pages 312–316.
- [36] Ben Fabry et al. “Scaling the microrheology of living cells”. In: *Physical review letters* 87.14 (2001), page 148102.
- [37] Xavier Trepap et al. “Universal physical responses to stretch in the living cell”. In: *Nature* 447.7144 (2007), pages 592–595.
- [38] Annafrancesca Rigato et al. “High-frequency microrheology reveals cytoskeleton dynamics in living cells”. In: *Nature physics* 13.8 (2017), pages 771–775.
- [39] Heinrich Hertz. “Ueber die Berührung fester elastischer Körper.” In: (1882).
- [40] Yuri M Efremov et al. “Measuring nanoscale viscoelastic parameters of cells directly from AFM force-displacement curves”. In: *Scientific reports* 7.1 (2017), page 1541.
- [41] Philip Kollmannsberger and Ben Fabry. “Linear and nonlinear rheology of living cells”. In: *Annual review of materials research* 41 (2011), pages 75–97.

A photograph of laboratory glassware on a reflective surface. In the foreground, a large clear plastic bottle with a white cap contains a yellowish liquid. To its right are several smaller clear plastic bottles, some containing red liquid. A green pipette is visible on the right side. The background shows more laboratory equipment, including a multi-well plate and a larger container. A semi-transparent green banner with white text is overlaid across the middle of the image.

## 4. Materials and Methods

### 4.1 Cell culture

MCF-7, MDA-MB-231 and MCF-10A cell lines were purchased from the American Type Culture Collection (ATCC<sup>®</sup>, USA). NCI-H226, A549 and NCI-H23 lines were kindly donated by Marcos Malumbres Lab from the Spanish National Cancer Research Center (CNIO).

When a cell line is cultured, each time it is subcultured it is named "passage number". It is not so easy to define the exact passage number of a cell culture, as an accurate method of determining this does not exist [42]. What is known is that higher passages of a cell line show altered protein levels and differences in morphology when compared to low passages [43]. In this thesis, the maximum passage number of the cell cultures has been ten.

MCF-7, MDA-MB-231 and A549 were grown in Dulbecco's modified Eagle's medium (DMEM, Gibco, Life Technologies Corporation, Rockville,

MD, USA) supplemented with 10% fetal bovine serum (FBS), 500U/mL penicillin and 0.1 mg/mL streptomycin.

MCF-10A cells were cultured in DMEM-F12 medium (Gibco) supplemented with 5% horse serum, 20 ng/mL epidermal growth factor, 0.5  $\mu$ g/mL hydrocortisone, 100 ng/mL cholera toxin, 10  $\mu$ g/mL insulin and 500 U/mL penicillin and 0.1 mg/mL streptomycin.

NCI-H226 and NCI-H23 cells were cultured in Roswell Park Memorial Institute medium (RPMI 1640, Biowest) supplemented with 25 mM HEPES, 10% fetal bovine serum (FBS), 500U/mL penicillin and 0.1 mg/mL streptomycin.

Cells were maintained at 37°C in 5% CO<sub>2</sub> in a humidified incubator.

For subculture, cells were detached from the plate floor by trypsinization (trypsin 0.25% with 1 g/L EDTA, HyClone<sup>®</sup>, GE Healthcare). After trypsin inactivation by adding fresh medium, cells were subcultured 2-3 times per week at a dilution of 1:5. All cell culture work was performed under sterile conditions.

To freeze cells, they were grown to 80% confluence, as described, in a 10 cm cell culture dish. Then, they were trypsinized and transferred to a 15 mL falcon tube to be centrifuged at 1400 rpm for 4 minutes in order to pellet the cells. Supernatant was aspirated and cells were resuspended into 1 mL of pre-cooled freezing solution (95% their culture medium and 5% DMSO for MCF-10A line, 92.5% FBS 7.5% DMSO for MDA-MB-231 and MCF-7 cell lines). Cells were afterwards transferred into a cryotube and placed directly in a -80° C freezer. After 48 hours, tubes were transferred to the liquid nitrogen cell storage (-196° C).

To recover frozen cells, they were directly thawed in a p-10 cell culture

dish with fresh complete medium and allowed to grow for one day. After this process, medium was replaced with fresh complete medium.

## 4.2 Immunocytochemistry

For perform immunocytochemistry, cover glasses were previously treated as follows: first, they were cleaned with piranha solution and covered with poly-lysine 0.1% for 15 minutes. Later, they were rinsed three times with Milli-Q<sup>®</sup> water and dried at room temperature. Once dried, cover glasses were kept under a UV light for 4 hours and cells were cultured on top of the covers.

Samples were fixed with freshly prepared 4% paraformaldehyde for 15 minutes at room temperature and washed three times with PBS for five minutes. Afterwards, cells were permeabilized for ten minutes with 0.25% Triton X-100 in PBS (PBST) and wash with PBS three times. Before staining, samples were blocked with 1% bovine serum albumin (BSA) in PBST for 30 minutes.

After three 5-minute rinses with PBS, we added phalloidin (Alexa Fluor<sup>®</sup> 488 Phalloidin, concentration 1:20) for 15 minutes, rinsed, and added DAPI 0.5  $\mu\text{g}/\text{mL}$  (Cell Signalling Technology<sup>®</sup>). After rinsing once more in PBS, we mounted the samples with ProLong<sup>®</sup> Antifade Reagent) and allowed them to dry 24 hours at room temperature. We sealed them with nail lacquer before imaging.

Confocal imaging was performed with a confocal microscope Nikon A1R HD25 at the SMOC (Servicio de Microscopía Óptica y Confocal, Centro de Biología Molecular Severo Ochoa, CBMSO).

### 4.3 Wound healing assay

Cells were seeded into p35 plates and allowed to grow to 80% confluency in their complete medium. Then cell monolayers were scratched with a sterile 200  $\mu$ L pipette plastic tip as described in [44]. Then, plates were washed three times with PBS, in order to remove cell debris, and Leibovitz's L-15 medium supplemented with 10% fetal bovine serum (FBS), 500 U/mL penicillin and 0.1 mg/mL streptomycin was added. Cells were incubated in a warm chamber under a Digital Holographic Microscope (DHM, Lynceé Tec.). Images were taken every 60 minutes with a 10x magnification. Cell occupation ratio is the remaining cell-free area compared to the initial scratched area, using ImageJ Wound Healing Tool for this calculation [45].

### 4.4 Knock-out of *TP53* and mutation of *KRAS* in lung cells

We performed an infection of the lung cancer cell lines by lentivirus. Malumbres Lab provided two plasmids: plentiCRISPR v2 sgP53 v2, which uses CRISPR/Cas9 to cut out TP53 gene; and pLenti-PGK-KRAS4B(G12V) to induce a G12V mutation in *KRAS*. These two plasmids were added with packaging plasmids pMDLg/pRRE (gag/pol, Addgene plasmid #12251), pRSV-Rev (Rev, Addgene plasmid #12253) and pMD2.g (VSVg, Addgene plasmid #12259) [46] to transfect HEK 293T cells using Lipofectamine<sup>TM</sup> 2000 reagent (Invitrogen<sup>TM</sup>, USA) according to the manufacturer's instructions. Viral particles were collected and filtered at 48 and 72 hours. Cells of interest were infected by this lentivirus plus polybrene 8  $\mu$ g/mL for 24 hours. Then, fresh medium was added for 48 hours. Finally, cells were selected with 2  $\mu$ g/mL puromycin for *TP53* and 200  $\mu$ g/mL hygromycin

for *KRAS* mutation (Figure 4.1).

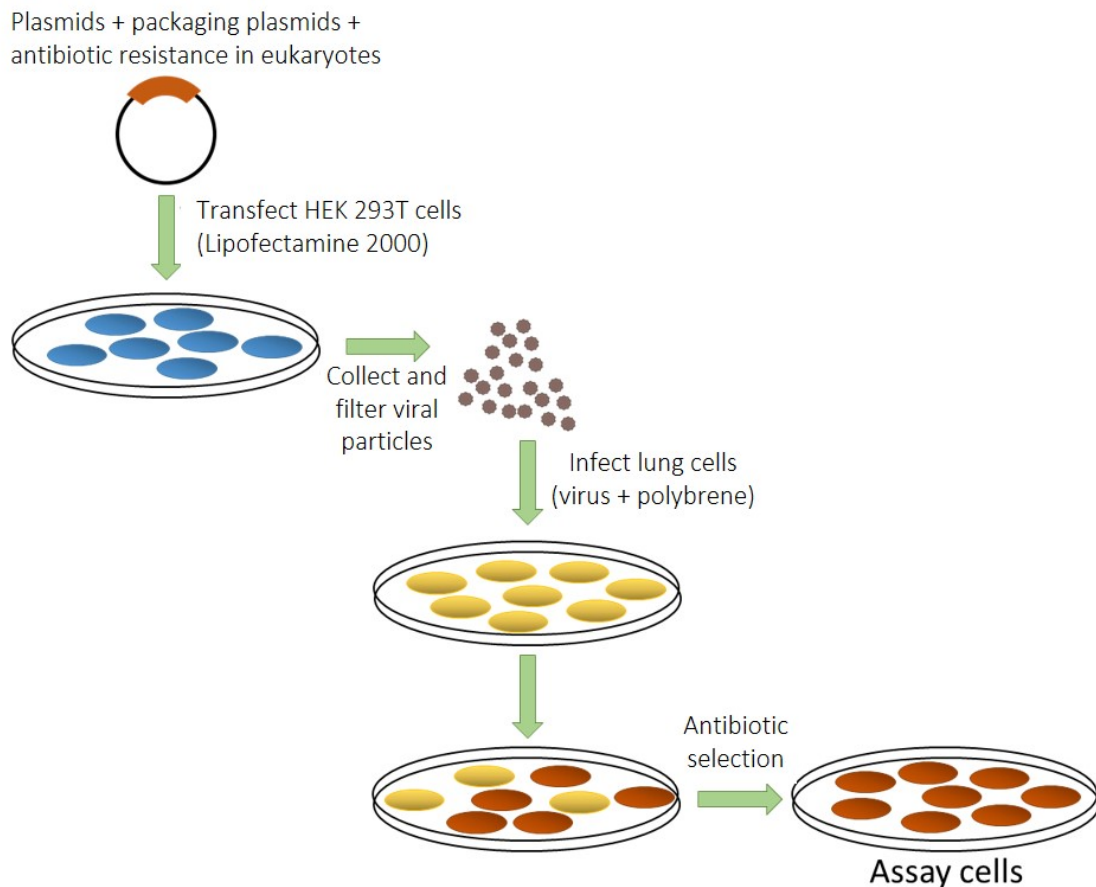


Figure 4.1: **Transfection of p53 and KRAS mutated in lung cells.** Scheme of infection of lentivirus with target genes of lung cancer cell lines via HEK 293T viral production.

## 4.5 Western blot analysis

Cultured cells were trypsinized (trypsin 0.25% with 1 g/L EDTA, HyClone<sup>®</sup>, GE Healthcare) and collected in a centrifuge tube with 5 mL of fresh medium to inactivate trypsin. Cells were centrifuged at 1400 rpm for 4 minutes. Resultant pellet was resuspended in 1 mL PBS and centrifuged again. The resultant pellet was conserved at -80° C.

Frozen pellets were lysed with RIPA lysis buffer (25 mM Tris-HCl pH 7.6, 150 mM NaCl, 1% NP-40, 1% sodium deoxycholate, 0.1% SDS)

for 30 minutes on ice. After, they were centrifuged for 20 minutes at 14.000 rpm. The concentration of protein in the supernatants was detected by Bradford method with an Eppendorf BioSpectrometer<sup>®</sup> at a 595 nm wavelength, using BSA for elaborating the pattern curve. Between 20 and 50  $\mu\text{g}$  of protein were loaded and separated by SDS-PAGE on 4-20% SDS-polyacrylamide gels (Bio-Rad). After electrophoresis, proteins were transferred onto nitrocellulose membranes, following Bio-Rad Criterion Blotter protocol.

Membranes were blocked for one hour with 5% skimmed milk in 0.1% TBS-Tween (5% BSA in 0.1% TBS-Tween for p53) prior to overnight incubation with the primary antibodies indicated in Table 4.1 at 4°C in the blocking buffer. After that, they were rinsed three times with 0.1% TBS-Tween for ten minutes each. Secondary antibody (Goat-Anti-Rabbit IgG-AP, Bio-Rad Laboratories, Inc., reference 1706518) was incubated for 1 hour at room temperature. Protein detection was performed using the AP (alkaline phosphatase) Conjugate Substrate Kit (Bio-Rad Laboratories, Inc.) according to the manufacturer's instructions. Imaging was obtained with a Gel Doc<sup>™</sup> EZ System (Bio-Rad Laboratories, Inc.).

Table 4.1: Primary antibodies used for Western Blot assay.

Name	Manufacturer	Reference	Dilution	Description
Anti-p53	CST <sup>®</sup>	#9282	1:1000	Monoclonal Rabbit
Anti-Ras (G12V)(D2H12)	CST <sup>®</sup>	#14412	1:1000	Monoclonal Rabbit



## 4.6 AFM experiments

Cells were placed on p35 culture dishes (Corning<sup>®</sup> CellBIND<sup>®</sup> Surface) at a density of  $2 \times 10^5$  cells/mL 24-36 hours before AFM experiments in order to guarantee confluence of cells.

AFM experiments were performed with a Bruker JPK NanoWizard<sup>®</sup>4 mounted on an inverted optical microscope (Leica DMI 6000-CS, Germany). Colloidal probes of 0.2 N/m and 10  $\mu\text{m}$  of diameter (CP-CONT-BSG, NanoAndMore GmbH, Germany) were used for force-distance curves (ramps). Before measurements, spring constant and sensitivity of the photodetector were calibrated by the automatic thermal noise analysis software of the instrument.

In Chapters 5 and 6, ramps were recorded at five approach tip velocities: 0.1  $\mu\text{m/s}$ , 0.33  $\mu\text{m/s}$ , 1  $\mu\text{m/s}$ , 3.3  $\mu\text{m/s}$  and 10  $\mu\text{m/s}$ ; but keeping the piezo length to 5  $\mu\text{m}$  and with a force threshold of 3 nN. Each cell was measured on top of the nucleus at the same position. The resulting power-law rheology parameters of each cell were first averaged at each loading rate, and the resulting values were then averaged across the five loading rates.

In Chapter 7, ramps were recorded at a 1  $\mu\text{m/s}$  tip velocity, 5  $\mu\text{m}$  of ramp length and a 3 nN threshold.

Power-law rheology analysis was performed by custom algorithms written in Wolfram Mathematica<sup>®</sup> (Wolfram Research) based on Efremov et al. method [40].



## Bibliography

- [40] Yuri M Efremov et al. “Measuring nanoscale viscoelastic parameters of cells directly from AFM force-displacement curves”. In: *Scientific reports* 7.1 (2017), page 1541.
- [42] ATCC. “Passage Number Effects in cell lines”. In: *ATCC Technical Documents* (2021).
- [43] Peyton Hughes et al. “The costs of using unauthenticated, over-passaged cell lines: how much more data do we need?” In: *Biotechniques* 43.5 (2007), pages 575–586.
- [44] Lijun Xu and Xingming Deng. “Protein kinase C $\alpha$  promotes nicotine-induced migration and invasion of cancer cells via phosphorylation of  $\mu$ - and m-calpains”. In: *Journal of Biological Chemistry* 281.7 (2006), pages 4457–4466.
- [45] Alejandra Suarez-Arnedo et al. “An ImageJ plugin for the high throughput image analysis of in vitro scratch wound healing assays”. In: *PloS one* 15.7 (2020), e0232565.
- [46] Tom Dull et al. “A third-generation lentivirus vector with a conditional packaging system”. In: *Journal of virology* 72.11 (1998), pages 8463–8471.





# Breast cancer cells

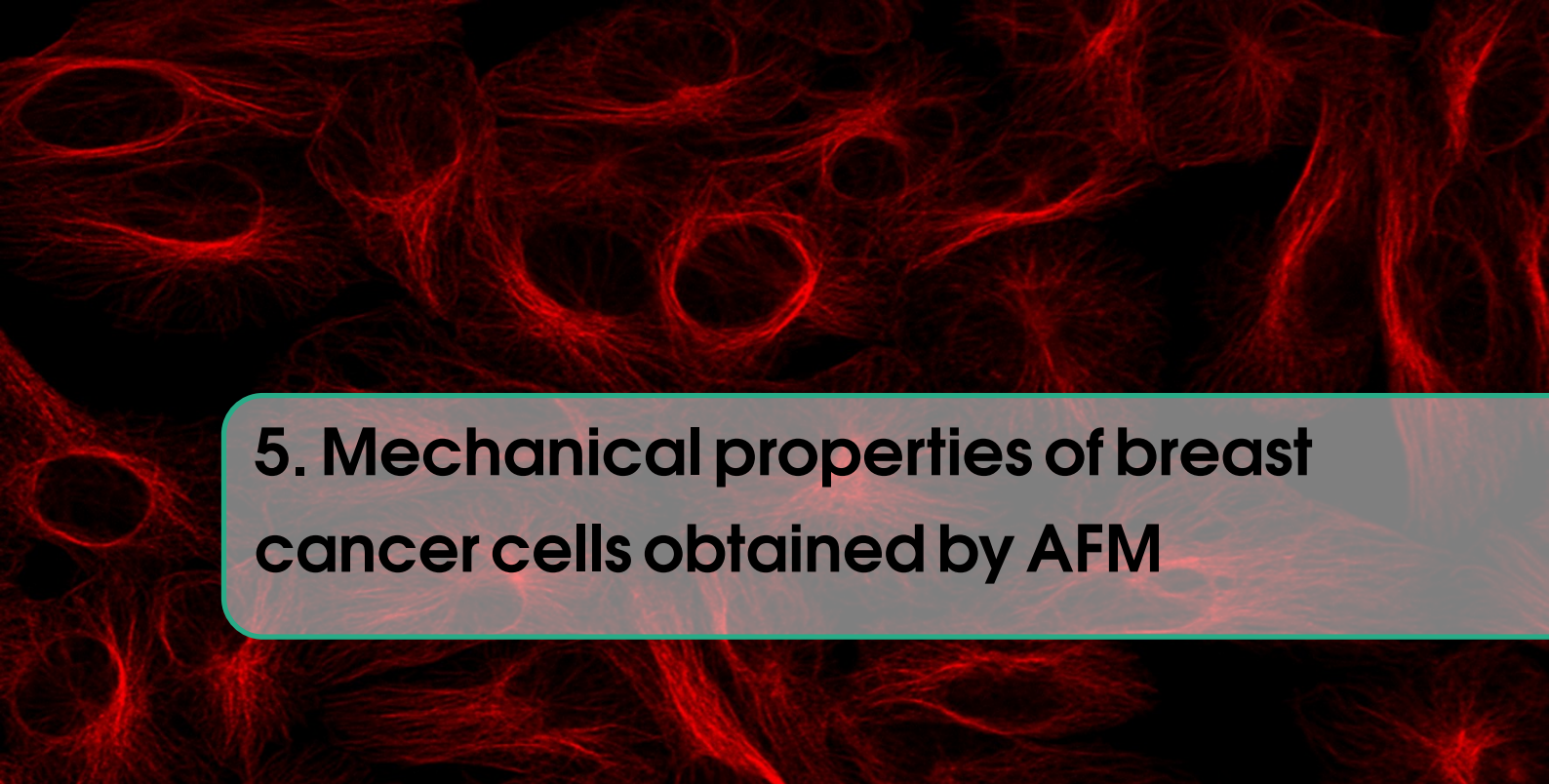
## **5 Mechanical properties of breast cancer cells obtained by AFM . 65**

- 5.1 Introduction
- 5.2 AFM results
- 5.3 Immunocytochemistry imaging
- 5.4 Wound healing assay of breast cancer cells
- 5.5 Conclusions
- Bibliography

## **6 Effects of energy metabolism on the mechanical properties of breast cells ..... 81**

- 6.1 Introduction
- 6.2 Breast cancer cells metabolism
- 6.3 ATP depletion and effect of drugs directed to the cytoskeleton
- 6.4 Immunocytochemistry imaging
- 6.5 Contribution of active processes to cell elasticity
- 6.6 Conclusions
- Bibliography





## 5. Mechanical properties of breast cancer cells obtained by AFM

### 5.1 Introduction

Breast cancer was the main diagnosed cancer in the world (11.7% of total cases) and the first cause of cancer death in females in 2020 [17]. Breast cancer incidence is higher in developed countries, but the majority of cases are detected in advanced states [47]. This is a very heterogeneous disease under the influence of both genetic and non-genetic risk factors [48].

According to the American Cancer Society<sup>®</sup>, metastasis occurs when cancer cells can spread to other sites in the body from where the cancer started, the so-called primary site, often by way of the lymph system or bloodstream.

In breast cancer, the model cell lines that have been used in this thesis have been widely studied before: MCF-10A cell line cells are considered as non-malignant counterparts, MCF-7 is a tumorigenic but non-invasive cell line, and MDA-MB-231 is an aggressive invasive, metastatic line.

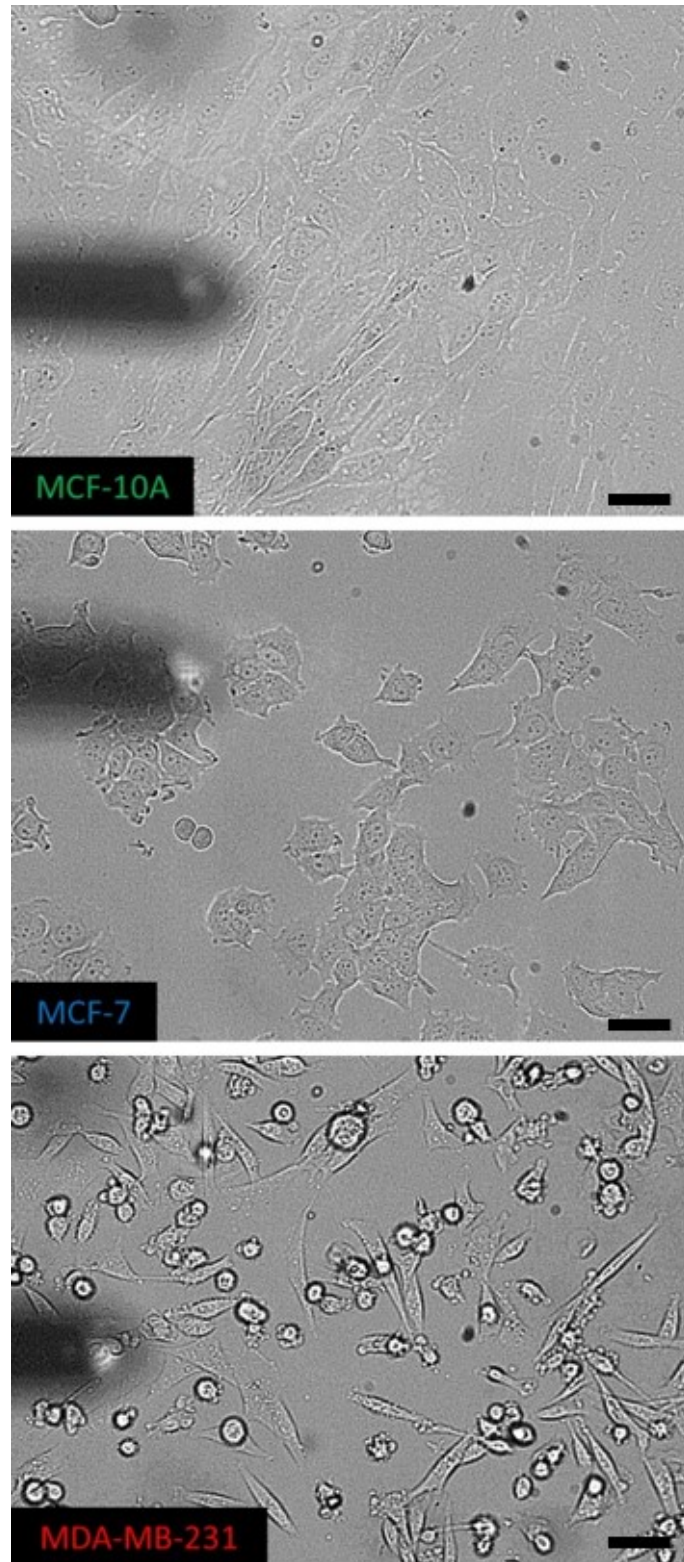


Figure 5.1: **Optical microscopy images of MCF-10A, MCF-7 and MDA-MB-231 lines during AFM measurements.** Scale bar  $50\mu\text{m}$ . Shadow at the left is the AFM cantilever retracted from the surface, bright spot is the laser placed on the back of the cantilever. Images were taken using a long free working distance HC PL Fluotar 10x/0,32 objective (Leica).



MCF-10A and MCF-7 form continuous mono layers with well-defined cell borders, while MDA-MB-231 cell line forms clusters of variable cell density, as seen in Figure 5.1.

In breast cancer cells, there is a reduction of actin stress fibers, resulting in a softer cytoskeletal network and providing tumoral cells the capacity to migrate [49, 50]. Their stiffness has been investigated in many works (Table 5.1), where the type of biophysical probe used in each experiment provides a different parameter of the cell related to its stiffness. All results agree that breast cancer cell lines MCF-7 and MDA-MB-231 are softer than normal cells. Living cells show a high heterogeneity, depending on the probe used to measure their mechanical properties, or even depending on the parameters used for a certain rheology technique.

Table 5.1: Summary of selected experiments on stiffness or related parameters of breast cancer cells. Results have been normalized to values for MCF-10A cells (considered as normal-like).

Cell type	Rheology Technique	Relative stiffness (or related parameters) wrt MCF-10A	Reference
MCF-7	Dielectrophoretic stretching	Strain response of MCF-10A is 2.5 times higher than MCF-7	[51]
MDA-MB-231	AFM-Confocal fluorescence microscopy	Cytoplasm: $E \sim 0.1875$ Nucleus: $E \sim 0.125$ Nucleoli: $E \sim 0.666$	[52]
MDA-MB-231	AFM	$E \sim 0.751$	[53]
MCF-7 MDA-MB-231	AFM	MCF-7 1Hz: $E \sim 0.714$ MDA-MB-231 1Hz: $E \sim 0.429$ MCF-7 250Hz: $E \sim 0.112$ MDA-MB-231 250Hz: $E \sim 0.1$	[49]

Table 5.1 continued from previous page

Cell type	Rheology Technique	Relative stiffness (or related parameters) wrt MCF-10A	Reference
MCF-7 MDA-MB-231	Microfluidic optical trap	MCF-7 optical deformability: $\sim 2.038$ MDA-MB-231 optical deformability: $\sim 3.210$	[54]
MCF-7	Optical tweezers	Cytoplasm stiffness is 30% smaller in MCF-7 cells than MCF-10A. Effective spring constant of the cytoplasm is larger in the MCF-10A.	[55]
MCF-7	Microfluidics	MCF-7 entry time: $\sim 0.255$ Elongation index: $\sim 1.041$	[56]
MDA-MB-231	AFM	Cytoplasm: $E \sim 0.769$ Nucleus: $E \sim 0.250$	[57]
MDA-MB-231	Microfluidic pipette array	$E \sim 0.467$	[58]
MCF-7	AFM	$E: 0.555 \sim 0.714$ at the same value of the loading rate	[50]
MCF-7	Microfluidic optical stretching	Optical stretching of MCF-7 five times higher than that of MCF-10A	[59]
MDA-MB-231	Optical tweezers	Shear modulus: $\sim 0.444$	[60]
MDA-MB-231	AFM	$E \sim 0.278$	[61]
MDA-MB-231	Microfluidics	Predicted Young modulus: $\sim 0.506$ Predicted viscosity: $\sim 0.514$	[62]
MCF-7 MDAMB-231	AFM force mapping	Shear modulus MCF-7: $\sim 0.182$ Shear modulus MDA-MB-231: $\sim 0.504$	[63]
MCF-7 MDA-MB-231	Force clamp mapping	At both sparse and confluent density, stiffness of MCF-7 and MDA-MB-231 is significantly lower than that of MCF-10A	[64]
MCF-7	Piezoresistive microcantilever deformation	MCF-7 have higher viscosity and higher deformability than MCF-10A	[65]
MDA-MB-231	AFM	$E \sim 0.651$	[66]

Table 5.1 continued from previous page

Cell type	Rheology Technique	Relative stiffness (or related parameters) wrt MCF-10A	Reference
MCF-7 MDA-MB-231	AFM	MCF-7: $E \sim 0.640$ MDA-MB-231: $E \sim 0.507$	[67]

The deformability of cells has been considered as a biomarker of metastatic potential. In this chapter, we study the differences in stiffness and actin fiber organization among three epithelial breast cancer cell lines with different degrees of malignancy by AFM.

## 5.2 AFM results

Cell lines were cultured as indicated in Chapter 4. According to sources, MCF-10A stiffness depends on cell confluence, while MCF-7 and MDA-MB-231 do not [64]. To avoid those cell confluence artifacts, experiments on MCF-10A and MCF-7 were performed on continuous mono layers, whereas for experiments on MDA-MB-231 we chose high-density cell regions, as seen in Figure 5.1.

AFM experiments were performed as referred in Chapter 4. A spherical probe of  $10 \mu\text{m}$  diameter attached to the free end of a compliant cantilever was used for indentation of the cells (Figure 5.2). The microcantilever was approached to reach a maximum force of about  $3\text{nN}$  at five tip velocities:  $0.1 \mu\text{m/s}$ ,  $0.33 \mu\text{m/s}$ ,  $1 \mu\text{m/s}$ ,  $3.3 \mu\text{m/s}$  and  $10 \mu\text{m/s}$ . Indentation depths range from  $100 \text{ nm}$  to  $2 \mu\text{m}$ .

The results show that, as expected, tumorigenic cells are softer than healthy ones. As seen in figure 5.3 A,  $E_0$  is  $1.14 \pm 0.65 \text{ kPa}$  for MCF10-A,

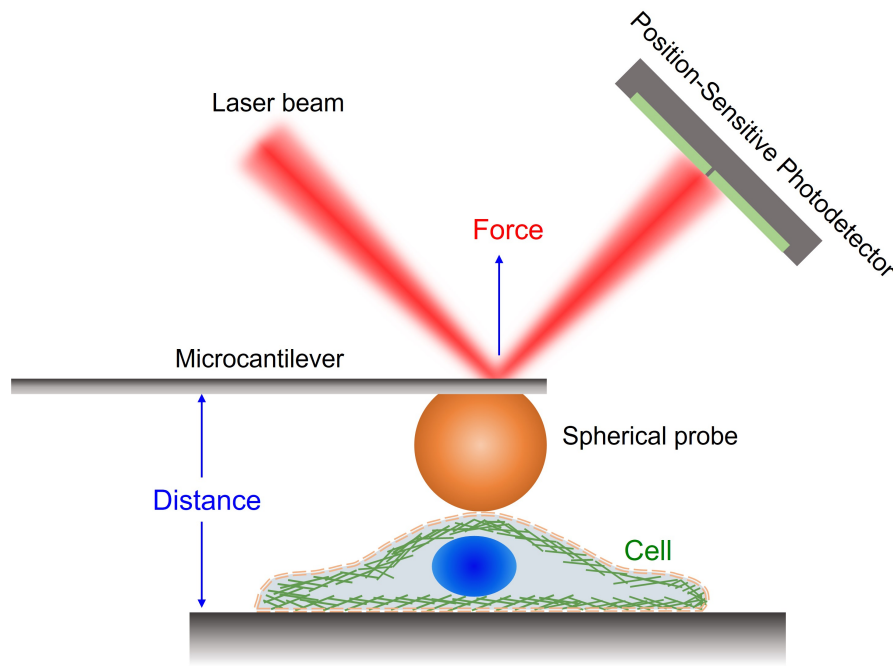


Figure 5.2: **Experimental setup of the AFM used in the experiments.** A spherical probe of  $10\mu\text{m}$  diameter attached to the free end of a compliant cantilever is placed above the nucleus of a adherent cell. Not in scale.

$0.26 \pm 0.16$  kPa for MCF-7 and  $0.46 \pm 0.24$  kPa for MDA-MB-231. Although stiffness and cell deformability have been proposed as physical biomarkers for metastatic potential [68, 69], our results do not show an evident difference in stiffness between non-invasive and invasive cells lines taking into account just this parameter.

The other parameter we obtained is the power-law exponent  $\beta$ , which is  $0.186 \pm 0.049$  for healthy cells,  $0.234 \pm 0.060$  for the tumorigenic cell line and  $0.147 \pm 0.061$  for the invasive cell line (Figure 5.3 A). This means that non-invasive cells show more fluid-like behavior than healthy counterparts, being invasive MDA-MB-231 cell line the one with lowest power-law exponent. This elastic-like behavior could ease migration and transiting through narrow pores, which also would require a robust actomyosin cortex to perform these tasks and which would explain why MDA-MD-231 cell

line is stiffer than MCF-7.

If both parameters,  $\beta$  and  $E_0$ , are plotted together, we observe different distinguishable behaviors for each of the cell lines (Figure 5.3 B). Cancerous cells are softer than healthy ones, but invasive cells are stiffer than non-invasive MCF-7 cell line. Also, healthy and highly invasive cells are more fluid than the tumorigenic non-invasive line. Therefore, if we take into account these two mechanical properties at the same time, a phenotyping of cancerous cells with different malignancy degrees could be performed.

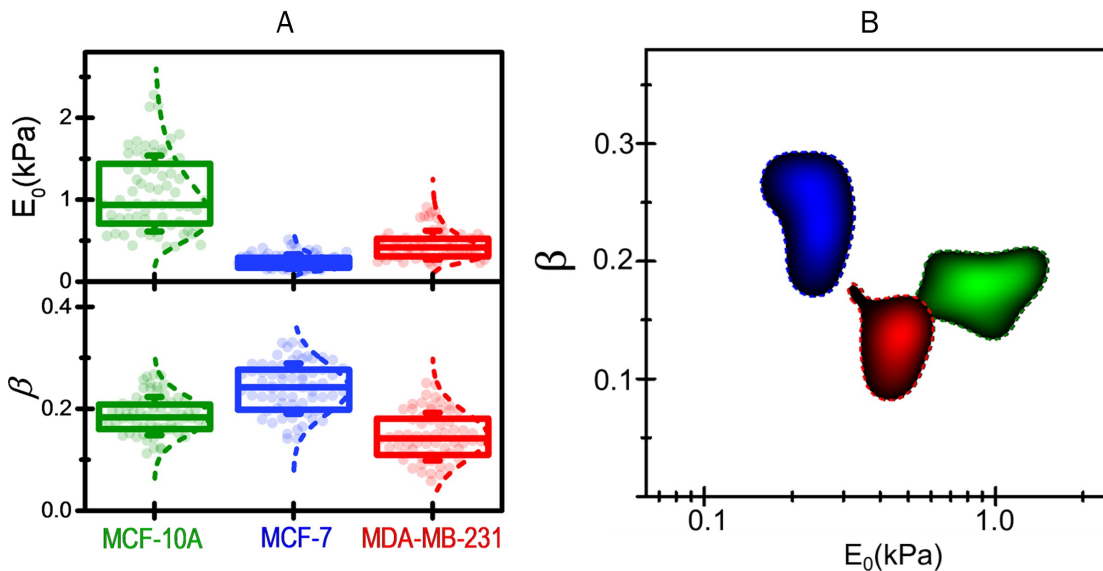


Figure 5.3: **PLR parameters of breast cancer cells.** **A.** Box plots of the apparent elastic modulus at a reference time of 1 s ( $E_0$ ) and the power-law exponent ( $\beta$ ) for the three cell lines. Symbols represent experimental data, the box shows the 25% and 75% quartiles and the error bar the standard deviation.  $E_0$  values were fitted to a logarithmic, normal distribution, while  $\beta$  values were fitted to a normal distribution. **B.** Plot of both parameters obtained by AFM,  $\beta$  and  $E_0$ . The three different cell lines (MCF-10A in green, MCF-7 in blue, MDA-MB-231 in red) can be distinguished by their mechanical properties.

### 5.3 Immunocytochemistry imaging

To directly observe the cytoskeleton arrangement in the cells, we labeled the filamentous actin with phalloidin in the three cell lines. We confirmed that

healthy cells and MCF-7 cell lines showed a well-organized cytoskeleton, while highly aggressive cells do not (Figure 5.4).

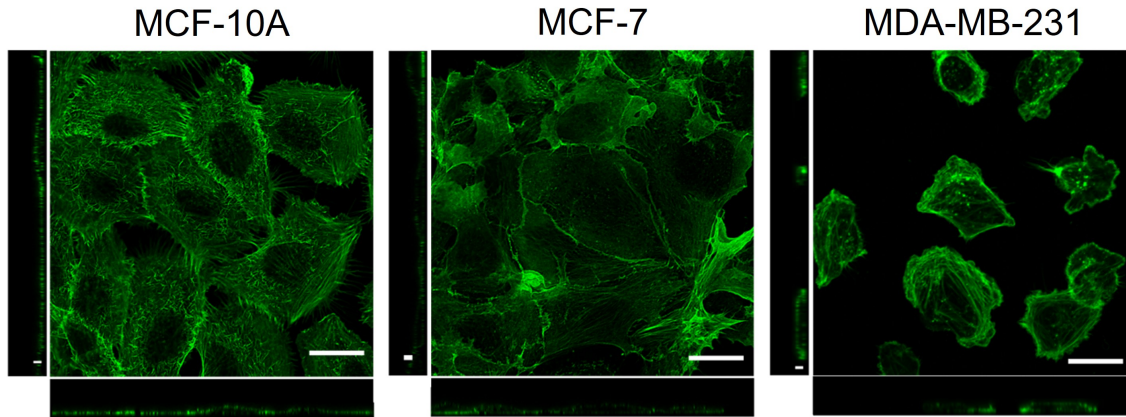


Figure 5.4: **Confocal fluorescence images that show changes in the organization of the actin cytoskeleton of MCF-10A, MCF-7 and MDA-MB-231.** Scale bar is  $20\mu\text{m}$ . For each image, orthogonal cuts are represented.

This is consistent with the idea that in healthy cells filamentous actin of the cytoskeleton is well organized and forms stress fibers [49] that give stiffness to MCF-10A. Although MCF-7 cells show an organized actin net, they do not form stress fibers in their apical domain, and highly aggressive MDA-MB-231 do not arrange a typical organized actin cytoskeleton.

#### 5.4 Wound healing assay of breast cancer cells

Cell motility is considered as an indicator of metastatic potential of cancer cells. To assess this motility, the three cell lines of human breast cancer were examined by wound healing assay.

After six hours (see Figure 5.5), malignant MDA-MB-231 occupies almost 14% of the gap, while MCF-10A and MCF-7 barely do by 5.98 and 4.01% respectively. By 12 hours MDA-MB-231 reached the 26.7%, MCF-10A the 11.24% and MCF-7 the 11.92% of their gaps. By the end of

---

the experiment, MCF-7 slowed down its gap occupation (16.71%), while healthy and metastatic cells continued their growth (27.37% and 32.45% respectively).

This suggests that healthy and metastatic cells want to develop and need some robustness for invasion, while MCF-7 cells do not need it, as their occupying performance is not so aggressive.

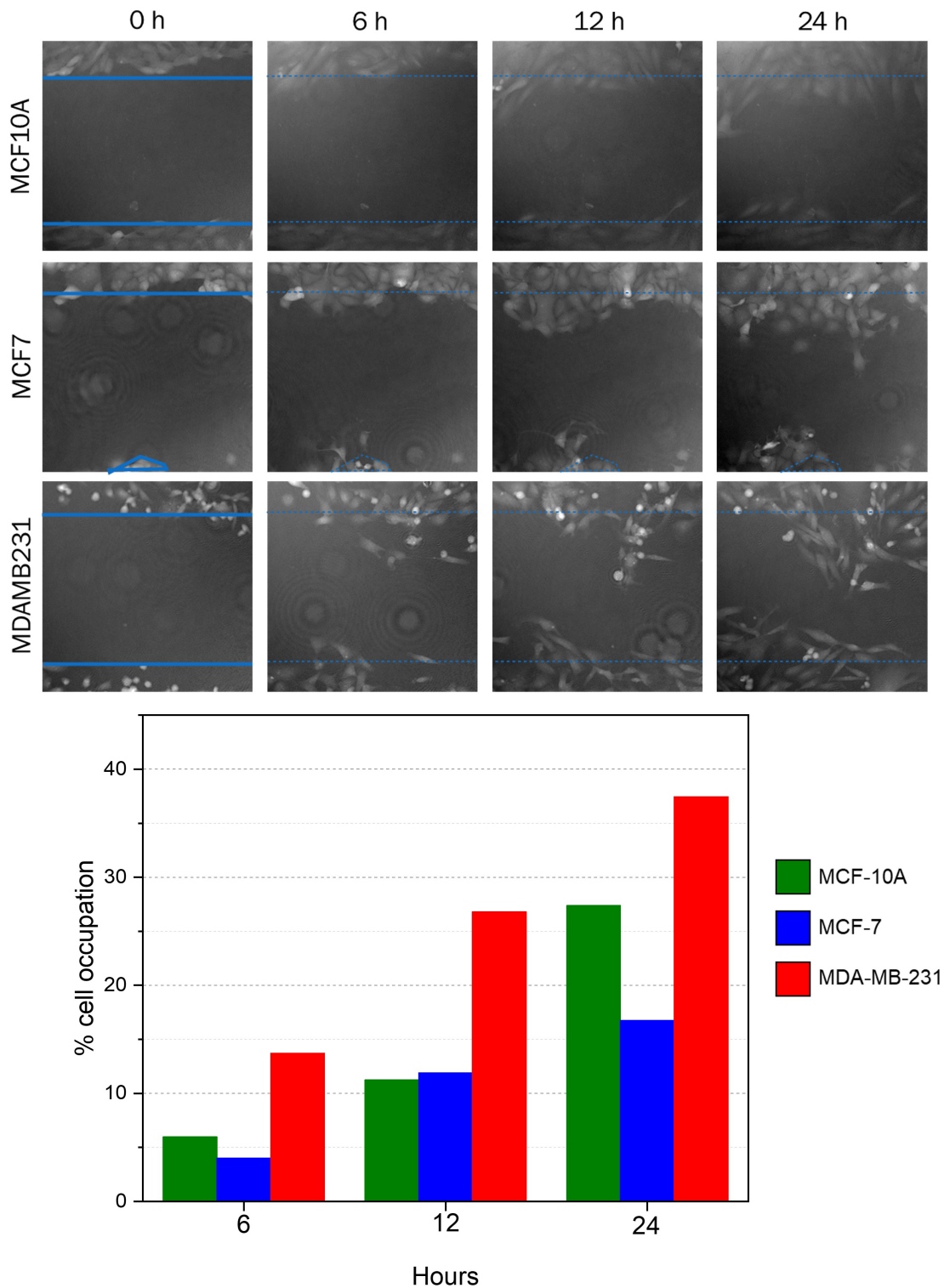


Figure 5.5: **Wound healing assay in breast cancer cells.** **Top:** representative images of the three cell lines during wound healing assay. Cells were scratched and recorded for 24 hours. Images were taken using a DHM (Lyncee Tech) at indicated periods. Magnification 10x. **Bottom:** quantitative closure (% of cell occupation) of the cell lines.



## 5.5 Conclusions

From this chapter, five conclusions can be reached:

1. Cancer cells are softer than healthy cells.
2. We use an AFM methodology that provides two-dimensional mechanical phenotyping of cells, based on PLR parameters,  $\beta$  and  $E_0$ . Healthy-like, non-invasive cancer and metastatic cell lines exhibit three distinguishable mechanical properties.
3. MCF-7 cell line, a tumorigenic but noninvasive cell line, is softer and more fluid than highly invasive counterparts.
4. MCF-10A and MCF-7 cell lines arrange their actin network. Healthy cells form stress fibers, which could give stiffness and strength to them, while cancerous cells do not.
5. MCF-10A and MDA-MB-231 exhibit a higher speed of invasion than MCF-7, as seen in wound healing experiments.



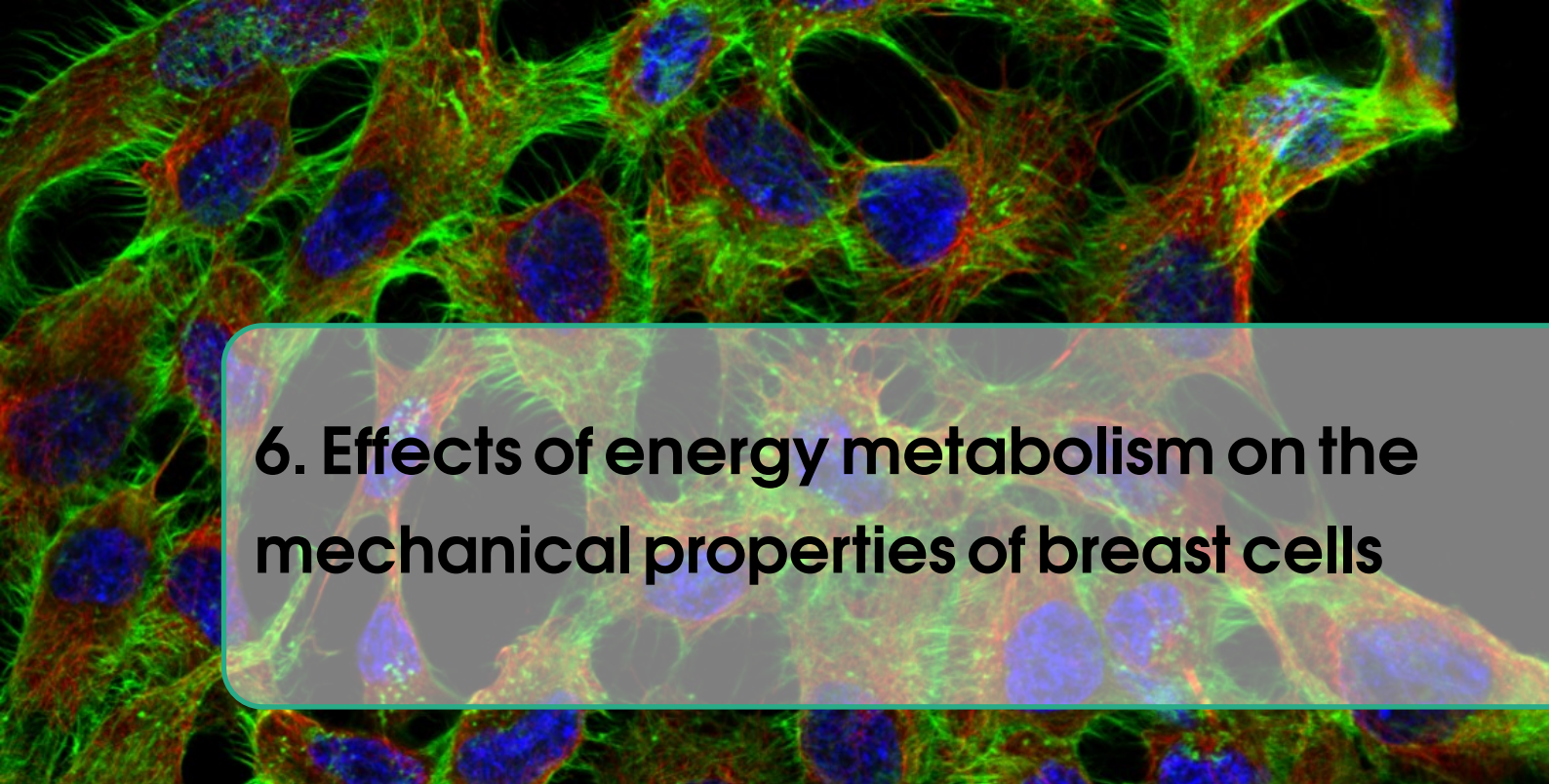
## Bibliography

- [17] Hyuna Sung et al. “Global cancer statistics 2020: GLOBOCAN estimates of incidence and mortality worldwide for 36 cancers in 185 countries”. In: *CA: a cancer journal for clinicians* 71.3 (2021), pages 209–249.
- [47] Karla Unger-Saldaña. “Challenges to the early diagnosis and treatment of breast cancer in developing countries”. In: *World journal of clinical oncology* 5.3 (2014), page 465.
- [48] Kara L Britt, Jack Cuzick, and Kelly-Anne Phillips. “Key steps for effective breast cancer prevention”. In: *Nature Reviews Cancer* 20.8 (2020), pages 417–436.
- [49] Alicia Calzado-Martín et al. “Effect of actin organization on the stiffness of living breast cancer cells revealed by peak-force modulation atomic force microscopy”. In: *ACS nano* 10.3 (2016).
- [50] QS Li et al. “AFM indentation study of breast cancer cells”. In: *Biochemical and biophysical research communications* 374.4 (2008), pages 609–613.
- [51] Isabella Guido, Magnus S Jaeger, and Claus Duschl. “Dielectrophoretic stretching of cells allows for characterization of their mechanical properties”. In: *European Biophysics Journal* 40.3 (2011), pages 281–288.

- [52] David B Agus et al. “A physical sciences network characterization of non-tumorigenic and metastatic cells”. In: *Scientific reports* 3 (2013), page 1449.
- [53] H Babahosseini et al. “Sub-cellular force microscopy in single normal and cancer cells”. In: *Biochemical and biophysical research communications* 463.4 (2015), pages 587–592.
- [54] Jochen Guck et al. “Optical deformability as an inherent cell marker for testing malignant transformation and metastatic competence”. In: *Biophysical journal* 88.5 (2005), pages 3689–3698.
- [55] Ming Guo et al. “Probing the stochastic, motor-driven properties of the cytoplasm using force spectrum microscopy”. In: *Cell* 158.4 (2014), pages 822–832.
- [56] Han Wei Hou et al. “Deformability study of breast cancer cells using microfluidics”. In: *Biomedical microdevices* 11.3 (2009), pages 557–564.
- [57] Meng-Horng Lee et al. “Mismatch in mechanical and adhesive properties induces pulsating cancer cell migration in epithelial monolayer”. In: *Biophysical journal* 102.12 (2012), pages 2731–2741.
- [58] Lap Man Lee and Allen P Liu. “A microfluidic pipette array for mechanophenotyping of cancer cells and mechanical gating of mechanosensitive channels”. In: *Lab on a Chip* 15.1 (2015), pages 264–273.
- [59] Bryan Lincoln et al. “Deformability-based flow cytometry”. In: *Cytometry Part A* 59.2 (2004), pages 203–209.
- [60] Kalpana Mandal et al. “Mapping intracellular mechanics on micropatterned substrates”. In: *Proceedings of the National Academy of Sciences* 113.46 (2016), E7159–E7168.
- [61] Mehdi Nikkhah et al. “Evaluation of the influence of growth medium composition on cell elasticity”. In: *Journal of biomechanics* 44.4 (2011), pages 762–766.
- [62] A Raj et al. “A combined experimental and theoretical approach towards mechanophenotyping of biological cells using a constricted microchannel”. In: *Lab on a Chip* 17.21 (2017), pages 3704–3716.

- 
- [63] Jan Rother et al. “Atomic force microscopy-based microrheology reveals significant differences in the viscoelastic response between malignant and benign cell lines”. In: *Open biology* 4.5 (2014), page 140046.
- [64] Nicolas Schierbaum, Johannes Rheinlaender, and Tilman E Schäffer. “Viscoelastic properties of normal and cancerous human breast cells are affected differently by contact to adjacent cells”. In: *Acta biomaterialia* 55 (2017), pages 239–248.
- [65] Sangjo Shim et al. “Dynamic characterization of human breast cancer cells using a piezoresistive microcantilever”. In: *Journal of biomechanical engineering* 132.10 (2010), page 104501.
- [66] TN TruongVo et al. “Microfluidic channel for characterizing normal and breast cancer cells”. In: *Journal of Micromechanics and Microengineering* 27.3 (2017), page 035017.
- [67] Jinshu Zeng et al. “Nano-mechanical and biochemical characterization of different subtypes of breast cells using atomic force microscopy and Raman spectroscopy”. In: *Laser Physics* 26.11 (2016), page 115702.
- [68] Wenwei Xu et al. “Cell stiffness is a biomarker of the metastatic potential of ovarian cancer cells”. In: *PloS one* 7.10 (2012), e46609.
- [69] Angelyn V Nguyen et al. “Stiffness of pancreatic cancer cells is associated with increased invasive potential”. In: *Integrative biology* 8.12 (2016), pages 1232–1245.





## 6. Effects of energy metabolism on the mechanical properties of breast cells

### 6.1 Introduction

As seen in the previous chapter, breast cancerous cells are softer than their healthy counterparts, but noninvasive and highly aggressive cell lines display very different mechanical properties.

Actomyosin cortex is sustained by active processes within the cell that require ATP. As seen in the introduction, one of the proposed hallmarks in cancer is the ability of cancerous cells to reprogram their energy metabolism in order to proliferate, survive and invade [1].

In this chapter, we try to shed light on how the cell metabolism, the actin organization and the cortical tension build up cell stiffness, and how these contributions are modified in cancer and metastasis in breast cells by the AFM methodology, as explained in the previous chapter.

## 6.2 Breast cancer cells metabolism

There are differences in the mitochondrial metabolism, glucose consumption, intracellular ATP levels and lactate production in the three studied cell lines [70]. Glucose consumption is greater in healthy cells and it decays with the malignancy of cells. Also, healthy cells display higher levels of intracellular ATP and higher mitochondrial activity (by MTT assay) than MCF-7 and MDA-MB231.

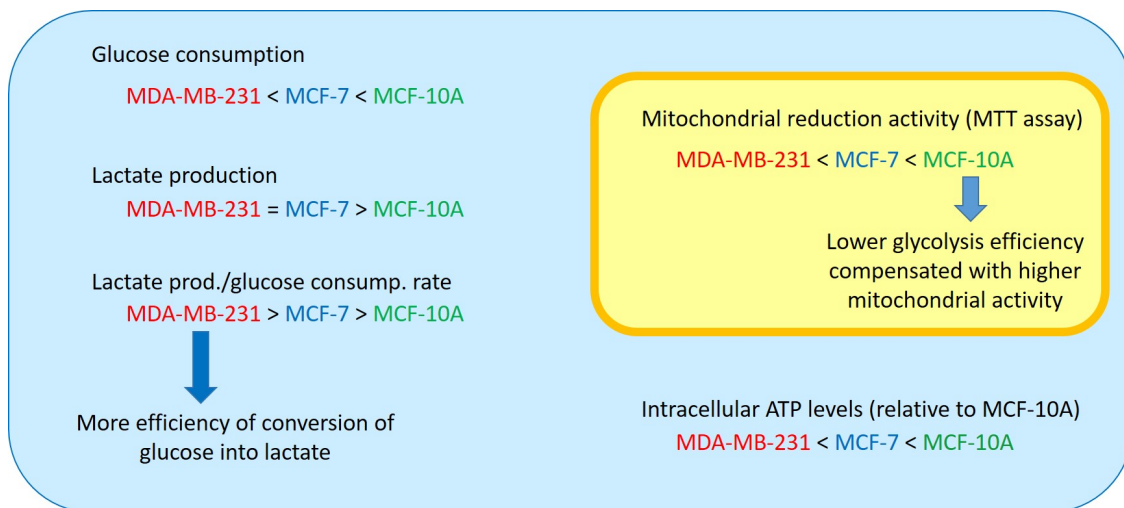


Figure 6.1: **Sketch of differences in glucose consumption, lactate production, lactate production and glucose consumption rate, mitochondrial activity and intracellular ATP levels.** Adapted from [70].

Although lactate production is similar in MCF-7 and MDA-MB-231, the ratio between this lactate production and glucose consumption is higher in metastatic cells. This could indicate an enhanced glycolytic efficiency in the latter ones, meaning that they convert glucose in lactate in a more effective way. Another possible explanation is that degradation of glutamine through glutaminolysis in MCF-7 and MDA-MB-231 generates lactate, increasing its levels in cancerous cells.



### 6.3 ATP depletion and the effect of drugs directed to the cytoskeleton studied by AFM

As explained before, there are three main protagonists in cell stiffness and mechanical resistance: metabolism, through ATP driven processes, actin network arrangement and myosin II forces, which causes cortical tension in the cytoskeleton.

In order to completely deplete the ATP in the cell culture, inhibition of oxidative and glycolytic metabolism was required. A glucose-free medium with 20 mM of sodium azide ( $\text{NaN}_3$ ) and 5 mM 2-Deoxy-D-glucose was supplied to cultures and cells were incubated for one hour with this medium before measuring.

2-Deoxy-D-glucose inhibits the first step of glycolysis [71], while  $\text{NaN}_3$  inhibits cytochrome C oxidase in the electronic transport chain (inhibiting oxidative phosphorylation) [72]. This prevents the generation of ATP from ADP and an inorganic phosphate. So, with this cell media, oxidative phosphorylation and glycolysis were depleted and cells ran out of ATP.

To inhibit just actin polymerization, cell cultures were incubated with cytochalasin D ( $5 \mu\text{g/mL}$ ) for ten minutes before measuring. This treatment disrupts the organization of the actin network, causing the formation of aggregates and increasing the actin filaments ends that cannot bind with others [73].

Finally, for non-muscle myosin II inhibition, blebbistatin was added to cell medium ( $50 \mu\text{M}$ ) for one hour prior to the AFM measurement. Drug doses and incubation times were well above the threshold for reaching the saturation response of the cells [74, 75, 76, 77], but keeping their viability

[78, 79, 80]. Treatments were not removed while measuring with the AFM, which was performed as described in Chapter 5. Power-law rheology parameters are plotted in Figure 6.2.

In noninvasive tumoral cells, stiffness remained unaltered with an increase of fluidity in ATP depletion conditions. CytoD also conspicuously affected PLR parameter  $\beta$  and slightly modified stiffness. Finally, blebbistatin reduced rigidity and lightly boosted  $\beta$ . Comparing the three, MCF-7 cell line is the one that shows less changes when treatments are applied.

In healthy cells, ATP depletion and cytochalasin D (cytoD) treatments caused the most drastic effect in stiffness, making cells softer. In the case of cytoD, cells also showed an increased fluidity.

Disarrangement of the actin cortex makes cell stiffness rely on other cell mechanical components. Recent works point out to the importance of the largest part of the cell, the cytoplasm, in the mechanical resistance of the cell to deformation [81, 82]. In our experiments, we observe a large increase of fluidity when actin cortex is affected, so we consider that the response of the cytoplasm acts as viscous fluid, as the cytoplasm is mainly composed by water.

MDA-MB-231 cells are significantly altered by all narcotics regarding stiffness and fluidity, being cytoD condition the one that affects the cells the most.

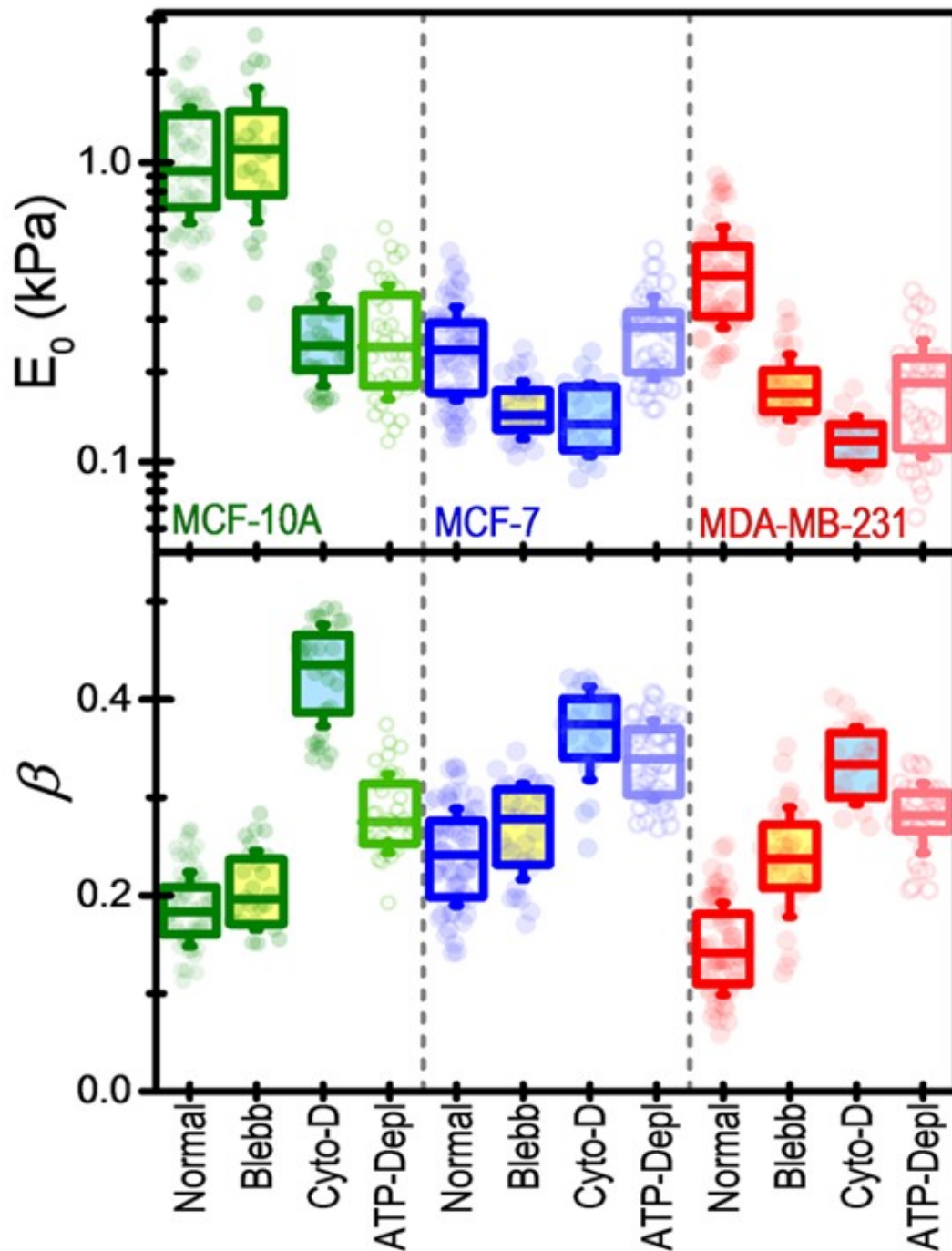


Figure 6.2: PLR parameters plot of treatments with blebbistatin, cytochalasin D and ATP depletion medium in each of the three cell lines studied.  $n$ : 66 MCF-10A cells in normal conditions, 37 MCF-10A cells in ATP depletion, 33 MCF-10A cells treated with cytochalasin-D, 25 MCF-10A cells treated with blebbistatin; 66 MCF-7 cells in normal conditions, 46 MCF-7 cells in ATP depletion, 26 MCF-7 cells treated with cytochalasin-D, 32 MCF-7 cells treated with blebbistatin; 61 MDA-MB-231 cells in normal conditions, 37 MDA-MB-231 cells in ATP depletion, 21 MDA-MB-231 cells treated with cytochalasin-D, 32 MDA-MB-231 cells treated with blebbistatin.

In Figure 6.3,  $\beta$  and  $E_0$  PLR parameters are represented regarding each other. There are visible effects of the drugs on the cell lines depending on the way cells build up their mechanical properties. We can observe that in MCF-10A cell lines, populations in normal and blebbistatin conditions overlap, so there is no effect on healthy cells. Although there are some alterations in MCF-7 cell groups, populations overlap, suggesting that MCF-7 are not so sensitive to these drugs, so their cell stiffness is not built up upon those mechanisms we are inhibiting. In normal and metastatic cells, similar effects are observed when ATP is depleted. Also, cytoD provokes a similar decrease in stiffness and an increase in fluidity in both cell lines.

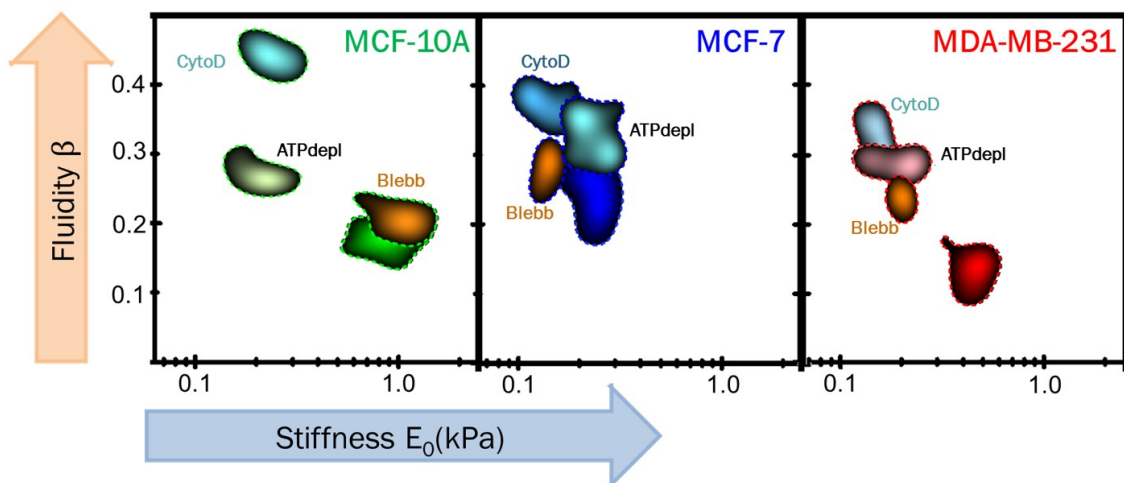


Figure 6.3: **Plots of PLR parameters  $\beta$  and  $E_0$  of the three cell lines with the applied treatments.** Groups not labeled are cell lines in normal conditions. MCF-10A mechanical properties are affected when cytoD or metabolism inhibitors are added, but not in presence of blebbistatin. MCF-7 cell line is the least altered by the addition of drugs or inhibition on metabolism. MDA-MB-231 is more fluid and softer in the presence of all narcotics.

## 6.4 Immunocytochemistry imaging

Again, we labeled the filamentous actin with phalloidin in the three cell lines to observe the effects of the drugs on the F-actin network arrangement (Figure 6.4).

In the three cell lines, we can see that actin filaments are well preserved in ATP depletion conditions and blebbistatin treatment. When cytoD is added, those actin filaments are disrupted. In the orthogonal slices, an increase in the height of cells is observed with both ATP depletion and cytochalasin D additions, but not in the presence of blebbistatin.



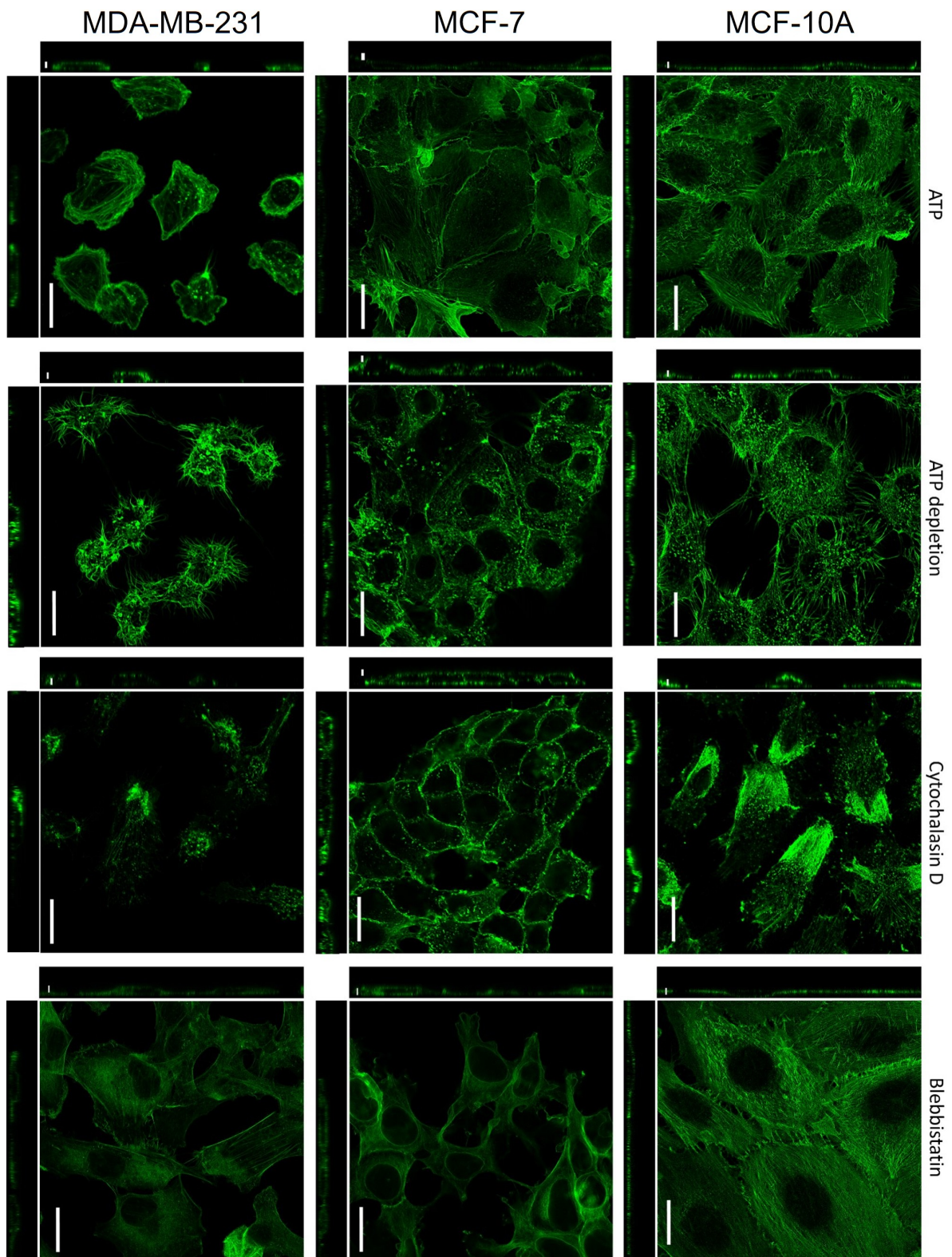


Figure 6.4: Confocal fluorescence images that show changes in the organization of the actin cytoskeleton of MCF-10A, MCF-7 and MDA-MB-231 in normal conditions, in ATP depletion with 20mM  $\text{NaN}_3$  and 5mM 2-Deoxy-D-glucose, with 5 $\mu\text{g/ml}$  cytochalasin D and 50 $\mu\text{M}$  blebbistatin. Scale bar 20 $\mu\text{m}$ .

## 6.5 Contribution of active processes to cell elasticity

We propose that stiffness relies on the contributions of actin cortex, myosin II and energy-driven mechanisms to cell stiffness, assuming that those factors are inhibited by cytochalasin D, blebbistatin and ATP depletion, respectively.

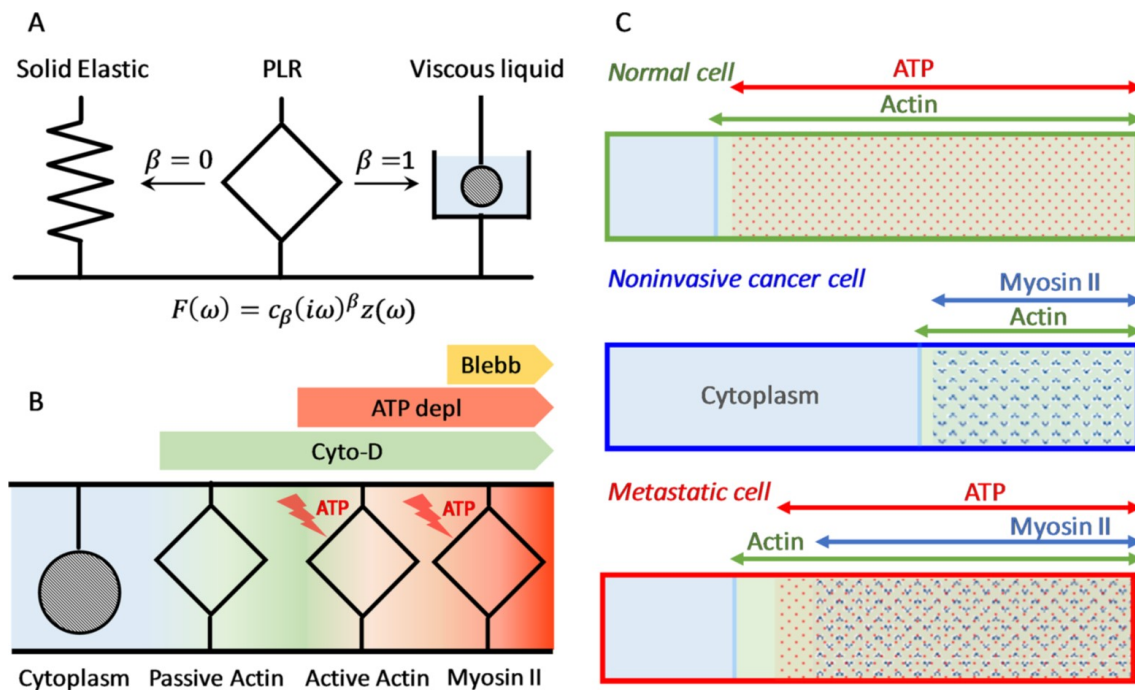


Figure 6.5: **Model of PLR response of breast cancer cells.** **A.** Sketch of the mechanical element used to represent PLR response (adapted from [83]). **B.** Scheme of the springpots that act in parallel to provide stiffness to the cell. Actin cortex components that support energy starvation are passive actin. Those that require energy consumption are active actin and myosin II. We assume fluid-like behavior for the cytoplasm in our experimental conditions. **C.** Relative contributions of the cytoplasm, actin network, myosin II and ATP hydrolysis to the overall elasticity of the studied breast cell lines.

We come up with a simple phenomenological model that describes the mechanical response of the cell as a result of mechanical elements arranged in parallel. Each mechanical component has a power-law response, a *springpot*, instead of a spring-dashpot system typically used for viscoelastic behaviors of materials. This springpot is between a spring ( $\beta = 0$ ) and a

dashpot ( $\beta = 1$ , Figure 6.5A) and describes the rheology of cells with only two parameters in an efficient way [83], and has been used previously to study viscoelastic properties of lung cells [84] and the relaxation response of smooth muscle cells [85], for example.

These mechanical elements are i) myosin II activity, ii) actin cortex components that support energy starvation ("passive actin"), iii) actin cortex components that require energy consumption ("active actin") and iv) cytoplasm. This last one also includes the rest of cell components and acts as a viscous fluid as discussed previously (Figure 6.5B). These differences between active and passive actin arise from the fact that, although actin polymerization is a major consumer of ATP, cells have well-conserved mechanisms to stabilize the actin cytoskeleton in absence of ATP [86, 87]. For example, when cells are in quiescent state, the actin cortex adopts a minimal but stable conformation. Based on this model, the relative contributions of these components to the elastic component of the stiffness given by  $E_0 \cos\left(\frac{\pi}{2}\beta\right)$  is represented in Figure 6.5C).

Our model indicates that 75-80% of the cell elasticity directly comes from actin cortex in healthy and metastatic cells. In noninvasive cancerous cells, this contribution is largely reduced to about 40%. MCF-7 are extraordinarily soft cells, which indicates that they have a minimal actin cortex configuration that is not affected by drug treatments.

In normal cells, most of the actin cortex elasticity is mostly based on ATP-driven processes, around a 95%, predominantly actin polymerization mechanism. On the other hand, myosin II activity contributes little to the cell elasticity.



Similarly, in metastatic cells, ATP hydrolysis sustains most of the actin cortex elasticity ( $\approx 85\%$ ). But most of the “active” actin cortex elasticity arises from myosin II activity ( $\approx 90\%$ ). These results reflect that normal and metastatic cells differ in the way in which they spend their energy.

Also, we can firmly state that actin is not a passive structure that provides mechanical resistance to the cell. This mechanical support is only achieved if the actin cortex is activated by ATP-driven processes.

MCF-7, non-invasive cancerous cells, exhibit an anomalous metabolic effect on elasticity. The actin cortex elasticity is insensitive to the lack of ATP and nutrients, but it drops about 75% when myosin II activity is inhibited. MCF-7 cells can sustain motor activity in starvation conditions. This is consistent with the idea that MCF-7 cells do not spend much of their energy on actomyosin cortex arrangement. Our hypothesis is that MCF-7 cells can use alternative routes to sustain some active processes in our starving medium.

As seen in the introduction, a common feature of cancer cell metabolism is the ability to acquire necessary nutrients from a nutrient-poor environment and utilize these nutrients to both maintain viability and build new biomass to proliferate [1].

## **6.6 Conclusions**

From this chapter, we extract the following conclusions:

1. Actin cortex needs to be activated by metabolic processes to act as a structure which is able to provide mechanical resistance to the cell.
2. Healthy cells build up cell stiffness by ATP-driven polymerization.
3. Metastatic cells use myosin II activity mostly for this purpose.
4. Noninvasive cancerous cells exhibit an anomalous behavior, as their stiffness is not considerably affected by the lack of nutrients and ATP, suggesting that energy metabolism reprogramming is used to sustain active processes at the actin cortex.
5. There is a close relationship between energy metabolism and cell stiffness, which are two relevant cancer hallmarks.
6. We propose an AFM methodology as a single-cell drug-assay.

# Bibliography

- [1] Douglas Hanahan and Robert A Weinberg. “Hallmarks of cancer: the next generation”. In: *cell* 144.5 (2011), pages 646–674.
- [70] Patricia Zancan et al. “Differential expression of phosphofructokinase-1 isoforms correlates with the glycolytic efficiency of breast cancer cells”. In: *Molecular genetics and metabolism* 100.4 (2010), pages 372–378.
- [71] Markus Ralser et al. “A catabolic block does not sufficiently explain how 2-deoxy-D-glucose inhibits cell growth”. In: *Proceedings of the National Academy of Sciences* 105.46 (2008), pages 17807–17811.
- [72] Helen M Duncan and Bruce Mackler. “Electron Transport Systems of Yeast: III. Preparation and properties of cytochrome oxidase”. In: *Journal of Biological Chemistry* 241.8 (1966), pages 1694–1697.
- [73] Manfred Schliwa. “Action of cytochalasin D on cytoskeletal networks.” In: *Journal of Cell Biology* 92.1 (1982), pages 79–91.
- [74] Yareni A Ayala et al. “Effects of cytoskeletal drugs on actin cortex elasticity”. In: *Experimental cell research* 351.2 (2017), pages 173–181.

- [75] Katarzyna Pogoda et al. “Depth-sensing analysis of cytoskeleton organization based on AFM data”. In: *European Biophysics Journal* 41.1 (2012), pages 79–87.
- [76] Tetsuro Wakatsuki et al. “Effects of cytochalasin D and latrunculin B on mechanical properties of cells”. In: *Journal of cell science* 114.5 (2001), pages 1025–1036.
- [77] Aaron F Straight et al. “Dissecting temporal and spatial control of cytokinesis with a myosin II Inhibitor”. In: *Science* 299.5613 (2003), pages 1743–1747.
- [78] Maruša Bizjak et al. “Combined treatment with Metformin and 2-deoxy glucose induces detachment of viable MDA-MB-231 breast cancer cells in vitro”. In: *Scientific reports* 7.1 (2017), pages 1–14.
- [79] Mark S Duxbury, Stanley W Ashley, and Edward E Whang. “Inhibition of pancreatic adenocarcinoma cellular invasiveness by blebbistatin: a novel myosin II inhibitor”. In: *Biochemical and biophysical research communications* 313.4 (2004), pages 992–997.
- [80] Caroline Hayot et al. “Characterization of the activities of actin-affecting drugs on tumor cell migration”. In: *Toxicology and applied pharmacology* 211.1 (2006), pages 30–40.
- [81] Emad Moeendarbary et al. “The cytoplasm of living cells behaves as a poroelastic material”. In: *Nature materials* 12.3 (2013), page 253.
- [82] Jiliang Hu et al. “Size-and speed-dependent mechanical behavior in living mammalian cytoplasm”. In: *Proceedings of the National Academy of Sciences* 114.36 (2017), pages 9529–9534.
- [83] Alessandra Bonfanti et al. “Fractional viscoelastic models for power-law materials”. In: *Soft Matter* 16.26 (2020), pages 6002–6020.
- [84] Bela Suki, Albert-László Barabasi, and Kenneth R Lutchen. “Lung tissue viscoelasticity: a mathematical framework and its molecular basis”. In: *Journal of Applied Physiology* 76.6 (1994), pages 2749–2759.
- [85] Jason D Hemmer et al. “Role of cytoskeletal components in stress-relaxation behavior of adherent vascular smooth muscle cells”. In: *Journal of biomechanical engineering* 131.4 (2009).

- 
- [86] Simon J Atkinson, Melanie A Hosford, and Bruce A Molitoris. “Mechanism of actin polymerization in cellular ATP depletion”. In: *Journal of Biological Chemistry* 279.7 (2004), pages 5194–5199.
- [87] Destiney Buelto and Mara C Duncan. “Cellular energetics: actin and myosin abstain from ATP during starvation”. In: *Current Biology* 24.20 (2014), R1004–R1006.





# Lung cancer cells

<b>7</b>	<b>Lung cancer cells .....</b>	<b>99</b>
7.1	Introduction	
7.2	Mechanical properties of lung cancer cell lines	
7.3	Effects of KRAS-G12V mutation and p53 knock-out	
7.4	Conclusions	
	Bibliography	







## 7. Lung cancer cells

### 7.1 Introduction

Lung cancer was the leading cause of death by cancers in 2020 and the most frequently diagnosed cancer during that same year [17].

Lung cancers are classified into two major groups: small cell lung cancers (SCLCs) and non-small cell lung cancers (NSCLCs). Those cancers arise due to genetic changes in tumor suppressor genes, such as *TP53*, and dominant oncogenes, such as *KRAS*.

In this chapter, we show how a substitution, missense mutation in *KRAS* and the suppression of *TP53* gene are able to change the mechanical properties of three different NSCLC lines.

#### 7.1.1 *KRAS* mutations

RAS proteins belong to the small GTPases superfamily. These proteins regulate cell growth, differentiation and proliferation [88]. *KRAS* (Kirsten

Rat Sarcoma Viral Oncogene Homolog) belongs to this *RAS* family and was one of the first oncogenes found to be mutated in human cancers, including lung, colorectal and pancreatic ones [89].

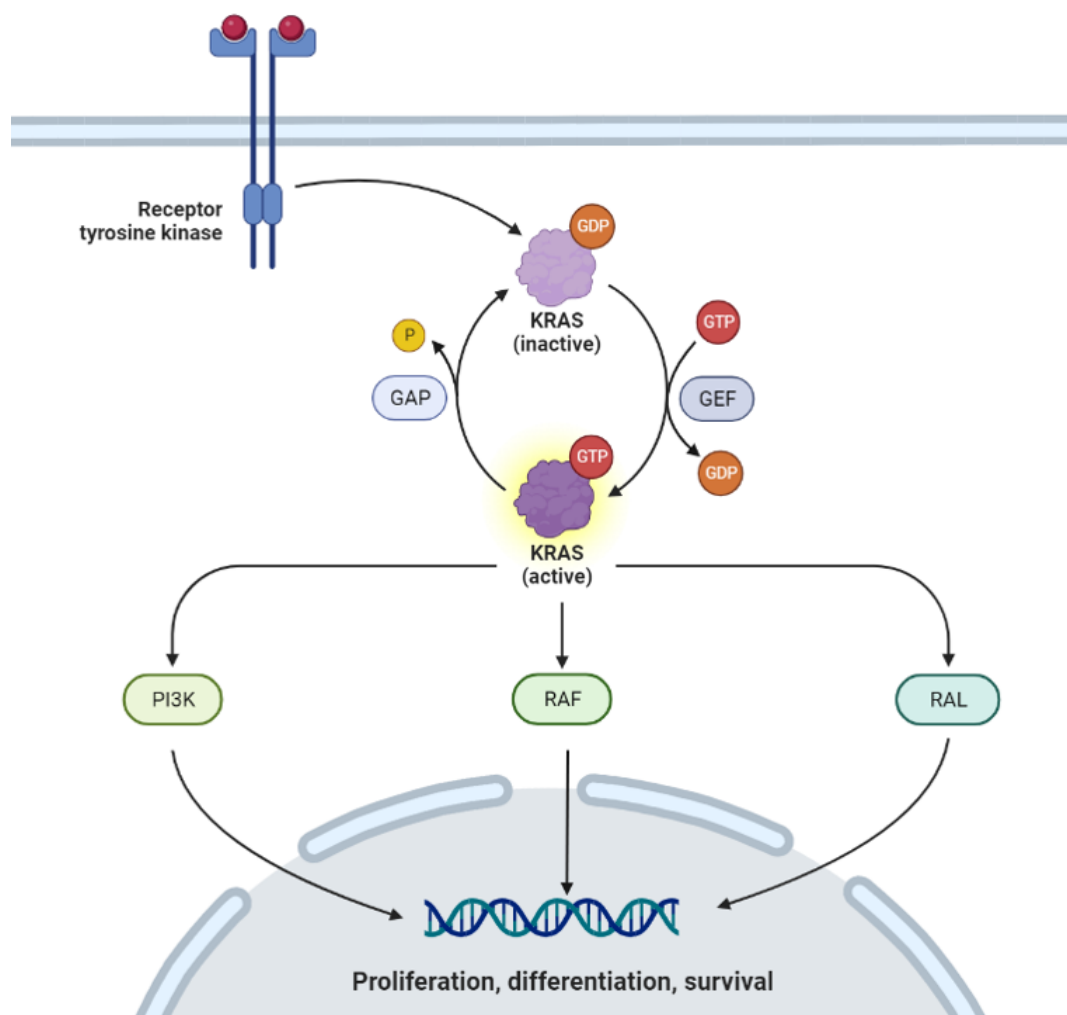


Figure 7.1: **KRAS activation and signalling cascade.** KRAS GTP-GDP cycling is regulated by GEFs and GAPs. Mutations in codon 12 affects KRAS, disrupting its regulation and allowing mutant KRAS protein to accumulate in an active state. With this, signalling cascades as PI3K, RAF and RAL are continuously active, as well as cell proliferation and survival are promoted. Created with BioRender.

*KRAS* mutations are frequent in NSCLC, whose treatment is based on chemotherapy with an average survival of 22 months [90]. In NSNLCs, the most frequently *KRAS* mutations happen at position 12 and 13, being *KRAS*-G12C (glycine-to-cysteine substitution) the most repeated codon

variant [91], but there are others like KRAS-G12V (glycine-to-valine substitution) and KRAS-G12D (glycine-to-aspartic acid substitution) [92]. Mutations in G12C and G12V are associated with worse prognosis compared to other *KRAS* mutants and are more common in smokers [93].

KRAS is a GDP-GTP switch, regulated by guanine nucleotide exchange factors (GEFs) and GTPase activating proteins (GAPs), as seen in Figure 7.1. These mutations in codon 12 affect the GTPase activity of the protein, activating KRAS by interfering with GAP binding and GAP-stimulated GTP hydrolysis. This way, KRAS is insensitive to its deactivation and keeps downstream signaling pathways on. This leads to cell survival, cancellation of apoptosis, altered cell metabolism, cytoskeleton rearrangement, and eventually to cancer [94].

In NSCLCs, KRAS mutations are also known to alter drug response and activate different routes for carcinogenesis [95]. In lung adenocarcinoma H838 cells (NSCLC), KRAS-G12V mutated cells show affected migration and metastasis, but not cell proliferation [96].

KRAS has been considered resistant to drug therapy due to its high affinity to GTP. Nevertheless, in recent years, the FDA approved a targeted therapy for lung cancer with KRAS G12C mutation [97].

### 7.1.2 Tumor suppressor *TP53*

*P53* (UniProt name) or *TP53* (*Tumor Protein 53*) is considered as the guardian of the genome due to its tumor suppressor function, which includes check and maintenance of cell cycle, DNA repair and induction of apoptosis [98]. This gene is located in the short arm of chromosome 17 and it is

translated to a protein of 53kDa in apparent molecular mass. More than 50% of human cancers show mutations in *TP53*, being almost 80% of these alterations missense mutations [99]. *TP53* is implicated in DNA repair, apoptosis, cell-cycle arrest and many other biological functions, as its result protein P53 is a transcription factor that activates transcription of downstream genes of these mentioned cell mechanisms (Figure 7.2). When *TP53* is mutated, there is a gain of function in cell-cycle progression and cell migration, the most important oncogenic activities [100].

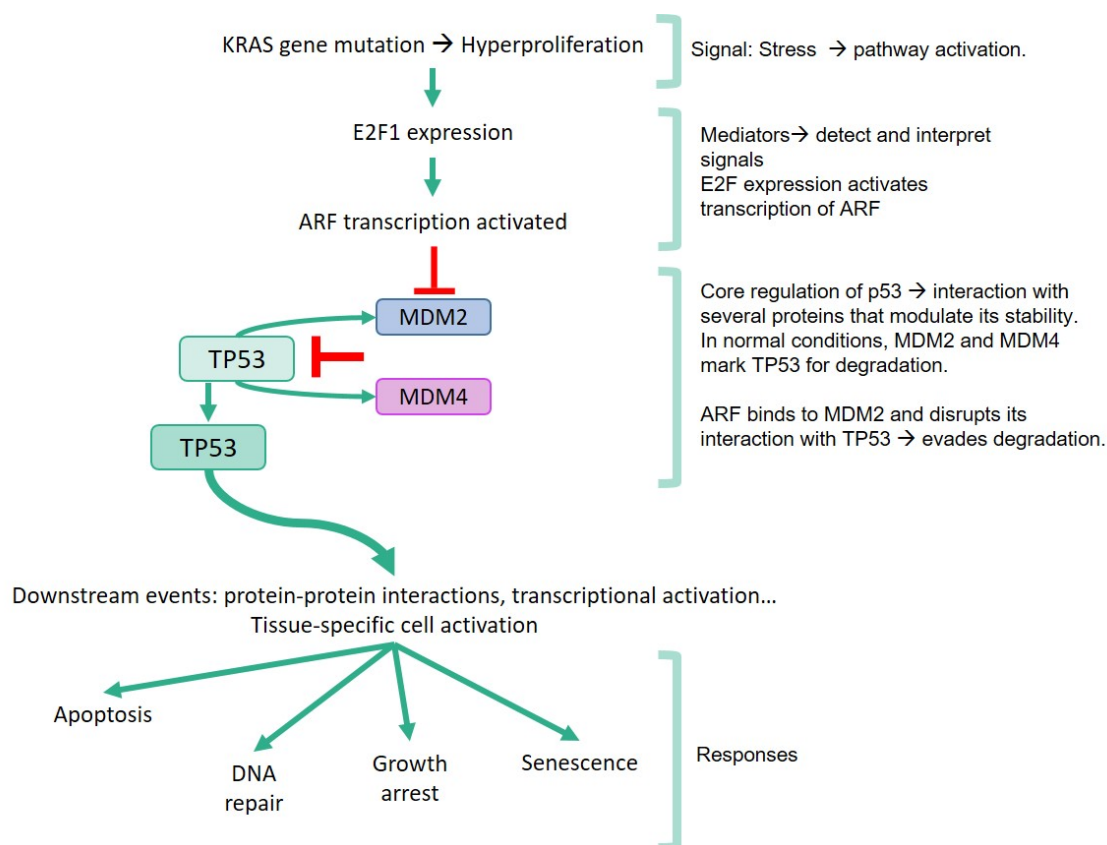


Figure 7.2: **TP53 pathway in response to hyperproliferative stress.** When mediators such as ARF are activated, MDM2 and MDM4, which mark p53 for degradation, are degraded. This prevents p53 from being degraded and activates signaling cascades that lead to apoptosis, DNA repair, cell cycle arrest and cellular senescence. Adapted from the p53 website [101].

*TP53* is known to control glycolysis, oxidative phosphorylation, redox balance, glutaminolysis and Krebs cycle in the cells [102]. In the case of *TP53* loss-of-function, mitochondrial respiration is decreased, which makes cells not be dependent on oxygen [103]. This allows their growth in hypoxic environments. This means that, in normal conditions, *TP53* can bypass the Warburg effect, as a tumor suppressor gene.

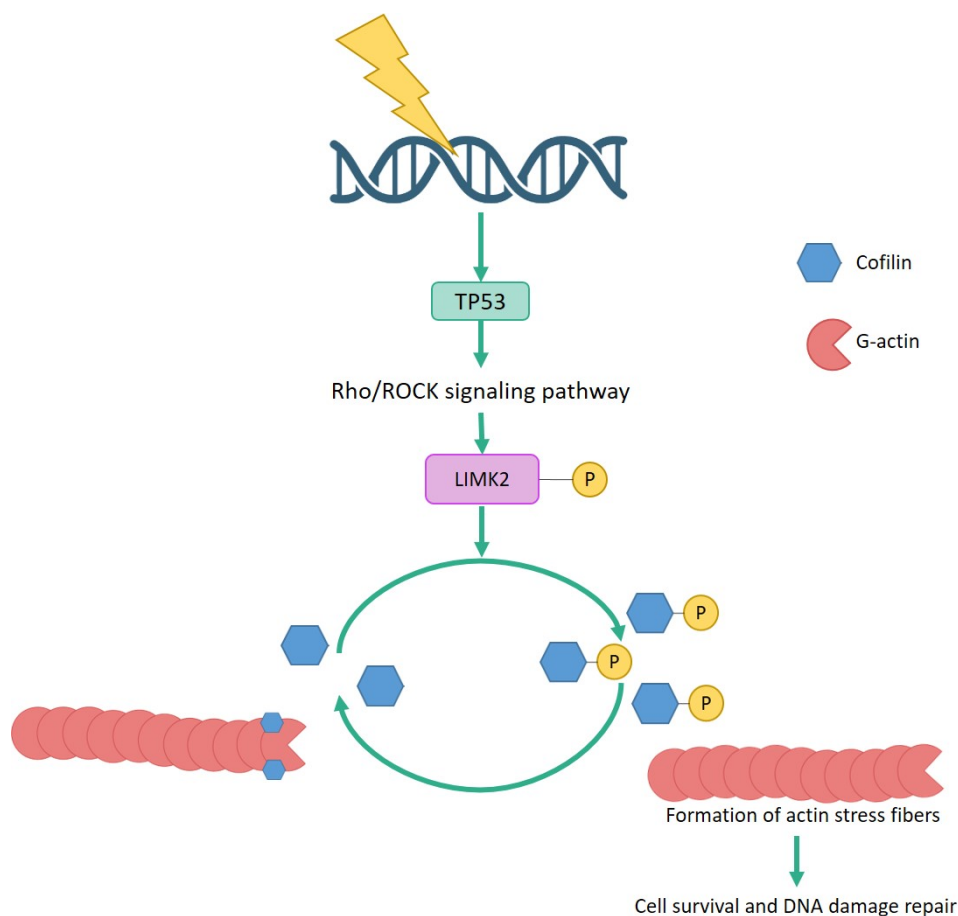


Figure 7.3: **TP53 and actin dynamics feedback in the case of DNA damage.** When DNA is damaged, P53 is activated and induces the activation of Rho/ROCK cascades. This leads to the inactivation of cofilin, reducing actin fibers depolymerization and stabilizing actin filaments. Adapted from [104].

P53 also regulates some actin-binding proteins, particularly those involved in lamellipodia or podosomes formation. In this way, TP53 modulates cytoskeleton dynamics [105].

In normal conditions, TP53 protein exists in the nucleus and it is quickly degraded, so it is hardly detected within the cell. Most missense mutations in *TP53* lead to a stable protein which accumulates in the cell nucleus, as it lacks their specific DNA-binding site. These mutant accumulated proteins are even present in distant metastasis [106].

When DNA is damaged, p53 is located in the cytoplasm and it promotes the formation of actin fibers. P53 is activated and induces the Rho/Rock pathway, which inactivates cofilin. Cofilin is an actin-binding protein that is able to break actin filaments. This way, actin depolymerization is inhibited and filaments are stable [104] (Figure 7.3).

*TP53* is highly mutated in SCLCs [107, 108] and, among NCLCs, 70% of cancers include p53 mutations or inactivations [106]. These mutations are frequent in cancers related to tobacco consumption, and the mutation rate is often higher in cancers from smokers than from nonsmokers, with an excess of G to T substitutions in their DNA sequence [109, 110].

## 7.2 Mechanical properties of lung cancer cell lines

Non-Small Cell Lung Cancer (NSCLC) accounted about 80-85% of the diagnosed lung cancers in United States, according to the American Cancer Society<sup>®</sup>. We chose three different NSCLC cell lines to perform AFM experiments: A549, NCI-H226 and NCI-H23.

A549 cells are adenocarcinomic human alveolar basal epithelial cells. They are an alveolar type II pulmonary epithelium model used for drug development [111]. NCI-H226 cell line was isolated from a squamous cell carcinoma in lungs, from a pleural mesothelioma. And NCI-H23 cell line



originates from an adenocarcinoma. This type of cancer has its origins in secretory cells of the lungs, which usually secretes mucus.

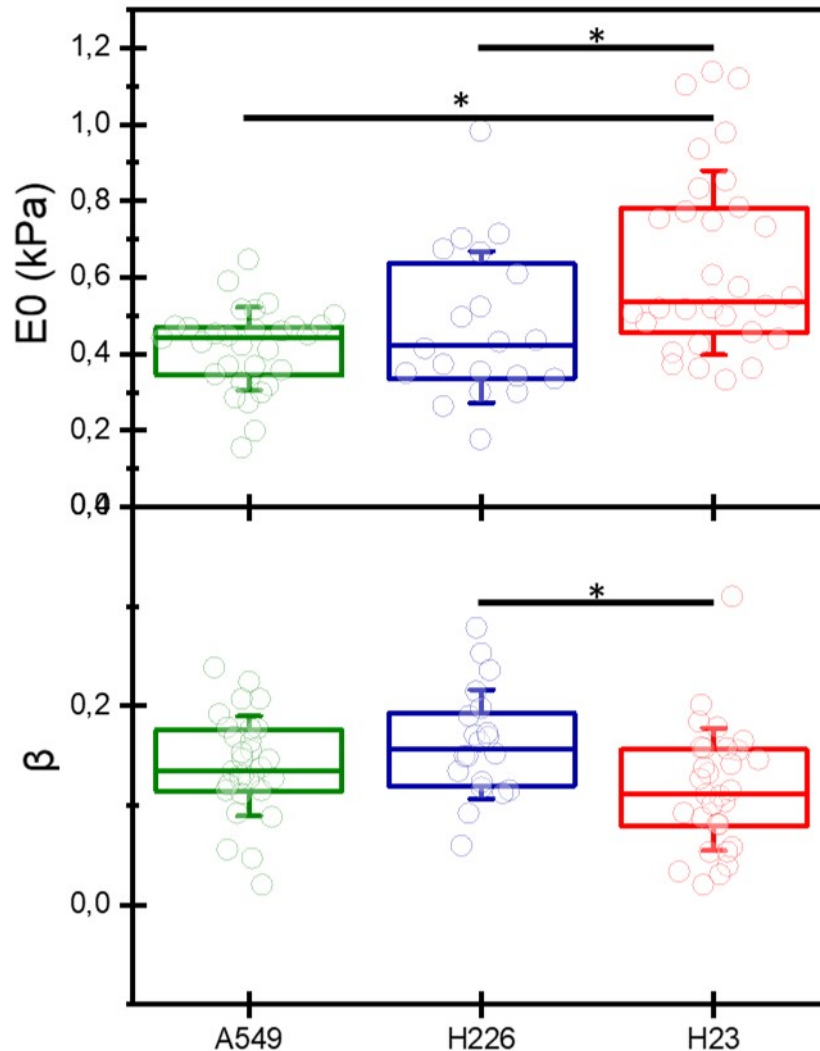


Figure 7.4: **Box plots of the apparent elastic modulus at a reference time of 1s ( $E_0$ ) and the power-law exponent ( $\beta$ ) for the three tested cell lines.** Significance at the 0.05 level is indicated by an asterisk.  $n$ : 30 A549 cells, 20 NCI-H226, 30 NCI-H23.

Figure 7.4 reflects the results for the AFM experiment. The values for the power-law exponent,  $\beta$ , is  $0.139 \pm 0.051$  for A549,  $0.161 \pm 0.054$  for NCI-H226 and  $0.116 \pm 0.061$  for NCI-H23. These low  $\beta$  values are consistent with the idea that these cell lines come from a tissue that is constantly under mechanical stress, implying that there are less energy

losses in the movement [112].

There are differences in A549 and H226  $E_0$  ( $0.41 \pm 0.108$  and  $0.471 \pm 0.198$  kPa, respectively) compared to NCI-H23  $E_0$  ( $0.638 \pm 0.241$  kPa).

As the cell lines we are testing are already tumoral, there are several cancer drivers that are modified in these cells, such as those displayed in Figure 7.5. Cancer drivers are those genetic mutations that induce directly uncontrolled cell growth [113].

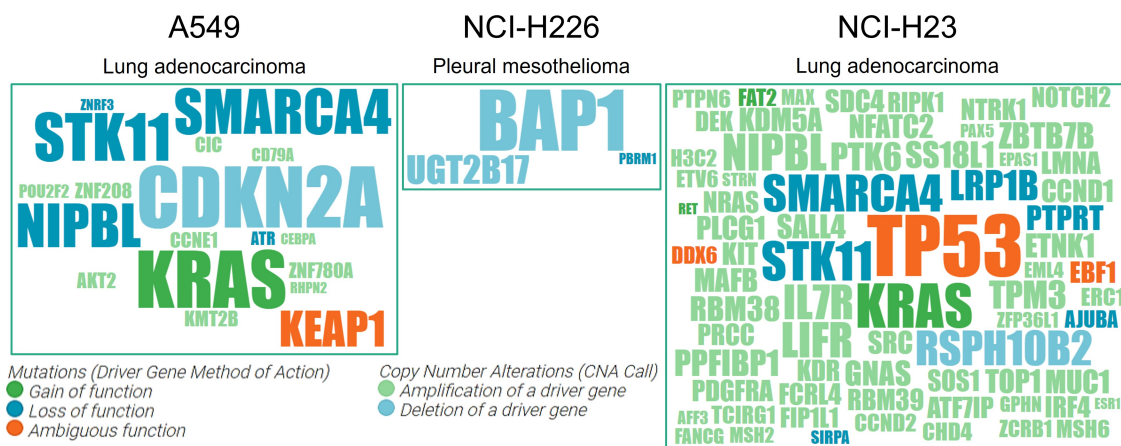


Figure 7.5: **Word clouds of cancer drivers in A549, NCI-H226 and NCI-H23.** For each cancer line, the frequency of mutations of each gene is represented by the size of the font. From Sanger Cell Model Passports.

NCI-H226 has the fewer number of cancer drivers and NCI-H23 the highest registered in the Sanger Cell Model Passports Database. Both A549 and NCI-H23 share common cancer driver modifications such as those in SMARCA4, STK11, NIPBL (A549 shows a loss of function while NCI-H23 have an amplification of this gene) and KRAS, and do not share any with NCI-H226. NCI-H23 is the cell line in which more cancer drivers alteration are studied of the three cell lines, including an ambiguous function of TP53.

NCI-H226 are wild-type for *KRAS* and *TP53*, A549 are wild-type for *TP53* but has a G12S substitution in *KRAS* and NCI-H23 are mutant to both



TP53 and KRAS. We wanted to explore if the differences in the mechanical properties of these three lines rely on alterations in these genes.

### 7.3 Effects of KRAS-G12V mutation and p53 knock-out

We decided to perform knock-outs of *TP53* in those cells that have a wild-type genotype and mutate *KRAS* with a G12V substitution in those lines with a wild-type one in the NSCLCs cell lines. With this methodology, each cell line acts as its own control and the function of both genes can be evaluated separately.

As explained before, A549 cells are wild-type for *TP53* [114], while NCI-H23 have *TP53* mutated, as seen in Table 7.1. NCI-H226 are referred to as *TP53* wild-type in the Catalogue Of Somatic Mutations In Cancer (COSMIC) [115], the NCI-60 cell line set [116] and the Cancer Dependency Map (DepMap, <https://depmap.org>)

Table 7.1: *TP53* mutations in NCI-H23. Adapted from *The Handbook of p53 mutation in cell lines* [101].

Cell line	Codon position (1-393)	WT sequence	Mutated sequence	WT AA	Mutant AA	Reference
NCI-H23	246	ATG	ATC	Met	Ile	[117, 116]

NCI-H226 cells are wild-type for *KRAS* [118], while A549 and NCI-H23 have missense mutations in *KRAS*, as seen in Table 7.2.

With this, mutations indicated in Table 7.3 were performed by infection of the lung cancer cell lines by lentivirus, as explained in Chapter 4.

Table 7.2: *KRAS* mutations in A459 and NCI-H23.

Cell line	Codon position	Nucleotide sequence change	AA change	Reference
A549	34	c.34G>A	Substitution - missense, position 12, Gly→Ser	[116]
NCI-H23	34	c.34G>T	Substitution - missense, position 12, Gly→Cys	[116]

Table 7.3: *TP53* and *KRAS* genes in the studied lung cell lines. Mutations and knock-outs performed are highlighted in color red.

Cell line	<i>TP53</i>	<i>KRAS</i>
NCI-H226	WT	WT
	WT	<b>MUT</b>
	<b>KO</b>	WT
	<b>KO</b>	<b>MUT</b>
A549	WT	MUT
	<b>KO</b>	MUT
NCI-H23	MUT	MUT

All cell sets (wild-types and mutants for each cell line) were obtained from the same cell stock. With this, we avoided discrepancies based on differences in stocks.

### 7.3.1 NCI-H226 cell line

To check that the G12V mutation in *KRAS* was successfully performed in the H226 cell line, we tested this by Western blot, also using this method to check the *TP53* knock-out (Figure 7.6).

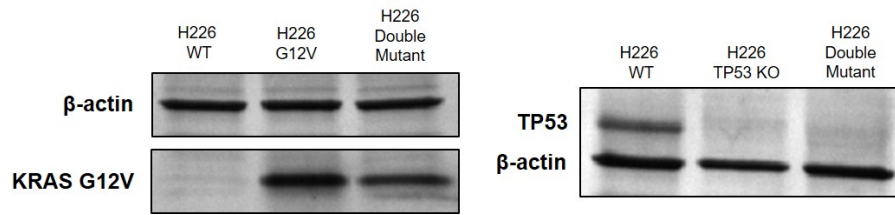


Figure 7.6: Western blot of H226 WT, G12V mutated and double mutant (KRAS-G12V and TP53KO).  $\beta$ -actin is used as control in the three cell lines.

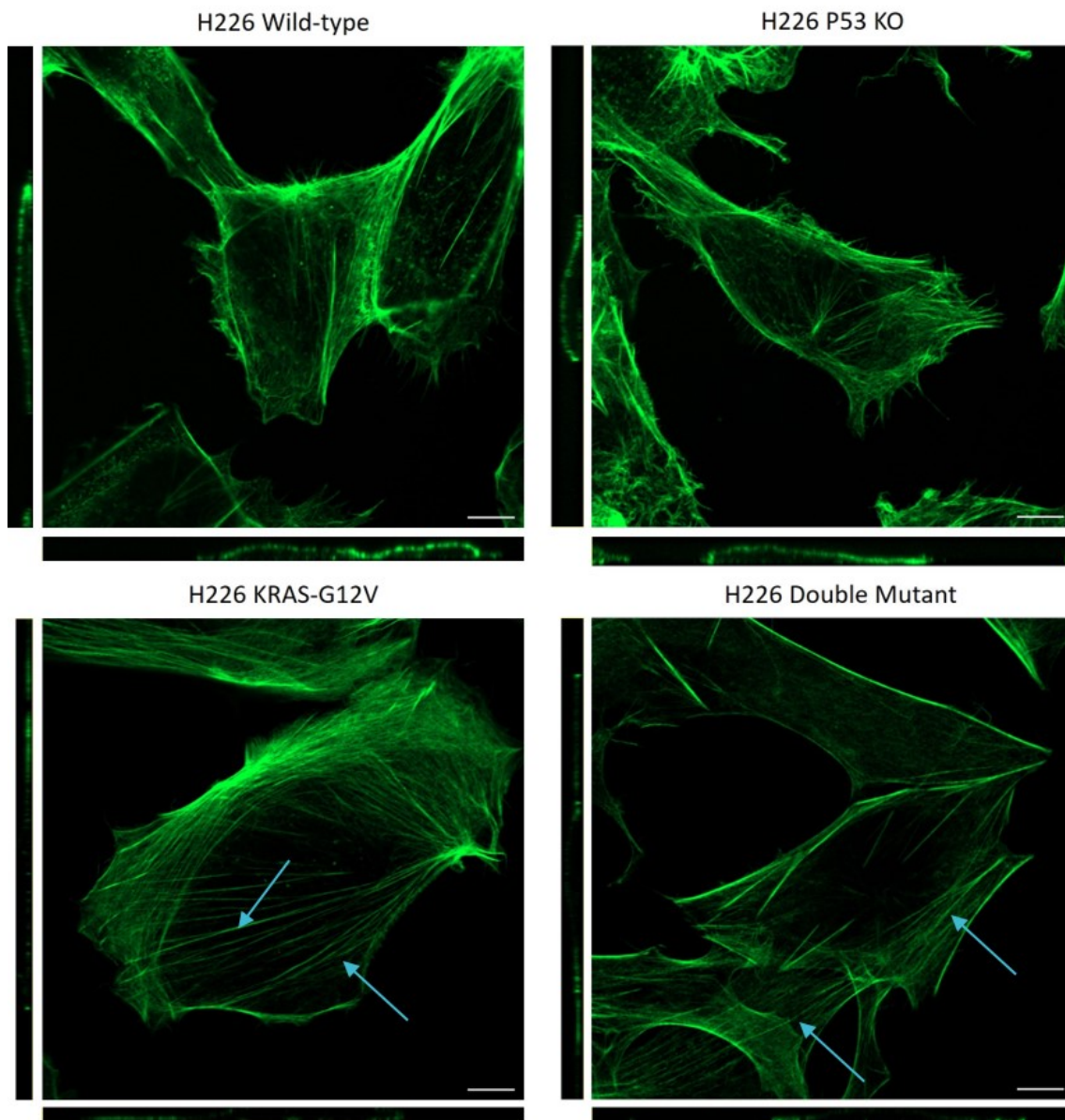


Figure 7.7: Immunofluorescence of H226 wild-type, KRAS G12V mutated cells, knock-out of TP53 cells and double mutant H226 cells. Scale bar 10  $\mu$ m. Actin stress fibers are indicated by arrows.

In the immunofluorescence confocal images of H226 shown in Figure 7.7, some changes in the actin network are observed. In the case of the KRAS-G12V cells, the appearance of well-defined thick filaments can be observed. This is consistent with the fact that KRAS G12V mutation produces an increase in stress fibers explained before. When only TP53 is affected, there is no observable effect compared to the wild-type sample. However, when both KRAS and TP53 are altered, actin seems to reorganize itself into dense fibers with almost no unsegregated actin in the cytoplasm.

Our results, displayed in Figure 7.8, show differences in NCI-H226 wild-type  $E_0$ ,  $0.64 \pm 0.36$  kPa, and NCI-H226 p53-knock out,  $0.47 \pm 0.19$  kPa. There are no differences for  $E_0$  of KRAS G12V mutant cells or the double mutant ( $0.54 \pm 0.24$  kPa and  $0.57 \pm 0.26$  kPa, respectively). No changes in  $\beta$  are observed.

As mentioned before, NCI-H226 cell line is already tumoral. With these genomic alterations, we were trying to make that cell line more malignant. The fact that stiffness can be a physical biomarker for malignity has been previously stated [15]. Although there is no statistical evidence, it seems like  $E_0$  drops a little when KRAS is mutated. But what is undoubtedly clear is that when both p53 is knocked-out and KRAS is mutated at the same time,  $E_0$  do not drop as much as if only TP53 is affected. This means that p53 is an important factor of cell stiffness, but G12V-KRAS can overpass this softening when p53 is released.

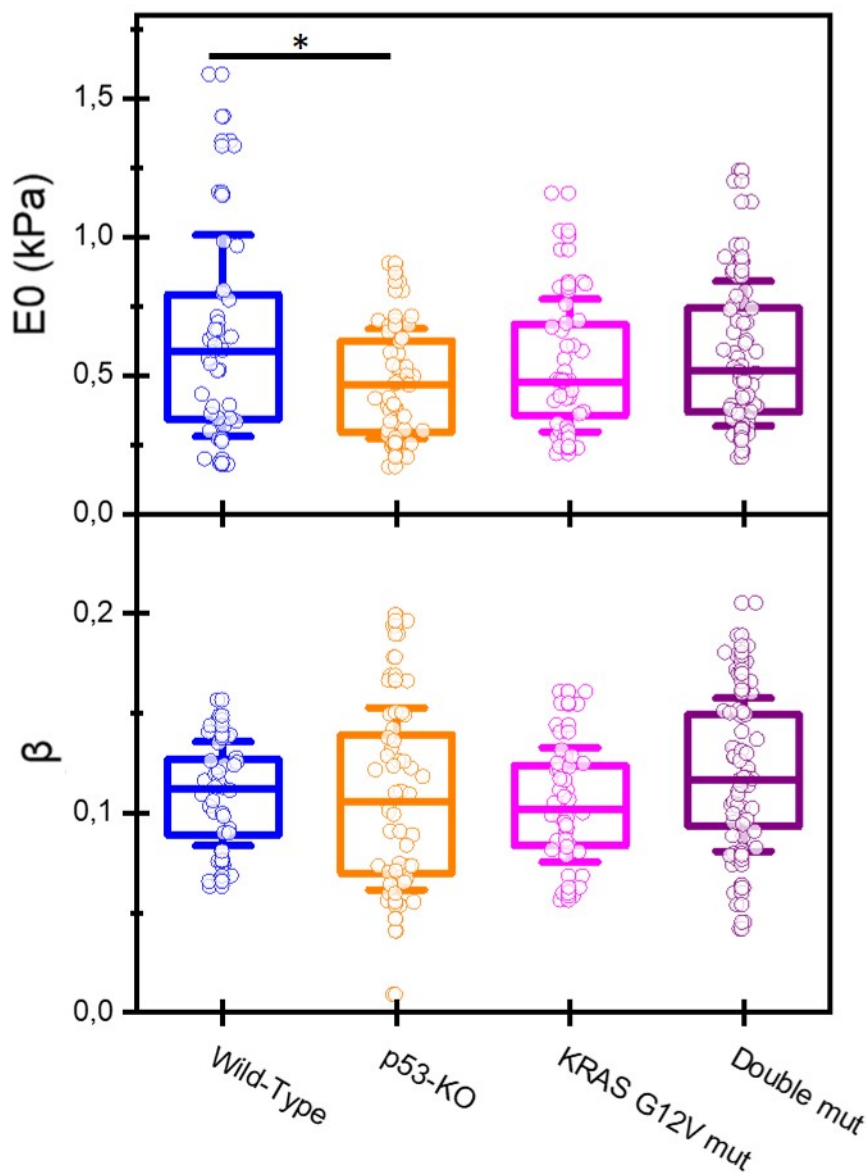


Figure 7.8: **PLR parameters plot of H226 cells WT, P53 knock-out, KRAS G12V mutant and double mutant (both p53 knock-out and KRAS G12V mutant).** Significance at the 0.05 level is indicated by an asterisk.  $n$ : 61 wild-type H226, 62 p53 KO H226 cells, 60 G12V mutant cells, 72 double mutant cells.

### 7.3.2 A549 cell line

As previously mentioned, A549 presents a G12S mutation in KRAS and is wild-type for TP53. So in this cell line, *TP53* was knocked-down and this was checked by Western blotting (Figure 7.9).

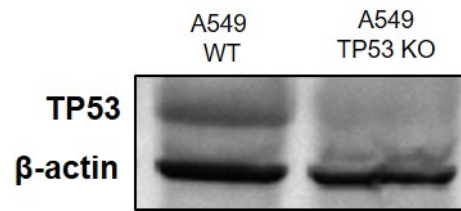


Figure 7.9: **Western blot of A549 WT and TP53 KO.**  $\beta$ -actin is used as control.

In the immunofluorescence confocal images of A549, shown in Figure 7.10, there are no observable differences in F-actin arrangement when p53 is depleted.

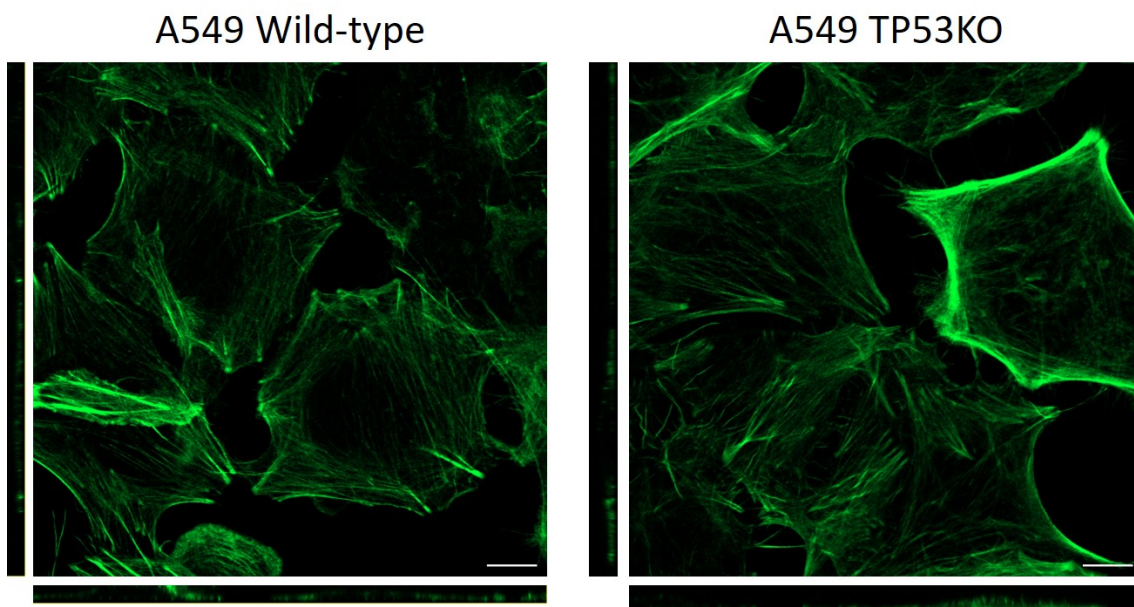


Figure 7.10: **Immunofluorescence of A549 wild-type and TP53 KO cells.** Scale bar  $10\mu\text{m}$ .

When p53 is inhibited in A549 cells in culture, growth or cell proliferation are not affected [119]. Figure 7.11 displays our AFM results. In the case of this cell line, TP53 knock-out provokes a visible effect on both  $E_0$  and  $\beta$  power-law rheology parameters. Cells not only become softer but more fluid as well. However, an increase in  $n$  is necessary to get more accurate statistics.

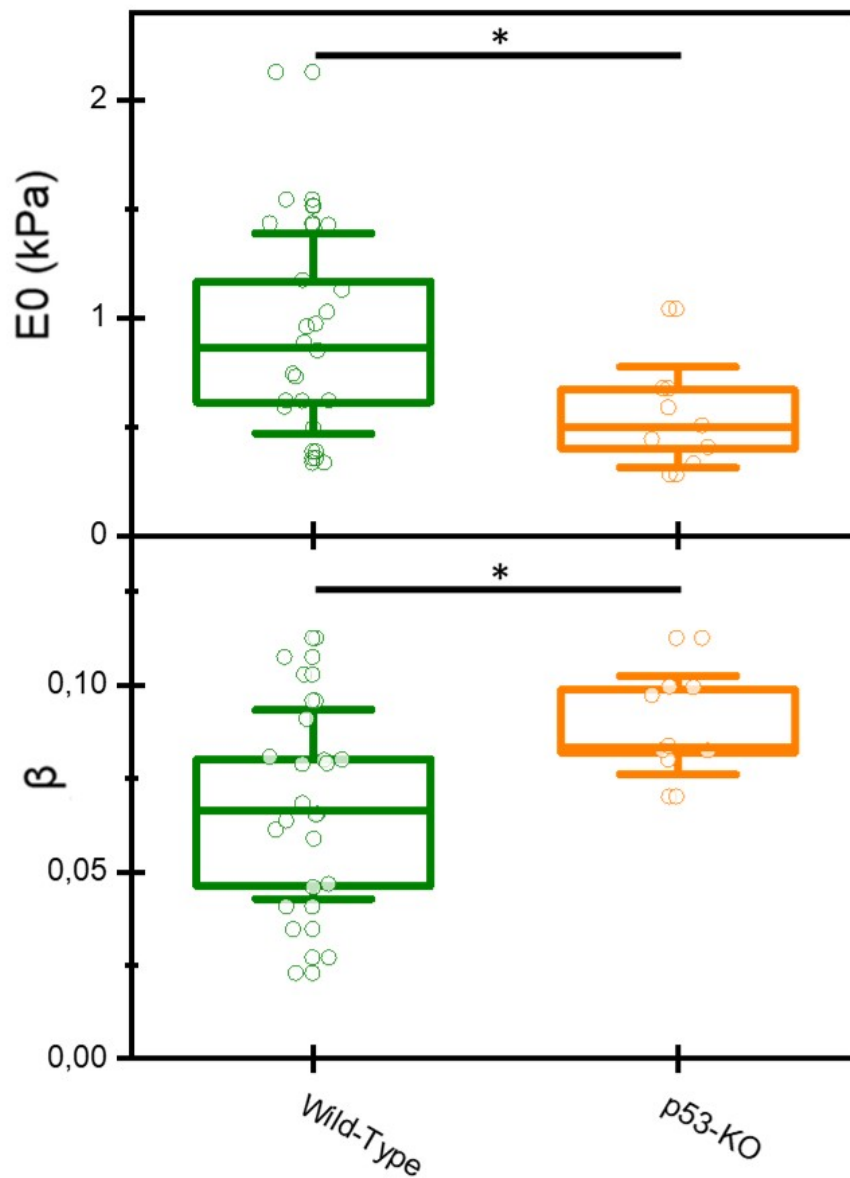


Figure 7.11: **PLR parameters plot of A549 cells WT and P53 knock-out cells.** Significance at the 0.05 level is indicated by an asterisk.  $n$ : 24 wild-type A549 cells and 15 p53-KO A549 cells.

As seen in the introduction of this Chapter, p53 is activated in response to hyperproliferative stress, such as provoked by KRAS mutation. In this case, as it is knocked out, it makes sense that this defensive route cannot be activated, so softening and "fluidization" of cells is observed.



As p53 plays a central role in cancer control by regulating processes that induce abnormal cells to repair themselves, it would be very interesting to over-express TP53 in A549 cell line to observe the changes in the mechanical properties caused by the protective role of p53.

## 7.4 Conclusions

From this chapter, we can conclude that:

1. TP53 has a role in stiffness in NCI-H226 and A549 cell lines, as TP53 knock-out cells are softer than wild types. In A549, TP53 plays an important function in the maintenance of mechanical properties, as its stiffness decreases and cells become more fluid when this tumor suppressor is knocked-out. This means that alterations in molecular pathways can change the stiffness of cells.
2. KRAS G12V mutation has no effect on H226 mechanical properties.
3. In H226, the stiffness of p53 KO and G12V KRAS mutant shows no differences in stiffness, so stiffness of p53 KO cells is recovered when KRAS is also mutated.



## Bibliography

- [15] Charlotte Alibert, Bruno Goud, and Jean-Baptiste Manneville. “Are cancer cells really softer than normal cells?” In: *Biology of the Cell* 109.5 (2017), pages 167–189.
- [17] Hyuna Sung et al. “Global cancer statistics 2020: GLOBOCAN estimates of incidence and mortality worldwide for 36 cancers in 185 countries”. In: *CA: a cancer journal for clinicians* 71.3 (2021), pages 209–249.
- [88] Marcos Malumbres and Mariano Barbacid. “RAS oncogenes: the first 30 years”. In: *Nature Reviews Cancer* 3.6 (2003), pages 459–465.
- [89] Gregory J Riely and Marc Ladanyi. “KRAS mutations: an old oncogene becomes a new predictive biomarker”. In: *The Journal of Molecular Diagnostics* 10.6 (2008), pages 493–495.
- [90] Mark M Awad et al. “Long-term overall survival from KEYNOTE-021 cohort G: pemetrexed and carboplatin with or without pembrolizumab as first-line therapy for advanced nonsquamous NSCLC”. In: *Journal of Thoracic Oncology* 16.1 (2021), pages 162–168.
- [91] Snjezana Dogan et al. “Molecular epidemiology of EGFR and KRAS mutations in 3,026 lung adenocarcinomas: higher susceptibility of women to smoking-related KRAS-mutant cancers”. In: *Clinical cancer research* 18.22 (2012), pages 6169–6177.

- [92] Badi El Osta et al. “Characteristics and outcomes of patients with metastatic KRAS-mutant lung adenocarcinomas: the lung cancer mutation consortium experience”. In: *Journal of thoracic oncology* 14.5 (2019), pages 876–889.
- [93] Nathan T Ihle et al. “Effect of KRAS oncogene substitutions on protein behavior: implications for signaling and clinical outcome”. In: *Journal of the National Cancer Institute* 104.3 (2012), pages 228–239.
- [94] Flávia Pereira et al. “KRAS as a Modulator of the Inflammatory Tumor Microenvironment: Therapeutic Implications”. In: *Cells* 11.3 (2022), page 398.
- [95] MC Garassino et al. “Different types of K-Ras mutations could affect drug sensitivity and tumour behaviour in non-small-cell lung cancer”. In: *Annals of oncology* 22.1 (2011), pages 235–237.
- [96] Pei-Shan Hung et al. “The inhibition of Wnt restrain KRASG12V-Driven metastasis in non-small-cell lung cancer”. In: *Cancers* 12.4 (2020), page 837.
- [97] Janelle E Mann. “Sotorasib (Lumakras™)”. In: *Oncology Times* 43.15 (2021), pages 12–17.
- [98] David P Lane. “p53, guardian of the genome”. In: *Nature* 358.6381 (1992), pages 15–16.
- [99] T Soussi. “The p53 pathway and human cancer”. In: *Journal of British Surgery* 92.11 (2005), pages 1331–1332.
- [100] Arnold J Levine. “p53, the cellular gatekeeper for growth and division”. In: *cell* 88.3 (1997), pages 323–331.
- [101] Bernard Leroy et al. “The TP53 website: an integrative resource centre for the TP53 mutation database and TP53 mutant analysis”. In: *Nucleic acids research* 41.D1 (2013), pages D962–D969.
- [102] Celia R Berkers et al. “Metabolic regulation by p53 family members”. In: *Cell metabolism* 18.5 (2013), pages 617–633.
- [103] Satoaki Matoba et al. “p53 regulates mitochondrial respiration”. In: *Science* 312.5780 (2006), pages 1650–1653.

- [104] Chun-Yuan Chang, Jyh-Der Leu, and Yi-Jang Lee. “The actin depolymerizing factor (ADF)/cofilin signaling pathway and DNA damage responses in cancer”. In: *International journal of molecular sciences* 16.2 (2015), pages 4095–4120.
- [105] Keigo Araki et al. “p53 regulates cytoskeleton remodeling to suppress tumor progression”. In: *Cellular and Molecular Life Sciences* 72 (2015), pages 4077–4094.
- [106] Akira Mogi and Hiroyuki Kuwano. “TP53 mutations in nonsmall cell lung cancer”. In: *Journal of Biomedicine and Biotechnology* 2011 (2011).
- [107] D D’amico et al. “High frequency of somatically acquired p53 mutations in small-cell lung cancer cell lines and tumors.” In: *Oncogene* 7.2 (1992), pages 339–346.
- [108] T Takahashi et al. “The p53 gene is very frequently mutated in small-cell lung cancer with a distinct nucleotide substitution pattern.” In: *Oncogene* 6.10 (1991), pages 1775–1778.
- [109] MS Greenblatt et al. “Mutations in the p53 tumor suppressor gene: clues to cancer etiology and molecular pathogenesis”. In: *Cancer research* 54.18 (1994), pages 4855–4878.
- [110] Gerd P Pfeifer et al. “Tobacco smoke carcinogens, DNA damage and p53 mutations in smoking-associated cancers”. In: *Oncogene* 21.48 (2002), pages 7435–7451.
- [111] A Tansu Koparal and Melih Zeytinoğlu. “Effects of carvacrol on a human non-small cell lung cancer (NSCLC) cell line, A549”. In: (2003), pages 207–211.
- [112] Hubert R Wirtz and Leland G Dobbs. “The effects of mechanical forces on lung functions”. In: *Respiration physiology* 119.1 (2000), pages 1–17.
- [113] Francisco Martínez-Jiménez et al. “A compendium of mutational cancer driver genes”. In: *Nature Reviews Cancer* 20.10 (2020), pages 555–572.
- [114] Li-Qun Jia et al. “Screening the p53 status of human cell lines using a yeast functional assay”. In: *Molecular carcinogenesis* 19.4 (1997), pages 243–253.
- [115] Reika Iwakawa et al. “Prevalence of human papillomavirus 16/18/33 infection and p53 mutation in lung adenocarcinoma”. In: *Cancer science* 101.8 (2010), pages 1891–1896.

- 
- [116] Ogechi N Ikediobi et al. “Mutation analysis of 24 known cancer genes in the NCI-60 cell line set”. In: *Molecular cancer therapeutics* 5.11 (2006), pages 2606–2612.
- [117] Takashi Takahashi et al. “p53: a frequent target for genetic abnormalities in lung cancer”. In: *Science* 246.4929 (1989), pages 491–494.
- [118] Wilbur A Franklin et al. “KRAS mutation: comparison of testing methods and tissue sampling techniques in colon cancer”. In: *The Journal of Molecular Diagnostics* 12.1 (2010), pages 43–50.
- [119] Anna A Sablina et al. “The antioxidant function of the p53 tumor suppressor”. In: *Nature medicine* 11.12 (2005), pages 1306–1313.

# IV

## Conclusiones

## Conclusions

**Conclusiones** ..... 121

**Conclusions** ..... 125

**List of publications** ..... 127





## Conclusiones

En esta tesis, se ha utilizado el AFM como una técnica que permite el fenotipado de células en base a sus propiedades mecánicas mediante dos parámetros relacionados con sus propiedades viscoelásticas: su módulo de elasticidad aparente,  $E_0$ , y su viscoelasticidad, a través del exponente  $\beta$ .

Hemos descubierto que, en células de mama, las células sanas son más rígidas que las cancerosas, pero el grado de malignidad de una línea celular no está relacionado con la rigidez de la misma.

También hemos utilizado esta metodología de AFM como un ensayo de tratamientos de drogas que afectan a la organización del citoesqueleto y al metabolismo de células individuales. Hemos tratado las líneas celulares con dismanteladores de filamentos de actina, inhibidores de miosina-II y hemos paralizado los procesos metabólicos a nivel celular. Con esto, hemos concluido que hay una relación muy estrecha entre el metabolismo y la rigidez celular, considerados como hitos de las células cancerígenas.

Tras los experimentos, hemos concluido que el cortex de actina necesita energía para poder mantener las propiedades mecánicas de las células. Las células de mama sanas utilizan la polimerización de fibras de actina para ello, mecanismo que conlleva gasto de ATP. Las células metastáticas, en cambio, utilizan la actividad de los motores moleculares de miosina-II para mantener su rigidez. Por otra parte, las células tumorales no invasivas muestran una reprogramación metabólica que les permite mantener sus propiedades mecánicas intactas, incluso en ausencia casi total de energía en forma de ATP.

En el caso de cáncer de pulmón, hemos empleado esta técnica de AFM con tres líneas de cáncer de pulmón de células no pequeñas, o no microcíticas, (NSCLC). En las líneas celulares A549 y NCI-H226, las propiedades mecánicas de células individuales son similares, mientras que son muy diferentes a las de la línea celular NCI-H23. Entre las mutaciones conductoras que muestran hay dos conocidos genes relacionados con el cáncer: el oncogén *KRAS* y el gen supresor de tumores *TP53*. NCI-H226 es wild-type para ambos, NCI-H23 muestra mutaciones en ambos, y A549 tiene mutado *KRAS*.

Hemos mutado *KRAS* con una sustitución G12V y hemos eliminado *TP53* en líneas celulares salvajes para ambos para ver si estas rutas moleculares afectan a las propiedades mecánicas. Así, cada línea actúa como control de sí misma.

Hemos concluido que *TP53* afecta a las propiedades mecánicas, en especial a la dureza de las células de las líneas NCI-H226 y A549. En esta última, el efecto de la eliminación de p53 causa cambios drásticos



tanto en el módulo de Young como en su fluidez, haciéndose más blanda y más fluida. Los resultados de KRAS mutado muestran que este oncogén no provoca alteraciones en la dureza de la línea NCI-H226, aunque sí que provoca la aparición de fibras de estrés en las células. Finalmente, la modificación de ambos en la línea celular NCI-H226 muestra que la mutación de KRAS rescata la dureza de las células cuyo TP53 ha sido eliminado. Así, se muestra que hay una conexión directa entre alteraciones en rutas moleculares y las propiedades mecánicas de las células.





## Conclusions

In this thesis we have developed an AFM methodology that provides two-dimensional phenotyping of cells based on two mechanical parameters: the apparent elastic modulus,  $E_0$ , and a power-law exponent  $\beta$ , which is related to viscoelasticity.

We have seen that breast cancer cells are softer than healthy breast cells, but this softness is not related to the grade of malignancy of the cell line.

We have also used this AFM methodology as a single-cell drug-test for breast cancer cells with treatments that affect cell cytoskeleton organization and single-cell metabolism. These drugs disrupt actin cortex, inhibit myosin-II activity and paralyze metabolic processes of cells. We have concluded that there is a close relationship between energy metabolism and cell stiffness, considered as two relevant cancer hallmarks.

In our experiments, we have concluded that actin cortex needs energy from metabolic processes to provide mechanical resistance to cells. Healthy

breast cell line builds up stiffness by ATP-driven polymerization, while metastatic cells use myosin-II for the maintenance of mechanical properties. We discovered that non-invasive ones show an energetic reprogramming that allows them to keep their mechanical properties unaltered even with energy deprivation.

In the case of lung cancer, we have employed the AFM technique with three non-small cell lung cancer (NSCLC) cell lines. In the A549 and NCI-H226 cell lines, the mechanical properties of individual cells are similar, while they are very different from those of the NCI-H23 cell line. Among the driving mutations shown, there are two known genes related to cancer: the KRAS oncogene and the TP53 tumor suppressor gene. NCI-H226 is wild-type for both, NCI-H23 shows mutations in both, and A549 has mutated KRAS. We mutated KRAS with a G12V substitution and deleted TP53 in wild-type cell lines for both genes to see if these molecular pathways affect the mechanical properties.

We have concluded that TP53 does affect the mechanical properties, especially the hardness of cells in the NCI-H226 and A549 lines. In the latter, the effect of p53 deletion causes drastic changes in both the elastic modulus and fluidity, becoming softer and more fluid. The results of mutated KRAS show that this oncogene does not cause alterations in the hardness of the NCI-H226 line. Finally, the modification of both in the NCI-H226 cell line shows that KRAS mutation rescues the hardness of cells whose TP53 has been deleted. Thus, it is shown that there is a direct connection between alterations in molecular pathways and the mechanical properties of cells.

## List of publications

Directly related publication:

- Yubero, M., Kosaka, P. M., San Paulo, Á., Malumbres, M., Calleja, M., & Tamayo, J. "Effects of energy metabolism on the mechanical properties of breast cancer cells". In: *Communications biology*, 3.1 (2020), pages 1-9.

Other publications:

- Martín-Pérez, A., Ramos, D., Yubero, M. L., García-López, S., Kosaka, P. M., Tamayo, J., & Calleja, M. "Hydrodynamic assisted multiparametric particle spectrometry". In: *Scientific Reports* 11.1 (2021), pages 1-9.
- Tamayo, J., Malvar, Ó., Ruz Martínez, J. J., García-López, S., Yubero, M. L., Cano, Á., Puerto, V., Sanz, A., Gil-Santos, E., Ramos Vega, D., San Paulo, Á., Kosaka, P. M. & Calleja, M. "Optomechanical devices for mechanobiological fingerprinting". In: *Frontiers of Nanomechanical*

*Systems*. (2020).

<https://digital.csic.es/handle/10261/261814>

- Martín-Pérez, A., Ramos, D., Gil-Santos, E., García-López, S., Yubero, M. L., Kosaka, P. M., & Calleja, M. "Mechano-optical analysis of single cells with transparent microcapillary resonators". In: *ACS sensors* 4.12 (2019), pages 3325-3332.

---

# AGRADECIMIENTOS

Detrás de este trabajo hay muchas personas:

En primer lugar, gracias a Javi y a Montse por la oportunidad. Gracias por confiar en mí y darme la bienvenida al grupo de Bionanomecánica, donde espero haber contribuido y dejado un pedacito de mí. También agradecer a Priscila su paciencia y la ayuda que me ha brindado, y a Álvaro por todos los consejos recibidos. También a los primeros: Alicia, Mario y Carmen. Vosotros me enseñásteis todo esto.

Mil gracias también a Jaime Ferrer, de la Universidad de Oviedo, por haberme aceptado aún sin conocerme de nada y ejercer como tutor de la tesis.

A los "mayores" de BioNano: Óscar (¿cómo estás?), Joselo y su bocata, y Edu y a Dani. A Alberto y a Juan por su show del muelle (¡buscadlo en YouTube!), a Adri y a Xavi. A los células, por todo lo vivido: Vero, Álvaro y a Carmen, los físicos, por haber compartido dramas y despacho por un tiempo. Y a Sergio, compañero de fatigas estos años. Y a las nuevas incorporaciones: Javier, Víctor y Mathieu, os deseo mil éxitos.

Mención muy especial a la sala de becarios, mi casa en los últimos momentos de la tesis: en especial a Sandra (ya me dirás si hay que rellenar alguna encuesta más), a Alicia y sus bacterias, a Elena (gracias por el vspace), a Andrés, Blanca y Rihab, Pablo, a Mica y su falafel, a Alba y a Alejandro, José María y tantos nuevos, y a Raquel (que siempre será de la sala de becarios) y a todo el IMM/IMN. Y sé que me dejo a muchas otras personas que han pasado por allí. A Margarita, por ayudarme con los papeleos, y a Manu, Vanesa y Ángela por hacernos la vida un poquito más fácil desde Recepción.

Tengo que agradecer también muchísimo al laboratorio 303 del departamento de Física de la Materia Condensada de la UAM. Pedro, muchas gracias por enseñarme qué es un AFM y dejarme trastear tanto tiempo en tu laboratorio. Aida, Merche y Álvaro: si sé usar un AFM es porque vosotros me enseñásteis, me habéis dejado el listón altísimo. Mariano, Natalia, Alba y Manuel. Os deseo lo mejor. Y al resto de compañeros: Pablo Ares, las dos Miriam, Diego, Bruno, Héctor...

Remontando a los inicios de mi carrera investigadora, dar las gracias también a Guillermo de Cárcer, por todo, por enseñarme lo que es la vida de laboratorio. Y a Begoña del CNIO, por toda la ayuda y los consejos con la parte más bio de esta tesis.

En lo personal, mil gracias a Kriscu, Álvaro y Nerea. Por CampaMola, por vuestra amistad, por todo. Si me pongo a escribir me sale otra tesis. A Sara y a Laura, porque sois Totonocoño y sabemos lo que eso significa. ¡Y a Bencenín!

A los ramireños: en especial a Alicia y a miniAli. Juntos conseguimos sobreBIVir y aquí seguimos detrás de Mamá Pato: Yolanda, Concha y Nacho, y Mab, por esta maravillosa plantilla de L<sup>A</sup>T<sub>E</sub>X.

A los Erasmus. Pillaremos un buen peo con Mateo junto a Aurora, Jacobo, Iván, Diego y las dos Rocíos. And my favourite Litochorou 37 girls: Ela and Alice (bocianie gniazdo!).

I have another family I was given some years ago. Meeting the Dangers was one of the best summers of my life: Anne-Marie, Hannah and Dan.

A los jerezanos en Madrid y en Jerez: en especial a Lucía y Rafa, Pili y Álvaro, Aida y Juansu, Larissa y Ángel, Marina, Ony, sin olvidarme "del Alfre". Y a mi familia política: Encarni por tratarme siempre tan bien como a una más, a Jose María por su temple y ejemplo, sin olvidarme de Alejandro y Agustín. Y a Eduardo, otro tipo de familia política.

A Josemari, porque siempre le acaba dando la vuelta a la tortilla y es la persona que más me enfada y más me hace reír. Y a Chili, Tequila y Tommy, claro.

A mi familia. A los que están y, sobre todo, a los que ya no están.

Y, cómo no, a ellos. A mis padres: Jesús y Rosana. Rosana y Jesús. Gracias por apoyarme desde siempre, desde pequeñita, gracias por la educación recibida y el amor mostrado y demostrado. Este libro es un triunfo vuestro. Gracias, mamá, por ayudarme tanto con esto, a pesar de no entender nada.

A todos. A los mencionados y a los que se me olvidan.

**GRACIAS**